Alterations of brain dendrite and synapse structure by the *Streptococcus pneumoniae* neurotoxin pneumolysin - Insights and pharmacological modulation

Morphologische Veränderungen von Dendriten und Synapsen durch das Neurotoxin Pneumolysin
- Einblicke und pharmakologischer Ansatz

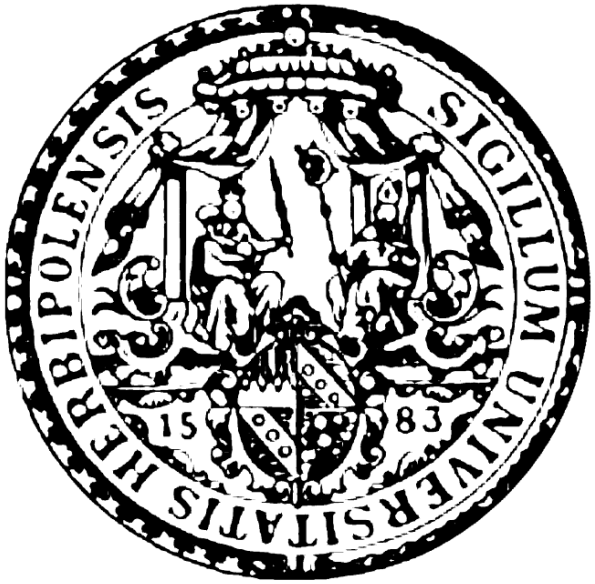

DOCTORAL THESIS

Julius-Maximilians-Universität Würzburg

Graduate School of Life Sciences – Section Biomedicine

Carolin Wippel

from

Frankenthal (Pfalz)

Würzburg, February 2012

Submitted on:

Members of the Thesis Committee:

Chairperson:	Prof. Thomas Dandekar
Primary Supervisor:	Dr. Asparouh Iliev
Supervisor (Second):	Prof. Timothy Mitchell
Supervisor (Third):	Prof. Erich Buchner
Date of Public Defense:	
Date of receipt of Certificates:	

I hereby confirm that my thesis entitled “Alterations of brain dendrite and synapse structure by the *Streptococcus pneumoniae* neurotoxin pneumolysin – insights and pharmacological modulation” is the result of my own work. I did not receive any help or support from commercial consultants. All sources and/or materials applied are listed and specified in the thesis.

Furthermore, I verify that this thesis has not yet been submitted as part of another examination process neither in identical nor in similar form.

Würzburg, 27.02.2012

„Der, die, das! - Wer, wie, was? Wieso, weshalb, warum - wer nicht fragt bleibt dumm.“

-Sesamstraße-

Index

Table of figures I

Index of tables III

List of abbreviations IV

Publications VIII

1 Abstract 9

English 9

Deutsch 11

2 Introduction 14

2.1 *Streptococcus pneumoniae* 14

2.1.1 Virulence factors 15

2.2 Bacterial meningitis caused by *Streptococcus pneumoniae* 16

2.2.1 Epidemiology 16

2.2.2 Pathogenesis 18

2.2.3 Diagnosis and Treatment 20

2.3 Pneumolysin 21

2.3.1 Contribution of PLY to the virulence of *S. pneumoniae* 22

2.3.2 Pore formation process 23

2.1 Cellular components of nervous tissue 24

2.1.1 Neurons 24

2.1.2 Neuroglia 26

2.1.3 The glutamate-glutamine cycle 27

2.2 Excitotoxicity 29

2.2.1 Glutamate receptors 30

2.2.1.1 NMDA receptors 30

2.2.2 Inhibitors 31

2.2.2.1 MK-801 31

2.2.2.2 AP5 32

3 Methods 33

3.1 Pneumolysin expression and purification 33

3.2 Cell culture 33
3.2.1 Primary neuronal culture 33
3.2.2 Primary astrocytic culture 34
3.3 Brain slice culture 35
3.3.1 Theory 35
3.3.2 Preparation 35
3.4 Transfection of primary neurons 36
3.4.1 Theory 36
3.4.2 Procedure 37
3.4.2.1 Multiplication of the plasmid 38
3.5 Cytotoxicity assay 38
3.5.1 Theory 38
3.5.2 Procedure 39
3.6 Glutamate assay 40
3.6.1 Theory 40
3.6.2 Procedure 40
3.7 Confocal imaging of brain slices 41
3.7.1 DiI staining 42
3.7.1.1 Procedure 42
3.7.2 Immunohistochemistry 42
3.8 Calcium imaging 43
3.8.1 Theory 43
3.8.2 Procedure 43
3.9 Statistics and analysis 44
4 Materials 45
4.1 Laboratory equipment 45
4.2 Buffers and solutions 49
5 Results 52
5.1 Live cell imaging of primary neurons 52
5.1.1 Sub-lytic amounts of pneumolysin induce morphological changes in primary neurons 52
5.2 Establishing an acute brain slice culture 55
5.2.1 C57BL/6 mice (p7) brain slices 57
5.2.2 C57BL/6 mice (p14) brain slices 59

5.2.2.1 Ctrl vs. PLY 59
5.2.3 Cell culture conditions modulating the toxicity of pneumolysin 62
5.2.4 Brain slices of mice with pneumococcal meningitis 63
5.2.4.1 Delta6 mutant 65
5.2.4.2 MK-801 – role in primary neuronal culture 65
5.2.4.3 MK-801 – role in brain slice culture 66
5.2.4.4 AP5 brain slice experiments 67
5.3 Glutamate measurement 69
5.4 Calcium imaging 71
6 Discussion 74
7 Concluding remarks and perspectives 83
8 References 84
Acknowledgment 95
Curriculum vitae ..... Fehler! Textmarke nicht definiert.

Table of figures

Figure 1: ***Streptococcus pneumoniae*** **(SEM) 14**
Figure 2: ***Streptococcus pneumoniae*** **incidence rate 17**
Figure 3: **Proposed protein structure of PLY 21**
Figure 4: **Pore formation process of pneumolysin 23**
Figure 5: **Neuron 24**
Figure 6: **Schematic of the tripartite synapse 27**
Figure 7: **The glutamate-glutamine cycle 28**
Figure 8: **Chemical structure of MK-801 ..... 31**
Figure 9: **Chemical structure of AP5 ..... 32**
Figure 10: **Principle of Magnetofection™ 36**
Figure 11: **Lactic dehydrogenase reaction 39**
Figure 12: **Glutamic acid 40**
Figure 13: **Principle of confocal imaging 41**
Figure 14: **Primary mouse neuron (DIV 14) 52**
Figure 15: **Primary mouse neuron 3 hours after observation 53**
Figure 16: **Live cell imaging of primary neurons incubated with PLY 54**
Figure 17: **Dying neuron 54**
Figure 18: **Cytotoxicity of two different brain slice culturing methods 56**
Figure 19: **Schematic of the brain slicing process 57**
Figure 20: **DiI stained neurons in the cortex of brain slices 58**
Figure 21: **Reduction of dendritic spines and number of varicosities in p7 mouse brain slices 59**
Figure 22: **DiI stained neurons in the cortex of 300 µm mouse brain slices 59**
Figure 23: **Dendrites of neurons in brain slices show morphological changes upon PLY challenge 60**
Figure 24: **Reduction of dendritic spines and induction of varicosities in brain slices incubated with sub lytic amounts of pneumolysin 60**
Figure 25: **MAP2 immunostaining of neurons in the cortex of C57BL/6 mice 61**
Figure 26: **MAP2 immunostaining brain slices after PLY challenge 62**
Figure 27: **Cell death induced by PLY (brain slice shaker method) 63**
Figure 28: **LDH release brain slices with differing calcium concentrations 63**

Figure 29: Relative synaptic density in the cortex of C57BL/6 mice suffering from pneumococcal meningitis 64
Figure 30: Live cell imaging of primary mouse neurons (DIV 14) incubated with PLY and MK-801 65
Figure 31: Live cell imaging of primary neurons (DIV 21) incubated with PLY and MK-801 66
Figure 32: Dendritic spines and varicosities per 100 µm dendrite in mouse brain slices (p14) 66
Figure 33: MAP2 immunostaining 67
Figure 34: AP5 (10 µM) effects of the number of spines and varicosities 68
Figure 35: Number of varicosities (50 µM AP5) 68
Figure 36: Glutamate levels in the supernatant of brain slice culture 69
Figure 37: Reuptake of glutamate into brain slices 70
Figure 38: Glutamate levels in brain slice culture over time 70
Figure 39: MAP2 immunostaining of brain slices 71
Figure 40: Example of a calcium chart 72
Figure 41: Evaluation of the calcium experiments 72
Figure 42: Rise of intracellular calcium 73

Index of tables

Table 1: Virulence factors of *Streptococcus pneumoniae* 15
Table 2: General laboratory equipment 45
Table 3: Chemicals 46
Table 4: Primary antibodies 47
Table 5: Secondary antibodies 48
Table 6: Software used for experiments and data evaluation 48
Table 7: Commercial kits used for experiments 48

List of abbreviations

°C	Centigrade
µg	Microgram
µl	Microliter
µm	Micrometer
µM	Micromolar
ACSF	Artificial cerebrospinal fluid
ALS	Amyotrophic lateral sclerosis
AM	Acetoxymethyl
AMPA	2-amino-3-(5-methyl-3-oxo-1,2- oxazol-4-yl)propanoic acid
AP5	2-amino-5-phosphonopentanoic acid
ATP	Adenosine triphosphate
BBB	Blood-brain barrier
BME	Basal medium eagle
BSA	Bovine serum albumin
ca.	circa
CaMKII	Ca^{2+}/calmodulin-dependent protein kinase
CDC	Cholesterol dependent cytolysin
CNS	Central nervous system
CSF	Cerebrospinal fluid
Cy	Cyanine

DABCO	1,4-diazobicyclooctane
DiI	1,1`-dioctadecyl-3,3,3`,3`-tetramethylindocarbocyanine perchlorate
DIV	Days in vitro
DMEM	Dulbecco‘s Modified Eagle Medium
DMSO	Dimethyl sulfoxide
DNA	Desoxyribonucleic acid
E	Embryonic day/day of gestation
E. coli	*Escherichia coli*
e.g.	*Exempli gratia* (= for example)
EAAT	Excitatory amino-acid transporter
EDTA	Ethylenediaminetetraacetic acid
FCS	Fetal calf serum
FITC	Fluorescein isothiocyanate
g	Gravitational force
GABA	γ-Aminobutyric acid
GAVI	Global Alliance for Vaccines and Immunization
GFP	Green fluorescent protein
h	Hour
HEPES	4-(2-hydroxyethyl)-1-piperazineethanesulfonic acid
HIV	Human immunodeficiency virus
hrs.	Hours
Ig	Immunoglobulin
iGluR	Ionotropic glutamate receptor

IL	Interleukin
l	Liter
LB	Lysogeny broth
LDH	Lactic dehydrogenase
LPS	Lipopolysaccharide
LSCM	Laser scanning confocal microscopy
LTP	Long-term potentiation
mACSF	Modified artificial cerebrospinal fluid
MAP2	Microtubule-associated protein 2
MAPK	Mitogen-activated protein kinase
mGluR	Metabotropic glutamate receptor
min	Minutes
MK-801	Dizocilpine
NADH	Nicotinamide adenine dinucleotide
NanA	Neuraminidase A
NMDA	N-methyl-D-aspartate
NMDAR	N-methyl-D-aspartate receptor
p	Postnatal
PAF	Platelet activating factor
PBS	Phosphate buffered saline
PCP	Phencyclidine
PD	Postnatal day
PFA	Paraformaldehyde

PFO	Perfringolysin O
PLO	Poly-L-Ornitine
PLY	Pneumolysin
rpm	Revolutions per minute
RT	Room temperature
SEM	Scanning electron microscopy
SEM	Standard error of mean
TNF-α	Tumor necrosis factor alpha
Trp	Tryptophan
VGLUT	Vesicular glutamate transporter
w/o	without
WHO	World Health Organization
wt	Wildtype

Publications

1.) Extracellular calcium reduction strongly increases the lytic capacity of pneumolysin from *Streptococcus pneumoniae*

Carolin Wippel*, Christina Förtsch*, Sabrina Hupp*, Elke Maier, Roland Benz, Jiangtao Ma, Timothy J. Mitchell, Asparouh I. Iliev

Journal of Infectious Diseases (2011) Sep, 204 (6): 930-6

*) authors contribute equally

2.) Astrocytic tissue remodeling by the meningitis neurotoxin pneumolysin facilitates pathogen tissue penetration and produces brain edema

Sabrina Hupp, Vera Heimeroth, **Carolin Wippel**, Christina Förtsch, Jiangtao Ma, Timothy J. Mitchell, Asparouh I. Iliev

Glia (2012) Jan, 60 (1): 137-46

3.) Dual role of Arp2/3 as a direct mediator of actin remodeling and modulator of lytic pore formation by the cholesterol-dependent cytolysin pneumolysin

Sabrina Hupp, Christina Förtsch, **Carolin Wippel**, Jiangtao Ma, Alexander Zürn, Timothy J. Mitchell, Asparouh I. Iliev

(submitted)

1 Abstract

English

Streptococcus pneumoniae (Pneumococcus) is one of the leading causes of childhood meningitis, pneumonia and sepsis. Despite the availability of childhood vaccination programs and antimicrobial agents, childhood pneumococcal meningitis is still a devastating illness with mortality rates among the highest of any cause of bacterial meningitis. Especially in low-income countries, where medical care is less accessible, mortality rates up to 50 % have been reported. In surviving patients, neurological sequelae, including hearing loss, focal neurological deficits and cognitive impairment, is reported in 30 to 50 %. Growing resistance of pneumococci towards conventional antibiotics emphasize the need for effective therapies and development of effective vaccines against *Streptococcus pneumoniae.*

One major virulence factor of *Streptococcus pneumoniae* is the protein toxin Pneumolysin (PLY). PLY belongs to a family of structurally related toxins, the so-called cholesterol-dependent cytolysins (CDCs). Pneumolysin is produced by almost all clinical isolates of the bacterium. It is expressed during the late log phase of bacterial growth and gets released mainly through spontaneous autolysis of the bacterial cell. After binding to cholesterol in the host cell membranes, oligomerization of up to 50 toxin monomers and rearrangement of the protein structure, PLY forms large pores, leading to cell lysis in higher toxin concentrations. At sub-lytic concentrations, however, PLY mediates several other effects, such as activation of the classic complement pathway and the induction of apoptosis.

First experiments with pneumococcal strains, deficient in pneumolysin, showed a reduced virulence of the organism, which emphasizes the contribution of this toxin to the course of bacterial meningitis and the urgent need for the understanding of the multiple mechanisms leading to invasive pneumococcal disease.

The aim of this thesis was to shed light on the contribution of pneumolysin to the course of the disease as well as to the mental illness patients are suffering from after recovery from pneumococcal meningitis.

Therefore, we firstly investigated the effects of sub-lytic pneumolysin concentrations onto primary mouse neurons, transfected with a GFP construct and imaged with the help of laser scanning confocal microscopy. We discovered two major morphological changes in the dendrites of primary mouse neurons: The formation of focal swellings along the dendrites (so-called varicosities) and the reduction of dendritic spines.

To study these effects in a more complex system, closer to the *in vivo* situation, we established a reproducible method for acute brain slice culturing. With the help of this culturing method, we were able to discover the same morphological changes in dendrites upon challenge with sub-lytic concentrations of pneumolysin. We were able to reverse the seen alterations in dendritic structure with the help of two antagonists of the NMDA receptor, connecting the toxin´s mode of action to a non-physiological stimulation of this subtype of glutamate receptors.

The loss of dendritic spines (representing the postsynapse) in our brain slice model could be verified with the help of brain slices from adult mice, suffering from pneumococcal meningitis. By immunohistochemical staining with an antibody against synapsin I, serving as a presynaptic marker, we were able to identify a reduction of synapsin I in the cortex of mice, infected with a pneumococcal strain which is capable of producing pneumolysin. The reduction of synapsin I was higher in these brain slices compared to mice infected with a pneumococcal strain which is not capable of producing pneumolysin, illustrating a clear role for the toxin in the reduction of dendritic spines.

The fact that the seen effects weren´t abolished under calcium free conditions clarifies that not only the influx of calcium through the pneumolysin-pore is responsible for the alterations. These findings were further supported by calcium imaging experiments, where an inhibitor of the NMDA receptor was capable of delaying the time point, when the maximum of calcium influx upon PLY challenge was reached.

Additionally, we were able to observe the dendritic beadings with the help of immunohistochemistry with an antibody against MAP2, a neuron-specific cytoskeletal protein. These observations also connect pneumolysin´s mode of action to excitotoxicity, as several studies mention the aggregation of MAP2 in dendritic beadings in response to excitotoxic stimuli.

All in all, this is the first study connecting pneumolysin to excitotoxic events, which might be a novel chance to tie in other options of treatment for patients suffering from pneumococcal meningitis.

Deutsch

Streptococcus pneumoniae ist einer der Hauptauslöser für bakterielle Meningitis, Lungenentzündung und Sepsis. Ungeachtet der Tatsache, dass es heutzutage viele Impfprogramme zur Prävention, sowie Antibiotika zur Behandlung gibt, ist die bakterielle Meningitis im Kindesalter, ausgelöst durch *S. pneumoniae,* immer noch eine ernstzunehmende Krankheit mit Sterberaten von bis zu 50 %. Dies gilt im Besonderen für Schwellen- und Entwicklungsländer, wo der Zugang zu medizinischer Versorgung sehr schwer bis unmöglich ist. Bei 30 bis 50 % der Patienten, die die Krankheit überstehen, bleiben teilweise schwere neurologische Störungen, wie z.B. Taubheit und Störungen kognitiver Fähigkeiten, zurück. Die steigende Resistenz des Erregers gegenüber herkömmlichen Antibiotika macht zudem die Dringlichkeit zur Entwicklung effektiver Therapieansätze und Impfstoffe deutlich.

Ein Hauptpathogenitätsfaktor von *Streptococcus pneumoniae* ist das Proteintoxin Pneumolysin (PLY). PLY gehört zu einer Familie strukturell verwandter Toxine; die sogenannten cholesterinabhängigen Cytolysine (CDCs). Pneumolysin wird von praktisch allen klinisch isolierten Pneumokokkenstämmen produziert. Die Expression findet in der späten log-Phase des Bakterienwachstums statt. Das Toxin wird hauptsächlich nach spontaner Autolyse des Bakteriums freigesetzt. Nach Bindung des Proteins an das Cholesterin in den Zellmembranen des Wirtsorganismus, Oligomerisierung von bis zu 50 Toxinmonomeren und Umordnung der Proteinstruktur, bildet das Toxin Poren in der Zellmembran, die in höheren Konzentrationen von PLY zur Zelllyse führen. In niedrigeren Konzentrationen löst das Toxin jedoch verschiedene andere Prozesse, darunter Apoptose und Aktivierung des Komplementsystems, aus.

Erste Experimente, die mit einem mutierten Pneumokokkenstamm (unfähig, Pneumolysin zu exprimieren) durchgeführt wurden, konnten eine reduzierte Virulez des Erregers zeigen, was die Beteiligung des Toxins am Verlauf der Krankheit verdeutlicht und klar macht, wie wichtig es ist, die Prozesse zu verstehen, die insbesondere zu einem schweren Verlauf der Krankheit führen.

Ziel vorliegender Arbeit war, die Beteiligung von Pneumolysin sowohl am Verlauf der bakteriellen Meningitis, hervorgerufen durch Pneumolysin, zu erforschen, als auch dessen Beteiligung an der Entstehung von neurologischen Störungen, wie sie auch nach Rehabilitation von einer Meningitis noch bestehen können.

Dafür wurden zuerst die Effekte von sublytischen Konzentrationen des Toxins auf primäre Mausneuronen (transfiziert mit GFP und mit Hilfe eines Konfokalmikroskopes aufgenommen) erfasst.

Dabei zeigten sich hauptsächlich zwei morphologische Veränderungen in den Dendriten der mikroskopierten Neurone: Die Entstehung von fokalen Schwellungen der Dendriten (sogenannte „varicosities“) sowie eine Verminderung der Anzahl von dendritischen Dornfortsätzen (sogenannte „dendritic spines“).

Um diese Effekte in einem komplexeren System näher untersuchen zu können, entwickelten wir eine reproduzierbare Methode um akute Gehirnschnitte über längere Zeit kultivieren zu können. Mithilfe dieser Methode konnten wir die Veränderungen, die wir schon in der Primärkultur beobachteten, auch in diesem komplexen System (das näher an der *in vivo* Situation ist) nachweisen. Die Entwicklung der fokalen Schwellungen der Dendriten konnten mithilfe zweier Antagonisten des NMDA Rezeptors rückgängig gemacht werden, wodurch erstmals eine Verbindung der Effekte mit einer Aktivierung von Glutamatrezeptoren aufgezeigt wurde.

Die Verminderung der Anzahl dendritischer Dornfortsätze im Gehirnschnittmodell wurde untermauert von den Ergebnissen, die wir durch Gehirnschnitte von Mäusen, die tatsächlich an pneumokokkaler Meningitis erkrankt waren, erlangen konnten. Durch immunohistologische Färbungen mit einem Antikörper gegen Synapsin I (ein präsynaptisches Protein) konnten wir eine Reduktion dieses Proteins im Cortex erkrankter Mäuse nachweisen. Die Reduktion des Synapsin I Signals war höher bei den Mäusen, die mit Pneumokokken infiziert waren, die zur PLY Produktion befähigt waren, im Vergleich zu den Hirnschnitten der Mäuse, die ebenfalls an einer Meningitis, jedoch hervorgerufen durch eine Mutante von *Streptococcus pneumoniae* (unfähig, Pneumolysin zu exprimieren) litten.

Die Tatsache, dass die morphologischen Veränderungen der Dendriten ebenfalls in calciumfreiem Puffer beobachtet werden konnten, macht deutlich, dass nicht nur der Calciuminflux durch die Pneumolysinpore verantwortlich ist für dessen Neurotoxizität. Diese These wird untermauert durch die Ergebnisse, die wir mithilfe der Calciummikroskopie erhielten: Die Applikation eines Antagonisten des NMDA Rezeptors konnte den Zeitpunkt des maximalen Calciuminfluxes in die Zelle nach Behandlung mit Pneumolysin hinauszögern.

Zudem konnten wir die Schwellungen in den Dendriten auch durch einen Antikörper gegen MAP2 (ein neuronenspezifisches Protein des Zytoskeletts) darstellen, was ebenfalls eine Verbindung von Pneumolysin zu „excitotoxicity“ (Toxizität aufgrund einer Übererregung von Glutamatrezeptoren) darstellt, da verschiedene Studien die Aggregation von MAP2 in fokalen dendritischen Schwellungen als Reaktion auf die Einwirkung von „excitotoxischen“ Stimuli nachweisen konnten.

Zusammenfassend lässt sich sagen, dass dies die erste Studie ist, die Pneumolysin in Zusammenhang mit einer Überaktivierung von Glutamatrezeptoren bringt, was eine komplett neue Sichtweise darstellt und eventuell neue Möglichkeiten der Therapie für Patienten, die an dieser Form der bakteriellen Hirnhautentzündung leiden, eröffnet.

2 Introduction

2.1 *Streptococcus pneumoniae*

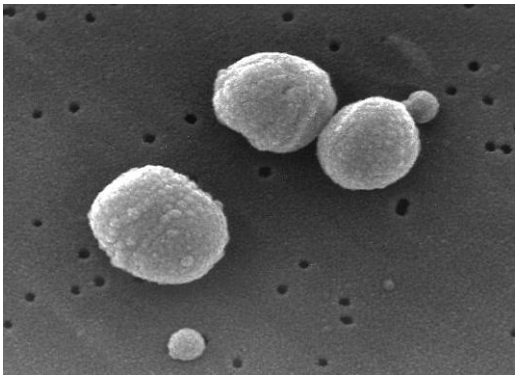

Figure 1: ***Streptococcus pneumoniae*** **(SEM)**

Scanning electron micrograph (SEM) of the pathogen. Gram-positive Pneumococci grow in pairs or short chains (source: http://phil.cdc.gov, picture provided by R. Facklam).

Streptococcus pneumoniae (see Figure 1) was isolated for the first time in 1881. Since then, it has been one of the most extensively studied microorganisms ever. Pneumococci belong to the family of gram-positive bacteria, and grow in pairs or short chains. The size ranges from 0,5 to 1,25 µm. The cocci are surrounded by a polysaccharide capsule. Because of their chemical structure, the capsule polysaccharides can be divided into different serotypes. Up to now, 90 different serotypes are known, which makes it difficult to develop a suitable vaccine against pneumococci. The pathogenicity of pneumocci has been attributed to various structures, most of which are located on its surface. However, the high morbidity and mortality caused by this microorganism are still poorly understood (AlonsoDeVelasco et al., 1995).

The most common forms of infections caused by *Streptococcus pneumoniae* include middle ear infections (acute otitis media), lung infections (pneumonia), blood stream infections (bacteremia) and meningitis.

The major ecological niche of *S. pneumoniae* is the nasopharynx. The carriage rate is highest in little children, mainly in their very early stages of life. The risk for nasopharyngeal carriage is higher in children less than 6 years of age, children with younger siblings and children with attendance in day

care centers. The risk factors for adults are mainly smoking, asthma and acute upper respiratory infections (Lynch and Zhanel, 2010). *S. pneumoniae* causes around 11 % of all deaths among children aged 1-59 months (O'Brien et al., 2009).

2.1.1 Virulence factors

Virulence factors enable microorganisms to establish themselves within a host and enhance their pathogenicity. *S. pneumoniae* produces several virulence factors which are involved in the illness process (see Table 1).

Table 1: Virulence factors of *Streptococcus pneumoniae*
(Mitchell and Mitchell, 2010)

Virulence factor	Main contribution to pathogenesis
Capsule	Antiphagocytic activity
Pneumolysin	Pore-formation in cell membranes Activation of complement pathway
LPXTG-anchored surface proteins (hyaluronidase, neuraminidase, etc.)	Breakdown of connective tissue Promotion of bacterial spreading Promotion of colonization
Pilus	Enhanced binding of pneumococci to cells Stimulation of cytokine production
Lipoproteins	Involved in iron uptake Enhanced adhesion of *S. pneumoniae*
Choline-binding proteins	Release of cell wall degradation products and pneumolysin Promotion of nasopharyngeal colonization Providing resistance to complement
Surface proteins without anchor motifs	Mediation of attachment to epithelial cells Facilitation of transmigration Reduced binding of complement to pneumococci
Gene and genome variation	Resistance to penicillin Adaption to changes in environment

One group of virulence factors, such as the capsule, provides resistance to phagocytosis and thus promotes the escape of pneumococci from the hosts´ immune defense. Other factors, including cell wall components and the intracellular toxin pneumolysin, are mainly involved in the inflammation caused by an infection. The inflammation process probably fully develops only after lysis of bacteria by autolysin, thereby releasing a number of virulence factors (AlonsoDeVelasco et al., 1995). From analysis of whole genome sequencing experiments, it is clear that different strains of pneumococci differ in their ability to produce virulence factors (Mitchell and Mitchell, 2010).

2.2 Bacterial meningitis caused by *Streptococcus pneumoniae*

Bacterial meningitis is an inflammation of the meninges in response to bacteria and bacterial products. It affects the pia mater, arachnoid and subarachnoid space.

The most common causes of bacterial meningitis nowadays are *Streptococcus pneumoniae* and *Neisseria meningitides,* because successful vaccination has virtually eliminated *Haemophilus influenzae* type b meningitis. However, mortality and morbidity vary by age and geographical location of the patient. Patients at high risk include newborns, those living in low-income countries, and immunocompromised people like HIV positives. Today, vaccination strategies have been employed with intent to reduce the incidence of pneumococcal meningitis (Brouwer et al., 2010).

2.2.1 Epidemiology

Invasive pneumococcal disease occurs, when the Pneumococcus reaches a normally sterile compartment like the brain. It most frequently affects children less than 2 years old and adults above 65 years of age.

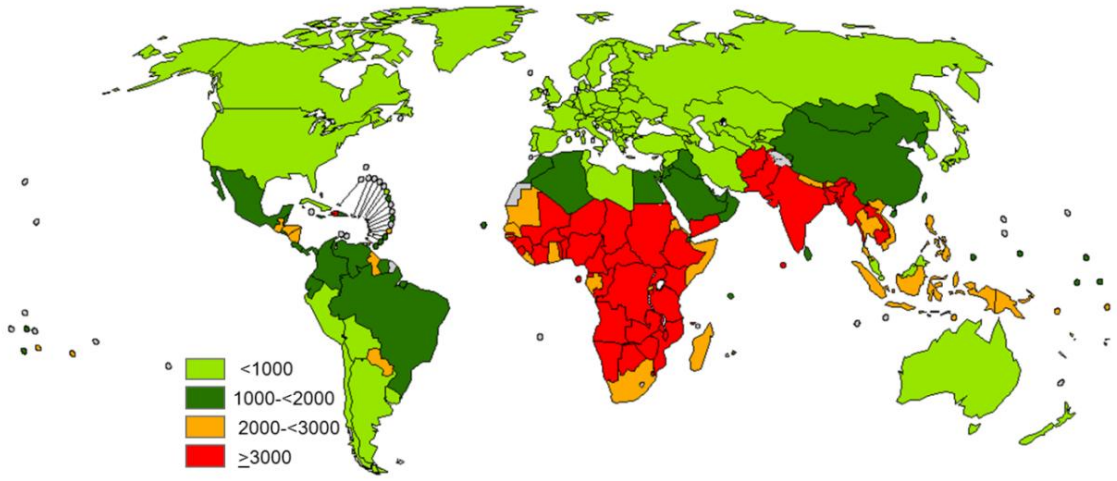

Figure 2: *Streptococcus pneumoniae* incidence rate

Incidence rate per 100,000 children under five years of age, 2000. Countries with resource poor settings are mainly affected by the disease (Data source: WHO, 2009).

The risk to suffer from an invasive pneumococcal infection is higher for children in developing countries, as they have less access to medical care, and laboratory support, as well as antibiotics are hardly available (Lynch and Zhanel, 2010).

In the developing world morbidity and mortality rates are dramatically higher than in industrialized countries (see Figure 2).

In countries with low medical standard, about 50 % of children with pneumococcal meningitis die while in hospital and up to 60 % of survivors suffer from clinical sequelae afterwards (Goetghebuer et al., 2000; Muhe and Klugman, 1999). Additional factors, such as HIV infection, malnutrition, and antibiotic-resistant bacteria, complicate the management of the infected patients (Scarborough and Thwaites, 2008). In comparison, mortality rates of this age group in industrialized countries are about 10 % and 30 %, respectively (Arditi et al., 1998; Kornelisse et al., 1995). In industrial countries, up to 60 % of survivors remain with neurological sequelae like seizures, hearing loss or impairment, cerebral palsy, learning and memory deficits and mental retardation. The most common sequelae is hearing loss. The risk of long-term disabling sequelae is highest in low-income countries, where the burden of bacterial meningitis is greatest (Edmond et al., 2010).

Despite on-going progress in antibiotic therapy and intensive care, the mortality rates, associated with invasive pneumococcal disease are among the highest for any major pathogen. Especially childhood pneumococcal meningitis remains a devastating disease (Chao et al., 2008). In 1999, the Global Alliance for Vaccines and Immunization (GAVI) was formed with the mission of ensuring that

every child in the world is protected against vaccine-preventable diseases. This alliance has been established to help developing countries to pay for new and underused vaccines and to improve their own current immunization services (see http://www.vaccinealliance.org) (Koedel et al., 2002).
Of particular concern for the clinical management of bacterial meningitis is the rising resistance to penicillin and other β-lactam antibiotics (Hoban et al., 2001).

2.2.2 Pathogenesis

The main reservoir for *Streptococcus pneumoniae* is the human nasopharynx. There, it normally leads to asymptomatic colonization. The carriage rates are highest among little children (up to 80 %). In the general adult population there is a carriage rate of only 4 % (Regev-Yochay et al., 2004). The bacterium gets transferred between people by coughing and sneezing. So, in crowded situations, such as they occur in hospitals, shelters and prisons, the carriage rate of adults can rise up to 40 % (Ihekweazu et al., 2010).
To colonize and invade the mucosa, bacteria have developed several virulence factors. The invasion requires prior adhesion of the pathogen to the endothelial cell surface. Previous studies showed that *S. pneumoniae* initially binds to carbohydrates displayed on epithelial cells, such as galactose beta 1-3 N-acetylgalactosamine (Gal(ß1-3)GalNAc) and sialic acid (Andersson et al., 1983).
Colonization of the nasopharynx is supported by further pneumococcal proteins such as the neuraminidase NanA and an IgA1 protease. NanA cleaves N-acetylneuraminic acid from mucin, glycolipids, glycoproteins and oligosaccharides and can thereby enhance colonization by decreasing the viscosity of the mucus or by exposing cell-surface receptors for the pneumococcus (Tong et al., 2000).
Also, pneumococci are able to counteract defense mechanisms of the hosts' immune system. The capsule promotes the colonization of the pneumococci and circumvents phagocytosis and activation of the complement system, thereby causing bacteremia, which means that bacteria have reached the blood stream (Gerber and Nau, 2010). The pneumococcal capsule represents an antigenic extracellular layer of polysaccharides, partly concealing the underlying bacterial cell surface from recognition by the immune system (Musher, 1992). Also, it has been shown that unencapsulated strains of *Streptococcus pneumoniae* are not able to cause invasive disease (Griffith, 1928).
After reaching the blood stream, blood circulation enables the bacteria to reach the blood-brain barrier, composed of specialized epithelial cells. Cerebral vascular endothelial cells differ from their systemic counterparts as they are tightly bound together by tight junctions. Also, they show low rates of pinocytosis as well as specific carrier and transport systems. In combination, these properties

restrict the non-specific transport of ions, proteins and pathogens into the brain. However, the pneumococcus manages to traverse the blood-brain barrier. Ring et al. showed that in human brain microvascular endothelial cell cultures, the pneumococci were able to adhere to the platelet-activating factor (PAF) receptor, enabling the pneumococcus to transmigrate through the endothelial cell to the basolateral site (Ring et al., 1998). Another possible mode of action is the disruption of the interepithelial tight junctions, enabling the pneumococcus to translocate into the CSF intercellularly (Quagliarello et al., 1986). However, it seems that the pneumococcus prefers to cross the blood-brain barrier by translocation through the cells rather than between them (Ring et al., 1998). Following the activation of the endothelial cell layer, the surface-expression of the PAF receptor is increased. This receptor binds phosphorylcholine of the pneumococcal cell wall (Cundell et al., 1995). The PAF receptor rapidly gets internalized after binding of a ligand. Accordingly, the pneumococcus seems to invade the endothelial cell in a vacuole together with the PAF receptor. Within the endothelial cell, the pathogen faces different fates including death within the vacuole and transmigration through the cell. Only transparent pneumococci seem to be able to transcytose through endothelial monolayers in a significant proportion (Ring et al., 1998).

The two morphological phenotypes of pneumococci are named opaque and transparent because of their appearance on transparent agar surfaces. The differences are the result of a process named phase variation. Phase variations are associated with differences in the expression of surface determinants that contribute to the ability of the pathogen to interact with the host. Transparent variants for example are more suited for colonization and invasion than opaque variants, whereas opaque variants show a better survival in the bloodstream. Once in the CSF, the pneumococcus is able to survive and replicate because immunoglobulin concentrations in the CSF are low and complement components are virtually absent. After reaching the stationary phase of replication (as well as in response to antibiotic treatment), autolysis of pneumococci leads to the release of several bacterial products (e.g. pneumolysin) that act as stimuli for the release of proinflammatory factors by the host. The early response cytokines IL-1, TNF-α, and IL-6 are produced shortly after pneumococcal recognition (van Furth et al., 1996). The release of these cytokines is the essential step in a cascade of evolving pathophysiologic alterations, including the recruitment of white blood cells into the CSF (Tauber and Sande, 1989).

Despite these early host defenses in the CSF, including recruitment of leucocytes, complement components, and immunoglobulins, they don’t seem to be very efficient in phagocytosis of *S. pneumoniae.* One reason for that is the lack of sufficient complement concentrations to achieve opsonic activity (Simberkoff et al., 1980; Stahel et al., 1997). Although the concentrations of IgG

increase during the course of bacterial meningitis, they also seem to remain below the concentrations which are required for an optimal opsonic activity (Smith and Bannister, 1973).

2.2.3 Diagnosis and Treatment

The survival of a patient suffering from invasive pneumococcal disease is dependent on rapid diagnosis and early treatment.

Pneumococcal diseases are basically treated with antibiotics. Since the resistance of bacteria towards antibiotics is rising, there is an urgent need to develop suitable vaccines to prevent infections. However, in some populations, resistance to antibiotics still remains a problem.

Another problem of antibiotic therapy is that killing the bacteria can lead to a massive release of biologically active bacterial products (like bacterial toxins and cell wall components) that potentiate inflammation and other pathophysiologic alterations (Tauber et al., 1987).

Over the past years, extensive research in the field of bacterial meningitis showed that neuronal damage after recovery of the disease is generally mediated by a severe inflammatory response of the host (Scheld et al., 2002). The hosts' immune system responds to bacterial toxins, cell wall components and cell lysis products, thereby perpetuating the inflammatory process. These findings led to new therapeutic approaches like the use of non-bacteriolytic antibiotics and the suppression of inflammation. For this purpose, corticosteroids like dexamethasone seemed to be the best choice as adjunctive anti-inflammatory treatment (Koedel et al., 2010).

Dexamethasone acts as an anti-inflammatory and immunosuppressive agent. It is recommended for adjunctive therapy of pneumococcal meningitis, as it reduces many of the pathophysiologic consequences of the disease. It down-modulates also many of the events that follow the initiation of antibiotic therapy (Tauber et al., 1985). However, a metaanalysis of 5 large recent trials of adjunctive dexamethasone, including more than 2000 participants, showed no effect of dexamethasone concerning the reduction in mortality and only slight effects in the reduction of hearing loss among the survivors (van de Beek et al., 2010).

Although some benefit of adjunctive dexamethasone therapy might be confined to patients with pneumococcal meningitis in high-income countries (McIntyre, 2010), in areas of the world where access to quality care is limited, the use of pneumococcal vaccine is particularly necessary to limit disease and save lives.

At present, strategies to prevent and treat bacterial meningitis are constrained by an incomplete understanding of the pathogenesis. Therefore, further research on meningitis pathogenesis is needed (Kim, 2010).

2.3 Pneumolysin

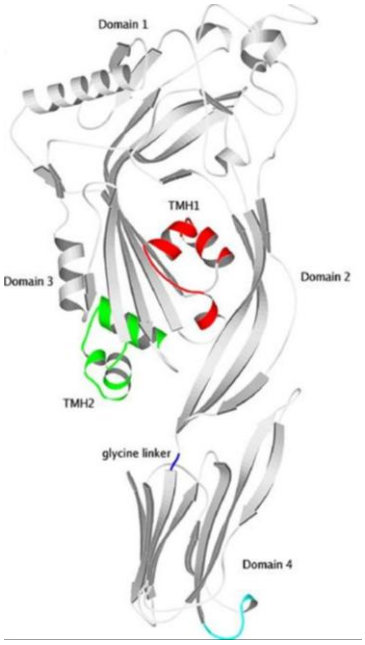

Figure 3: Proposed protein structure of PLY

The configuration of the toxin monomer is fitted to perfringolysin O. Pneumolysin is arranged in four structural domains. Domain 1 serves as a scaffold, domain 2 plays a role in the transformation process from prepore to the final pore, domain 3 is responsible for the penetration of the membrane and domain 4 is essential for the binding of the toxin to membrane cholesterol (Rossjohn et al., 2007).

Pneumolysin (PLY, see Figure 3) is one of the major virulence determinants of *Streptococcus pneumoniae.* PLY is a 53 kDa protein which belongs to a large family of highly homologous bacterial toxins; the so-called cholesterol-dependent cytolysins (CDCs). The activity of all family members takes place at membranes, but the proteins themselves are involved in diverse phenomena. The CDCs for example also include human proteins, like perforin and the membrane attack complex. PLY is expressed by almost all clinical isolates of *S. pneumoniae* during the late log phase of growth. It is located in the cytoplasm of the bacteria and mainly gets released when the pneumococci undergo autolysis (Paton, 1996). However, more recent studies show that *Streptococcus pneumoniae* also can release PLY independently of autolysis mediated by autolysin (Balachandran et al., 2001).

Pneumolysin is composed of 471 amino acids, arranged in four structural domains. The main effects of PLY on the host are mediated by two modes of action: the binding to the cell membrane, followed by pore formation, and the activation of the complement pathway in a non-immunospecific manner through direct interaction with the IgG domain F_c (Mitchell et al., 1991; Rossjohn et al., 1998).

The attachment of pneumolysin to the cell membrane is dependent on the cholesterol in the membrane. The binding to cholesterol is rapid, dependent on the pH but independent of temperature (Johnson et al., 1980). In 2004, Nollmann et al. showed that the haemolytic activity of pneumolysin could be anticipated by cholesterol and that the stoichiometry of the cholesterol-PLY complex is 1:1 (Nollmann et al., 2004).

Up to now, there is no model of the pneumolysin molecule in solution available, just low-resolution images from electron microscopy (Gilbert et al., 1998; Morgan et al., 1995). Pneumolysin shows high homology to perfringolysin O (PFO, a protein toxin produced by *clostridium perfringens*) as it has almost the same molecular mass and shares 48 % sequence identity with PFO. Therefore it has been possible to build a model for PLY, based on the homology with perfringolysin O, for which an atomic structure has been established (Solovyova et al., 2004).

2.3.1 Contribution of PLY to the virulence of *S. pneumoniae*

Pneumolysin plays a crucial role in the pathogenesis of pneumococcal meningitis, as mutant strains of *S. pneumoniae* which do not express pneumolysin, showed reduced virulence in a rat model of meningitis (Hirst et al., 2008; Reiss et al., 2011).

Using a microvascular endothelial cell culture model, it has been shown that pneumococci expressing pneumolysin were able to traverse the endothelial cells, whereas mutant pneumococci deficient in pneumolysin were unable to penetrate the cell barrier (Zysk et al., 2001). In 2000, Hirst et al. have shown that pneumolysin is toxic to ciliated ependymal cells, and that PLY inhibits ependymal ciliary beat frequency (Hirst et al., 2000a; Hirst et al., 2000b). There are several other biological effects of pneumolysin, like the lysis of red blood cells, the increase of alveolar permeability in rat lung, the inhibition of mitogen induced proliferation and antibody production by human lymphocytes as well as electrophysiological and histological damage after perfusion into the cochlea of guinea pigs (Mitchell and Andrew, 1997).

A major activity of pneumolysin is activation of complement via the classical pathway in absence of specific antibody (Paton et al., 1984). Additionally, it has been shown that pneumolysin is thereby able to decrease the opsonization of pneumococci (Yuste et al., 2005). Domain 4 of the protein toxin shows a structure similarity to the Fc portion of immunoglobulin (Gilbert et al., 1998). The ability of PLY to activate the complement pathway is probably due to nonspecific binding of the Fc portion of IgG by the toxin (Mitchell and Andrew, 1997).

Despite all these dramatic effects of pneumolysin, it is also able to induce mild damage to cells. It has been shown, that pneumolysin, in sub-lytic concentrations, leads to a phosphorylation of p38 MAPK

in epithelial cells. That seems to be a conserved response of epithelial cells to sub-lytic concentrations of bacterial pore-forming toxins, thereby acting as an early warning system to initiate an immune response while the local density of toxin-producing bacteria is still low (Ratner et al., 2006).

2.3.2 Pore formation process

For the pore formation process of CDCs, two mechanisms have been proposed. One suggests that the toxin inserts into the bilayer in its monomeric form, then assembles into oligomers and forms a pore (Morgan et al., 1994). According to the second, most favored theory, the toxin binds to the lipid bilayer, oligomerizes to form a pre-pore, which then inserts into the cell membrane (Tilley et al., 2005).

By studies of Gilbert et al. and Tilley at al., structures for the prepore complex, as well as for a fully inserted membrane pore have been introduced (Gilbert et al., 1999b; Tilley et al., 2005). By applying the structural findings of perfringolysin O to these structural findings of the pore complexes, the different conformational changes of the proteins during pore-formation have been proposed.

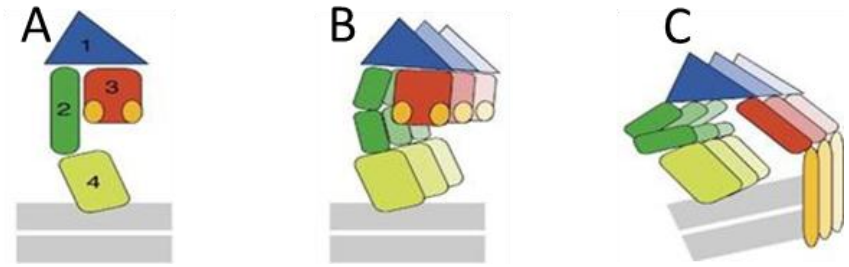

Figure 4: Pore formation process of pneumolysin

The pore forming process by pneumolysin takes place in several steps. Firstly, domain 4 binds to membrane cholesterol (A). By rising concentrations of pneumolysin, the toxin monomers assemble and oligomerize (B). By conformational changes, the α-helices in domain 3 transform into ß-hairpins, which then poke into the membrane, leading to the final pore (C) (Walz, 2005).

It has been shown, that the C terminal domain (domain 4) of pneumolysin is critical for the binding to cholesterol in cell membranes (Owen et al., 1994). The most conserved region in the cholesterol-binding sequence is the tryptophan (Trp) rich loop at the base of domain 4. This loop is responsible for entering the membrane (Gilbert et al., 1999), as the modification of the single cysteine in this Trp rich loop prevents PLY from binding to lipid bilayers (Gilbert et al., 1999a). It has been shown, that

direct binding of domain 4 of pneumolysin to membrane cholesterol is an essential step to exert lytic activity (Baba et al., 2001). Domain 1 serves as a scaffold, stabilizing the protein structure and allowing the other domains to rearrange around. When the concentration of pneumolysin rises, the monomers begin to assemble into oligomers, which needs the help of domains 1 and 3. The oligomerization process leads to a change in the orientation of domains 2 and 4 towards each other, thereby bending domain 2, leading to a loss of contact between domains 2 and 3. When domain 2 is completely detached from domain 3, the transformation from the prepore state to the final pore takes place (see Figure 4). Therefore, domain 3 moves towards the inner surface of the developing prepore complex. By this conformational change, the α-helices in domain 3 transform into ß-hairpins. A final bending of domain 2 moves domain 3 closer to the membrane leads to a poking of the ß-hairpins into the membrane, thereby forming the final pore (Gilbert et al., 1999b; Shatursky et al., 1999; Tilley et al., 2005).

2.1 Cellular components of nervous tissue

2.1.1 Neurons

Neurons (see Figure 5) are the basic working units of the brain. During their development, they emerge a highly polarized morphology which enables them to quickly transmit information to other nerve cells, muscle or gland cells. The brain contains between 1 billion and 100 billion neurons, depending on the species.

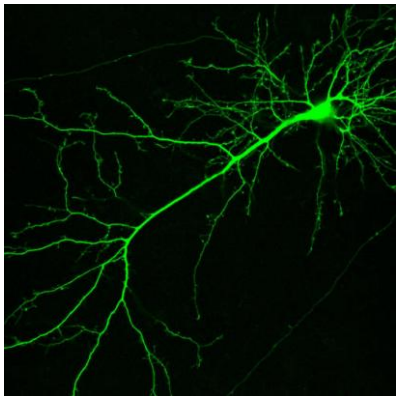

Figure 5: Neuron

Neurons are highly specialized cells. During development, they alter their morphology to become highly polarized cells, enabling them to quickly transmit information.

Morphologically, the neuron is divided into three major regions: a cell body (perikaryon), containing the nucleus and most organelles; dendrites, emerging from the neuronal cell body and a single excitable axon, which extends from the perikaryon and often splits up into smaller branches before ending at nerve terminals.

Many axons in the brain are covered with an insulating myelin sheath composed of oligodendrocytes, enabling the axon to spread the electric signal very fast along. In the peripheral nervous system, this sheath is made of Schwann cells.

Neurons send signals by transmitting electrical impulses along their axons. The electric signal is created by a difference in charge between the inner and the outer side of the cell membrane. This transmembrane potential difference is generated by the opening and closing of ion channels, which regulate the flow of ions through the membrane. The flow of these ions creates an electrical current that produces small voltage changes across the neuron´s cell membrane.

A nerve pulse arises, when a reversal in the membrane potential occurs at one point of the cell membrane. Then, the neuron´s internal negative charge switches to a positive charge state. This change is called action potential. The action potential then spreads along the axon at high speed. Axons contain several unmyelinated patches, the so-called nodes of Ranvier. These spots boost the signal by propagating the signal from one to another (saltatory conduction). In this way, neurons are able to fire impulses multiple times every second.

By reaching the end of the axon, the signal triggers the release of neurotransmitters into the synaptic cleft. Neurotransmitters are the chemical messengers of the brain. After getting released into the synaptic cleft, these transmitters diffuse across the intrasynaptic space, reaching the postsynaptic membrane, where they bind to specific receptor molecules on the surfaces of adjacent cells (other neurons, muscle or gland cells). The so-called dendritic spines resemble the postsynapses, where neurons receive input from the axons of other neurons. The receptor molecules on the postsynaptic membrane act as on-and-off switches for the next cell. Each receptor has a region that selectively recognizes a particular neurotransmitter. When the transmitter is connected to its receptor, this interaction alters the target cell's membrane potential and subsequent depolarization of this target cell leads to a further propagation of the signal. Increased understanding of neurotransmitters and signaling in the brain and the understanding how drugs can modulate these processes guides one of the largest fields in neuroscience (Squire, 2008).

2.1.2 Neuroglia

1859 introduced by Rudolph Virchow, the term neuroglia describes the connective tissue in the brain. There are 4 different types of neuroglia cells in the CNS of vertebrates: oligodendrocytes, astrocytes, microglia and ependymal cells.

Astrocytes, as one major subtype of glial cells, appear in many shapes and forms, although they are mostly star-shaped. They represent up to 50 % of the cells in the brain. Astrocytes are connected to each other via gap junctions. They strengthen the blood-brain barrier by inducing and maintaining the tight junctions between the epithelial cells which form the barrier. These highly specialized cells are the main reservoir for extracellular matrix proteins and adhesion molecules in the CNS (e.g. laminin and fibronectin). They also produce a large number of growth factors and cytokines, thereby contributing to the developmental function and regenerative capacity of the brain (Squire, 2008). Although for a long time they seemed to be only connective tissue in the brain ("brain glue"), research in the past years revealed they contribute to a lot of important functions in the brain. For example, it has been shown that astrocytes play eminent roles in neuronal signaling and in several diseases of the brain. They have been ignored in science for a long time, because their mode of action is more subtle and in an indirect manner (Ransom et al., 2003). Astrocytes are generally considered as nonexcitable cells. However, recent studies showed that astrocytes interact with neurons via calcium signaling (Nag, 2011). It has also been shown, that astrocytes can release glutamate themselves in response to elevated intracellular calcium levels (Parpura et al., 1994).

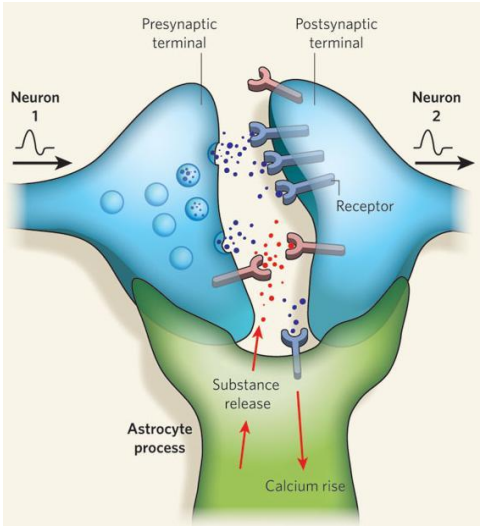

Figure 6: Schematic of the tripartite synapse

The latest model of synapses involves astrocytes in the complex mechanism of synaptic transmission. They ensheath prae- and postsynapse, thereby supporting the whole process of neuronal signaling (Allen and Barres, 2009).

This bidirectional communication between astrocytes and neurons is a quite recent topic in synapse research and has led to the term "tripartite synapse" which means the involvement of presynaptic neurons, postsynaptic neurons and astrocytes in synaptic transmission (see Figure 6), not only the involvement of two neurons, as it has been believed for a long time. The appearance of astrocytes at synapses enables them to monitor and to respond to synaptic activity (Allen and Barres, 2009).

2.1.3 The glutamate-glutamine cycle

One of the most important functions of astrocytes in the brain is the uptake of the neurotransmitter glutamate secreted by neurons and its recycling back into neurons. This process is termed glutamate-glutamine cycle (see Figure 7). Thereby it is ensured, that the balance of glutamate in the CNS is stable.

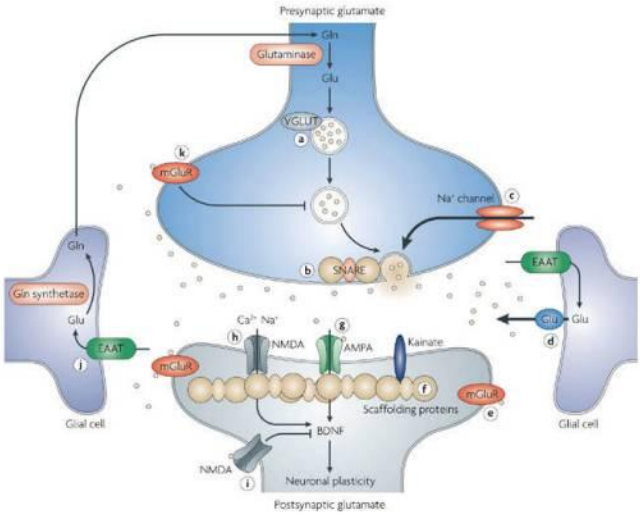

Figure 7: The glutamate-glutamine cycle

To ensure a balance of glutamate concentration in the brain, astrocytes take up the released glutamate, convert it into glutamine which is then taken up by neurons, which can then convert it back into glutamate (Sanacora et al., 2008).

Neurons are not able of a *de novo* synthesis of the neurotransmitter glutamate. Also, the blood-brain barrier bans serum glutamate from entering the CNS, and as a consequence, all brain glutamate has to be synthesized within the brain itself. So, neurons depend on astrocytes, which release glutamine as a precursor of glutamate (Bak et al., 2006).

After the release of glutamate through neuronal signaling, the ensheathing astrocytes (as a part of the tripartite synapse, see chapter 2.1.2) eliminate glutamate from the synaptic cleft by excitatory amino acid transporters (EAATs). Afterwards, glutamate reacts with ammonia to form glutamine through the activity of glutamine synthetase (a cytosolic, ATP-dependent enzyme, which is not expresses by neurons). This reaction is also important because of the fact that it detoxificates free ammonia. Glutamine then is secreted into the extracellular fluid. The release of glutamine into the synaptic cleft is uncomplicated, as glutamine has no transmitter activity. In neurons, glutamine is converted back into glutamate by the phosphate-activated mitochondrial enzyme glutaminase or by transamination of 2-oxoglutarate, an intermediate in the citric acid cycle (Hertz et al., 1999).

Synaptic glutamate is accumulated in vesicles. Each vesicle contains approximately 1200 molecules of glutamate. The accumulation of the transmitter is caused by specialized proteins in the vesicular membrane, the vesicular glutamate transporters (VGLUTs). After release of the vesicles, the cycle restarts. At GABAergic synapses, the cycle is called GABA-glutamine cycle, respectively (Siegel, 2006).

Interestingly, astrocytes also express a lot of the neurotransmitter receptors appearing on the cell membranes of neurons. Release of transmitters by neurons therefore leads to an intracellular calcium rise in astrocytes, triggering the release of several neuroactive compounds, thereby signaling back to the neurons. This interaction either leads to an enhancement or an inhibition of neuronal activity. Additionally, these highly specialized cells are able to communicate with each other through calcium waves (Allen and Barres, 2009). Quite recent experiments showed that human astrocytes also express NMDA receptors (Lee et al., 2010).

2.2 Excitotoxicity

Over the past several years, research has demonstrated that excitatory amino acids serve as the major excitatory neurotransmitters in the cerebral cortex and hippocampus. Neurons that contain excitatory amino acids play crucial roles in psychological functions such as learning and memory (Dong et al., 2009).

The term “glutamate excitotoxicity” was introduced by Olney, who described intracranial brain lesions in response to subcutaneous injections of glutamate in infant and adult mice (Olney, 1969).

Excitotoxicity is defined as cell death resulting from the toxic actions of excitatory amino acids. Because glutamate is the major excitatory neurotransmitter in the mammalian central nervous system, neuronal excitotoxicity usually refers to the injury and death of neurons arising from prolonged exposure to glutamate and the associated excessive influx of ions into the cell. The resulting calcium overload is particularly neurotoxic, leading to the activation of enzymes that degrade proteins, membranes and nucleic acids. For instance, Ca^{2+} -activated proteolytic enzymes (e.g. calpains) can destroy essential proteins. High intracellular calcium levels also activate the Ca^{2+}/calmodulin kinase II (CaMKII), leading to a phosphorylation of several enzymes, thereby increasing their activity (Berliocchi et al., 2005).

Overactivation of glutamate receptors impairs cellular calcium homeostasis and activates nitric oxide synthesis, generation of free radicals and programmed cell death (Sims and Zaidan, 1995).

Acute CNS insults such as ischaemia and traumatic brain injury have traditionally been the focus of excitotoxicity research. However, glutamate excitotoxicity has also been linked to chronic neurodegenerative disorders such as amyotrophic lateral sclerosis, multiple sclerosis, Parkinson’s disease and others. Despite the continued research into the mechanisms of excitotoxicity, there are currently no pharmacological interventions capable of providing significant neuroprotection in the clinical setting of brain ischaemia or injury (Lau and Tymianski, 2010).

The mechanisms underlying glutamate excitotoxicity are complex. However, especially in the acute pathologies, glutamate excitotoxicity is not a result of a genetic mutation or structural deficit in the channel. Instead, glutamate excitotoxicity can be thought of as a normal physiological response to a CNS insult. Chronic over-excitation of neurons elicited by glutamate is a newer concept that has linked glutamate excitoxicity to neurodegenerative processes in ALS, Huntington's disease, Parkinson's disease and Alzheimer's dementia (Lau and Tymianski, 2010).

2.2.1 Glutamate receptors

Glutamate receptors are mainly synaptic receptors, distributed throughout the central nervous system. They are divided into two classes: ligand gated ion channels (ionotropic receptors; iGluRs) and G-protein coupled channels (metabotropic receptors; mGluRs). The class of ionotropic glutamate receptors is composed of NMDA-, AMPA-, and kainate receptors, whereas the metabotropic glutamate receptor family includes 8 different receptors (mGluR1-8). Glutamate receptors are involved in neuronal communication, memory and learning processes. Furthermore, they play a role in the pathogenesis of some neurodegenerative disorders, like dementia and Alzheimer´s disease.

2.2.1.1 NMDA receptors

Of all the glutamate receptors known up to now, the N-methyl-D-aspartate receptor (NMDAR) is the most studied. It belongs to the group of ionotropic glutamate receptors. N-methyl-D-aspartate is the name of the compound that selectively activates the NMDAR. NMDARs are cation-channels that are highly permeable to calcium ions. They are involved in multiple brain activities, like learning and memory, as they are essential for the regulation of synaptogenesis and long-term plasticity changes in synaptic strength. The stimulation of NMDARs may be beneficial, but excessive stimulation, followed by rising intracellular calcium concentrations, causes the activation of intracellular pathways leading to both physiological (e.g. learning and memory) and pathological processes (e.g. excitotoxic injury) (Benarroch, 2011).

NMDARs are large heteromeric complexes composed of four homologous subunits derived from three related families: NR1-3. According to the current proposed nomenclature, these subunits are termed GluN1, GluN2, and GluN3, respectively. Because of these manifold possibilities of NMDA receptor composition, NMDARs exist as diverse subtypes with distinctive patterns of expression (Paoletti, 2011). The NMDAR exhibits a complex gating mechanism, requiring not only binding of various ligands but also cellular depolarization. The depolarization is necessary to remove a magnesium ion from inside the channel which normally blocks the NMDA receptor (Lau and

Tymianski, 2010). When activated, the NMDAR allows the influx of cations, though most notably calcium. Because of their involvement in several neurological disorders like Alzheimer´s and Parkinson´s disease, NMDARs are of course also targets of therapeutic interest. The development of drugs to block or stimulate NMDA receptors to treat neurological and psychiatric disorders is of particular interest.

2.2.2 Inhibitors

Since the association of glutamate excitotoxicity with several neurological diseases, various attempts have been made to attenuate neuronal damage by glutamate receptor function. The NMDAR itself has a number of sites to manipulate pharmacologically, including the ion channel pore, the glutamate-binding site, the glycine-binding site and the polyamine interaction site. Antagonists of the NMDA subclass of glutamate receptors may offer new approaches for the prevention and treatment of ischemic brain injury. This strategy is supported by encouraging results in a variety of *in vivo* and *in vitro* experimental models (Albers et al., 1989).

2.2.2.1 MK-801

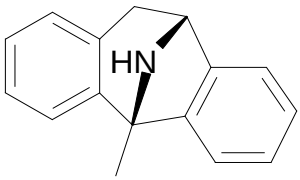

Figure 8: Chemical structure of MK-801

MK-801 is a potent inhibitor of NMDA receptors.

(+)-5-methyl-10,11-dihydro-5H-dibenzo[a,d]cyclohepten-5,10-iminemaleate (dizocilpine; MK-801, see Figure 8) originally had been invented as an anticonvulsant. Later studies using a cortical slice preparation revealed that MK-801 is a potent, non-competitive antagonist of N-methyl-D-aspartate (NMDA)-induced depolarization. In these experiments, MK-801 was able to block responses to NMDA and quinolinic acid but had no effect on responses produced by kainic acid or quisqualic acid. Another effect of the compound was, that MK-801, parenteral administered, showed neuroprotective effects. It also caused complete protection against loss of neurons produced by

injection of neurotoxic doses of NMDA or quinolinic acid into the striatum or hippocampus (Woodruff et al., 1987).

However, dizocilpine was not approved for human use, for it had cardiovascular side effects and in behavioral studies using a variety of species, including rhesus monkeys, appeared to have the same psychotomimetic properties as phencyclidine (PCP; “angel dust”) (Koek et al., 1988). MK-801 blocks the NMDAR at the level of the channel pore, thereby reducing calcium entry.

2.2.2.2 AP5

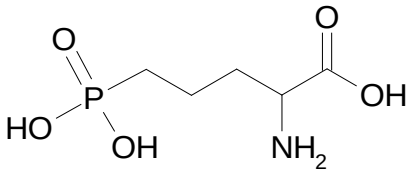

Figure 9: Chemical structure of AP5

AP5 serves as a competitive NMDA receptor antagonist.

AP5 (2-amino-5-phosphonopentanoic acid, see Figure 9), in contrast to MK-801, is a competitive NMDA receptor antagonist. It selectively blocks the NMDA receptor by binding to the same site glutamate is binding. AP5 can block depolarization induced by NMDA but is ineffective against kainate and quisqualate-induced depolarization. This NMDAR antagonist blocks the induction of sustained depolarization by high-frequency stimulation as well as the propagation of epileptiform discharges in hippocampal slices (Herron et al., 1986). AP5 is able to block hippocampal long-term potentiation (LTP) *in vivo*, without effecting normal synaptic transmission (Morris, 1989).

3 Methods

3.1 Pneumolysin expression and purification

Pneumolysin and mutants were kindly provided by Prof. Timothy Mitchell, Institute of Infection, Immunity and Inflammation, University of Glasgow.

PLY was prepared as follows. The toxin was expressed in E.coli XL-1 cells and purified by hydrophobic interaction chromatography as described in Mitchell et al., 1989. The lipopolysaccharide (LPS) content of purified toxin was determined by using the Limulus Amebocyte Lysate Kinetic-QCL Kit. All purified proteins had <0.6 endotoxin units/µg of protein. The purified wild-type toxin had an activity ≈5 x 104 hemolytic units/mg. One hemolytic unit was defined as the minimum amount of toxin needed to lyse 90 % of 1.5 x 108 human erythrocytes per ml within 1 h at 37 °C. The non-toxic delta6 version of the plasmid was constructed by site-directed mutagenesis (Mitchell et al., 1989).

3.2 Cell culture

All animal experiments were performed according to the regulations of the German Protection Law with approval from the Government of Lower Franconia, Bavaria, Germany.

3.2.1 Primary neuronal culture

To obtain optimal growth of the cells on the cell culture slides/dishes, they have to be coated prior to the seeding of the cells. Therefore, the dishes and slides get incubated overnight with a solution of Poly-L-ornithine (PLO) in an incubator at 37 °C. To prepare a culture of primary hippocampal cells, we used C57BL/6 mice at day 13 of gestation (E 13).

Firstly, the mother C57BL/6 mouse is killed by vertebral dislocation. Then, the abdomen skin is cut in the sagittal line without opening the peritoneum. After administering alcohol all over, the peritoneum is cut, the uterus bicornus gets extracted and the vessels are cut by scissors. The embryonic sacs get instantly transferred into a sterile petri dish, filled with chilled PBS on ice. The embryonic sacs are then cut in the area opposite to the placenta; thereby the embryos easily drop out. The heads are cut off and immediately transferred into another petri dish, filled with PBS on ice. While fixing the skull with sharp forceps through the eyes, the heads are cut in the midline, using micro scissors. The skin and the lamina are pushed aside with sharp forceps. Pushing from beneath the brain with a small spoon, the brain can easily be pulled outside the skull. The brains immediately

get placed in chilled, sterile PBS on ice. Firstly, the cerebellum and brain stem have to be removed. Secondly, the brain is cut in two halves. By using forceps, the meninges can be removed from the cortex with caution.

From each hemisphere, the hippocampus gets removed by cutting the hemispheres from beneath. The hippocampi are then collected in 7 ml chilled PBS in a 15 ml falcon tube. By pipetting up and down several times, the cells get dispersed. The cell suspension then is centrifuged at 4 °C and 1500 rpm for 5 minutes. After removal of the PBS, the cells get resuspended in cell cuture medium (Basal Medium Eagle (BME), supplemented with 1 % FCS, 1 % Glucose, 1 % Penicillin/Streptomycin and 2 % B-27). Prior to seeding, the vital cells get counted by placing 20 µl cell suspension, diluted 1:1 with a 0,4 % solution of trypan blue in a Neubauer cell counter under a stereomicroscope.

The cell suspension is adjusted to 150.000 vital cells per ml and seeded in cover slip bottom chamber slides (1 ml cell suspension per chamber) for live cell imaging and in permanox chamber slides for immunocytochemistry.

After a few days without changing the medium, the cells begin to interconnect and establish synapses. Two weeks after seeding, the neurons build up a network with a lot of established synapses. Then, they are ready for experiments.

3.2.2 Primary astrocytic culture

As culture medium for primary astrocytes, we use Dulbecco's Modified Eagle Medium (DMEM) GlutaMax high glucose, supplemented with 10 % fetal calf serum (FCS) and 1 % penicillin/streptomycin).

The astrocytes are prepared from C57BL/6 mice at postnatal day 6 to 7 (PD 6-7). The pubs get killed by decapitation. After distribution of alcohol all over the skull, the skin is removed from the cranium and kept aside. The skull gets cut along the middle line with small scissors. The brain is then removed by using a small spoon, pushing from beneath. After chopping off the cerebellum, the meninges get removed. The brains are cut in two halves and collected in chilled PBS in a small falcon tube (15 ml) on ice. By pipetting up and down, the tissue gets disrupted. The brain suspension is then centrifuged at 4 °C and 1600 rpm for 5 minutes. The PBS gets replaced by culture medium and the cells are resuspended by several times of pipetting up and down. Per 75 cm^2 culture flask, 2 brains are sufficient. The cells are seeded onto culture flasks which were previously coated with PLO (see 3.2.1). The cells grow in monolayer. To obtain optimal growth, the medium is replaced by fresh medium every two days.

For seeding, the cells get washed once with PBS before getting trypsinated by adding 2 ml of 0.05 % EDTA Trypsin into a cell culture flask with astrocytes. After 10 - 12 minutes incubation at 37 °C, 5 % CO_2 and 95 % humidity, the trypsin is inactivated by adding 8 ml fresh culture medium. The cells can be harvested by flushing them several times with medium. Afterwards, they get collected in a 15 ml falcon tube on ice. After a centrifugation step (4 °C and 1600 rpm for 5 minutes), the medium is replaced by fresh medium and the cell pellet can be resuspended by several times of pipetting up and down. The cells are then seeded at a density of 200 000 cells/ml.

3.3 Brain slice culture

3.3.1 Theory

The advantages of brain slices over primary culture are multiple: Brain slices remain the tissue architecture of the brain regions they are generated from. Also, they represent a high similarity to the *in vivo* situation, as the neuronal activities and circuits remain functional in the tissue context.
Organotypic slice cultures are typically prepared from mice at postnatal days 3-9. At this age, they have a high degree of plasticity and resistance to mechanical trauma during the slice preparation. Also, basic synaptic connections have been established, particularly in the CA1 area of the hippocampus; but mature synapses have not yet been established in the brain. They usually develop during the following 2-3 weeks *in vivo* (Cho et al., 2007).
For experiments, we used mice at PD 6-7 and PD 14-15, to compare toxin effects between different stages of development.

3.3.2 Preparation

For the preparation of acute brain slices, the mouse gets killed by decapitation. After administering some ethanol, the brain is removed by cutting the scalp with small scissors. The soft skull then gets opened with scissors. Afterwards, the cranial plates are removed by small forceps. Then the whole brain gets detached by pushing from beneath with a small spoon. After transferring the brain into chilled PBS on ice, the cerebellum is cut off by a scalpel. The cerebrum is placed on top of a specimen holder and gets stuck there by adhesive bonding. The specimen holder is then positioned in a cooled container filled with chilled and carbogenated artificial cerebrospinal fluid (ACSF). During the whole cutting process, the ACSF is constantly gassed with carbogen. The brain gets sliced up by coronal

sectioning with a vibratome, starting from a position 5 mm rostral from the olfactory bulb up to 9 mm, cutting the brain into 300 µm thick slices.

Prior to incubation with toxin, the slices are allowed to adapt at 37 °C for 30 minutes in carbogenated BME, supplemented with 1 % glucose and 1 % penicillin/streptomycin. Subsequently to toxin challenge, the brain slices get fixed in a 37 °C preheated solution of paraformaldehyde (PFA).

3.4 Transfection of primary neurons

To investigate single neurons by live cell fluorescence imaging approaches, it is inevitable to use a transfection method which shows low toxicity and long-lasting protein expression. As neurons (especially in culture) are sensitive to cytotoxicity and difficult to transfect with most methods, we used the Magnetofection™ approach for gene transfer. This method is cost-effective, easy to perform and does not require the preparation of complex constructs, such as viruses, which are known to be widely used for gene delivery into neurons (Buerli et al., 2007)

3.4.1 Theory

Transfection is a method to integrate DNA into eukaryotic cells. There are several methods for transfection existent. The principle of Magnetofection™ is to attach the DNA of interest to magnetic nanoparticles coated with cationic molecules.

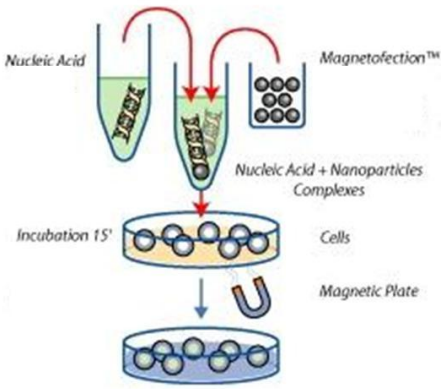

Figure 10: Principle of Magnetofection™

With the help of this method, the DNA of interest gets attached to magnetic beads. During incubation on top of a magnetic plate, the DNA gets transfected into the cell by magnetic force.

The DNA couples to the magnetic beads by salt-induced colloidal aggregation and electrostatic interaction. The magnetic beads then directly get applied onto the cells. By putting the culture plates on top of a magnetic plate, the beads (with the DNA attached on their surface) get traversed through the cells by magnetic force, leaving the DNA in the cytoplasm of the cells (Scherer et al., 2002).
The method is very mild towards the cells, which makes it a suitable application for the vulnerable primary neurons. The membranes of the transfected cells stay intact which represents an advantage over other physical transfection methods. Another advantage is that per each well, just a few cells get transfected. As the transfected gene in our case encodes the green fluorescent protein (GFP), it is possible to observe single neurons in a high magnification to follow how they change under several conditions.

3.4.2 Procedure

For live cell imaging, the cells are seeded onto chambered coverglass slides in a concentration of 150 000 cells/chamber.
At DIV (days *in vitro*) 10-12, the cells are dense enough and ready for transfection. First of all, the NeuroMag^{TM} reagent has to be vortexed. Per 1 µg DNA (Plasmid: pSyn-NGFP) 1 µl transfection reagent is sufficient. The transfection solution is prepared as follows. For each slide (4 chambers) to be transfected, 100 µl BME medium without serum is placed in a small vial. Then 4 µg (1 µg per chamber) of plasmid DNA is added, before adding the NeuroMag^{TM} reagent. All is mixed by vigorous pipetting and incubated at room temperature for 20 minutes. Afterwards, the mixture is filled up to 400 µl with BME medium, briefly vortexed and 100 µl per chamber is added to the cells. The slide is then placed on top of the magnetic plate during 15 minutes. After removing the plate, the cells are cultivated at 37 °C in a CO_2 incubator until evaluation of GFP expression, which takes approximately 24 hours.
Prior to observation, medium gets exchanged by a clear live cell imaging buffer, to avoid disturbances of fluorescence by phenol red. The microscope is improved by a heating chamber and a heating plate to remain temperature at stable 37 °C.
In each chamber, one transfected (thereby glowing in a light, green manner), healthy neuron is selected for observation.

3.4.2.1 Multiplication of the plasmid

To replicate the plasmid DNA, *Escherichia coli* DH5α cells were used for transformation. This *E. coli* strain represents a chemically competent bacterial strain, which means, the cells are able to take up naked DNA by a heat shock.

The cells get thawed on ice for about 15 minutes. After agitating with caution, 50 ng plasmid DNA per approach is used and mixed with the cells carefully. The cells are then incubated for 30 minutes on ice. To transverse the DNA into the cells, they get a heat shock at 42 °C for 1,5 minutes in a water bath. After putting the cells on ice for another 1,5 minutes, 900 µl LB (Lysogeny broth) medium per approach is added. For 1 h, the cells are then mixed at 37 °C and 400 rpm in a thermomixer. The cells afterwards get centrifuged at 4 °C and 6 000 rpm for 3 minutes. 800 µl of the supernatant gets discharged, the rest is resuspended. The cells (100 µl cell suspension) then are plated onto ampicillin containing agar plates, because the plasmid features an ampicillin resistance gene. Thus it is ensured, that only bacteria which incorporated the plasmid grow on the agar plates. For optimal growth, the plates are kept at 37 °C in an incubator overnight. The next day, the colonies can be picked. Each colony is placed in a 5 ml tube filled with LB medium containing 100 µg/ml ampicillin. After 12 hrs shaking at 37 °C, the bacteria culture are processed by using the Quiagen Miniprep kit which is used according to manufacturer´s instructions. The gained plasmid DNA is stored at -20 °C until usage.

3.5 Cytotoxicity assay

3.5.1 Theory

To measure cytotoxicity in brain slice culture medium or in the supernatant of cell culture, the lactic dehydrogenase assay is the method of choice.

When cells get destroyed or damaged, their cell membranes get loosen up. When the cell membranes are disrupted, the enzyme lactic dehydrogenase (LDH) leaves the cytosol and gets transferred into the extracellular space.

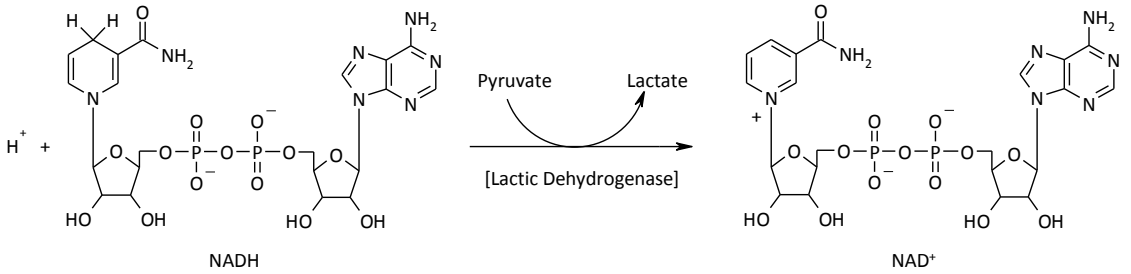

Figure 11: Lactic dehydrogenase reaction

Lactic dehydrogenase (LDH) is released by damaged cells. This enzyme reduces pyruvate to lactate under consumption of NADH. By measuring the decrease of NADH, one can calculate the correlating cell death in the supernatant of cell culture, e.g.

LDH reduces pyruvate to lactate under consumption of reduced nicotinamide adenine dinucleotide (NADH) (see Figure 11). NADH, in contrast to the oxidized form NAD^+, has a second absorption peak at 340 nm. By measuring the decrease of the absorption at 340 nm with a photometer, one can conclude the amount of lactic dehydrogenase in the culture medium, which correlates with cell death (Moran and Schnellmann, 1996).

3.5.2 Procedure

For measuring LDH in the supernatant, the medium gets collected subsequent to the incubation. To avoid adulteration of results by phenol red in the medium, ACSF is used instead. For brain slice culture, 1 ml ACSF per incubation gets collected in a small vial. To obtain a positive control, 2 brain slices get placed in 3 ml ACSF in one well of the 6 well plate. In contrast to the incubated brain slices, they don´t get carbogenated and Triton X 100 is added to the culture medium in a final concentration of 0,1 %. After incubation, the brain slices in the positive control get destructed by frequent pipetting up and down. ACSF serves as a negative control.

After collecting the samples, they are shortly centrifuged at 4 °C. To perform the assay, 100 µl supernatant per sample is placed in a 96 well plate. 100 µl working solution are added, and the plate has then to be incubated at room temperature in avoidance of light for 30 minutes. Afterwards, the absorbance is measured at a wavelength of 490 nm.

3.6 Glutamate assay

3.6.1 Theory

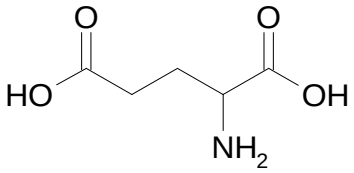

Figure 12: Glutamic acid

Glutamic acid is the most abundant excitatory neurotransmitter in the mammalian brain.

Glutamic acid (see Figure 12) is a key element in cellular metabolism. As one of the two acidic proteinogenic amino acids, it is the most abundant swift excitatory neurotransmitter in the mammalian nervous system. It is also believed to be involved in learning and memory and has appeared to be involved in several diseases like cerebral ischemia, head and spinal cord injury, and prolonged seizure activity (Bittigau and Ikonomidou, 1997). The carboxylate anions and salts of glutamic acid are known as glutamates.

3.6.2 Procedure

To measure glutamate concentrations in the supernatant of the brain slice culture, we used a Glutamate Assay Kit, which resembles a sensitive and simple fluorometric method. The enclosed glutamate Enzyme Mix recognizes glutamate as a specific substrate leading to proportional color development. Therefore the amount of glutamate in the tissue culture supernatant can easily be quantified by colorimetric measurement in a plate reader (spectrophotometry at a wavelength of 450 nm), measuring optic density.

Thus, for each well of a 96 well plate, 100 µl reaction mix have to be prepared, containing 90 µl assay buffer, 8 µl glutamate developer and 2 µl glutamate enzyme mix. 100 µl of this reaction mix is added to each well containing the glutamate standard and the test samples. After mixing, the reaction gets incubated for 30 minutes at 37 °C in the dark. Then, optic density is measured at 450 nm in a microplate reader. To correct the background, the value derived from the 0 nmol glutamate control

has to be substracted from all the sample readings. Then, glutamate concentrations can be calculated with the help of the standard curve.

3.7 Confocal imaging of brain slices

Developed by Marvin Minsky in the 1950s, scanning confocal imaging nowadays serves as a general tool for live cell imaging applications. It can also be used to image fixed cells and tissue, labeled with one or several fluorescent probes. The fact, that confocal imaging can be used for optical sectioning, enables researchers to also address diverse biochemical questions (e.g. gene expression and cytoskeletal dynamics).

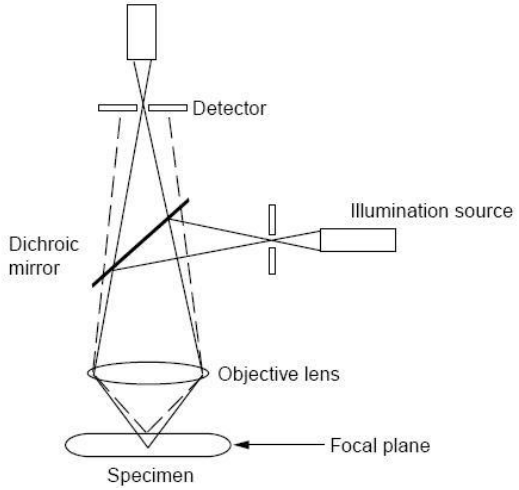

Figure 13: Principle of confocal imaging

(Emptage, 2001)

The term confocal microscopy derives from the fact that both the illumination and the detection unit are at the same **con**jugate **focal** plane (see Figure 13). Thereby, signals are only collected from the plane of focus. Additionally, a pinhole in front of the detector eliminates out-of-focus light. The most common form of confocal microscopes is the laser scanning confocal microscope (LSCM) (Watson, 1997). In contrast to a common wide-field microscope, a confocal microscope can reveal the three-dimensional structure of a specimen, by imaging a series of optical sections at different depths of the sample (Smith, 2008).

With the help of antibodies, coupled to fluorescent dyes, it is possible to image different properties of cells concurrently. Fluorescent dyes are agents that emit light of a particular wavelength, after they got excited by light.

3.7.1 DiI staining

DiI (1,1`-dioctadecyl-3,3,3`,3`-tetramethylindocarbocyanine perchlorate) belongs to the family of carbocyanine dyes. DiI is weakly fluorescent in water but reaches a high fluorescence when it is incorporated into membranes.

The major mechanism of the staining process is lateral diffusion. The dye molecules diffuse along the cell membrane and become incorporated with their alkyl chains embedded in the lipid bilayer, resulting in a staining of the entire cell. DiI is maximally excited in the green and fluoresces bright red-orange, when viewed through a rhodamine filter. One big advantage is, that the dye is intensely fluorescent and that the fluorescence fades much more slowly than rhodamine fluorescence, e.g., making it a suitable approach for the staining and observation of neurons in brain slices (Honig and Hume, 1989). DiI and its analogs usually exhibit very low cell toxicity, making them also suitable for the staining of living cells. However, moderate inhibition of electron transport chain activity has been reported for some analogs of DiI (Anderson and Trgovcich-Zacok, 1995).

3.7.1.1 Procedure

To stain a small portion of neurons in the cortex and hippocampus of brain slices, the slices remain in the cell nets. The PBS gets removed, so that the slices still are slightly wet and don't desiccate. Under a stereomicroscope, single crystals of DiI get applied with caution to the very surface of the brain slices. The tissue then is placed in a dark environment for 4 hours to ensure the dye had enough time to diffuse along the neuronal membranes. Afterwards, the slices get washed in PBS for 20 minutes and then mounted in mowiol. The slides are kept at 4 °C in the dark until observation.

3.7.2 Immunohistochemistry

For immunohistochemical staining, the brain slices get fixed in 4 % PFA overnight at 4 °C. Then, they get washed in PBS at room temperature on a shaker at 100 rpm for 10 minutes. To avoid waste of antibody, the brain slices are then transferred into a 24 well culture plate – each slice in one well. After washing, the brain tissue gets incubated with 1 % Triton-X 100 in PBS (1 ml per slice) at 100 rpm on a shaker at room temperature for 6 hours. To obtain a good membrane permeabilization, the slices remain in the Triton solution in the fridge at 4 °C overnight. On the next day, the brain slices get incubated with 4 % bovine serum albumine (BSA) in PBS (2 hours, RT, 200 rpm) to avoid unspecific binding of antibody. After aspiration of the BSA and a short washing step with PBS, the slices get incubated (300 µl per slice) with the primary antibody (mouse-anti-MAP2), diluted 1:200 in

PBS on a shaker at RT, 200 rpm overnight. On the next day, the tissue is washed five times with PBS, in each case for half an hour. The secondary antibody (Cy3-conjugated Goat-anti-mouse IgG) is diluted 1:200 in PBS (300 µl per brain slice), and the tissue is incubated at room temperature on a shaker (100 rpm) for 2 hours. After 5 washing steps of 30 minutes each, the brain slices get mounted in mowiol.

3.8 Calcium imaging

3.8.1 Theory

As many cellular functions are tightly regulated by calcium, and PLY is supposed to lead to an influx of calcium into cells, the measurement of intracellular calcium concentrations is of high importance. To measure intracellular calcium levels ($[Ca^{2+}]_i$), the fluorescent dye fura-2 is widely used. Fura-2 is very sensitive and specific, and it can be loaded into intact living cells without disruption of cellular functions (Hayashi and Miyata, 1994).

One big advantage of fura-2 is that upon calcium binding, the peak excitation wavelength shifts to shorter wavelengths. So the measurement of two excitation wavelengths can be used to measure $[Ca^{2+}]_i$ independently of dye concentration and cell thickness. Another advantage is the considerably improved selectivity for Ca^{2+} over other divalent cations (Grynkiewicz et al., 1985).

The acetoxymethyl (AM) derivates of fura-2 (fura-2 AM) are very useful compounds for the study of living cells. The modification of carboxylic acids with AM ester groups results in uncharged molecules that can permeate cell membranes easily. Once inside the cell, the lipophilic blocking groups are cleaved by nonspecific esterases, rendering a charged form that leaks out of cells far more slowly than the uncharged molecules (Roe et al., 1990).

3.8.2 Procedure

For calcium measurements, we use primary astrocyte culture. The cells get seeded onto PLO-coated square cover slips. To avoid waste of cells and reagents, we use silicone inserts. After approximately 5 days, the cells are 90 % confluent and ready for measurements. To get rid of the phenol red in the cell culture medium (to avoid disturbances in fluorescence), the cells are rinsed with PBS once. Fura-2 AM is dissolved in Dimethyl sulfoxide (DMSO) to obtain a stock solution of 1 mM.

To load the cells with the fura-2 dye, we use modified artificial cerebrospinal fluid (mACSF). Per 1 ml of mACSF, 5 µl fura-2 stock solution are needed to to obtain a 5 µM solution of fura-2 AM in mACSF.

For the loading process, 200 µl of the fura-2 solution are applied to the cells, which then remain in the CO_2 incubator for 30 minutes. After that time period, the cells are rinsed with mACSF once, and then placed in the incubator for another 30 minutes. Then, they are ready for measurement. To measure changes in intracellular calcium levels, the coverslip is observed with the help of an IonOptix microscope.

3.9 Statistics and analysis

Statistical analysis was carried out with Microsoft Excel 2007 and GraphPad Prism, version 4.2 for Windows (Graph Pad Software, Inc.).

Analysis of pictures was carried out with ImageJ software, version 1.46a for windows (National Institute of Health, Bethesda, MD, U.S.).

4 Materials

4.1 Laboratory equipment

Table 2: General laboratory equipment

Equipment	Manufacturer
Autoclaves	Systec (V 150), HMC (HV-110)
Balance	Kern 572
Carbogen gas	Linde
Centrifuge (table)	Hettich Mikro 120
Centrifuge for bacteria	Eppendorf Centifuge 5417R
Centrifuge, cooled 15/50 ml tubes	Hettich
Chambered coverslips	Nunc
Cooling module	BioRad
Drying chamber	Memmert UNE 300
flexiPerm culture inserts	Sarstedt
Freezer	Heraeus (Hera freeze, -80 °C)
Ice machine	Scotsman (AF 200)
Incubators	Heraeus (Hera Cell 240), Memmert
Instruments for cell preparation	WPI, Hartenstein, Roth
Labware (cell culture plastics etc.)	Sarstedt, Roth, StarLab, Eppendorf, Millipore, BD Falcon
Laminar flow cabinet	BDK Luft- und Reinraumtechnik GmbH
Maxi Sorp plates	Nunc, BD Falcon
Microscope for cell culture	Leica DMIL
Needles	Braun
Orbital shaker	NeoLab Shaker DOS-10L
pH meter	Hanna Instruments
Photometer	Perkin Elmer Instruments
Pipettes (2,5-1000 µl)	Eppendorf, Gilson
Pipettus	accu-jet pro

Plastic cuvettes	Roth
Plate Reader	BioTek (EL 800)
Power supply units	BioRad (Power Pac 3000), Consort (EV 231)
Precision balance	Sartorius
Razor blades	Valet Auto Stop Blades
Refrigerators	Liebherr
Stirrer	Heidolph
Surgical disposable scalpels	Braun
Surgical Instruments	Roth, Hartenstein
Syringes	Braun
Thermomixer	Eppendorf
Variable speed pump	BioRad
Vibratome	World Precision Instruments (WPI) NVSLM
Vortex	IKA
Water bath	Memmert

Table 3: Chemicals

Chemicals	
Aqua purificata	Roth
Acetone	Roth
Ampicillin	Roth
N-Methyl-D-aspartic acid (NMDA)	Sigma
Boric acid	Sigma
Bovine serum albumine (BSA)	Roth
D-AP5	BIOMOL International L.P.
DABCO	Roth
'DiI'; DiIC18(3) *crystalline*	Invitrogen
Dimethylsulfoxide (DMSO)	Roth
Ethanol, ≥70%, p.a.	Roth
Ethanol, ≥99,8%, p.a.	Roth
D-(+)-Glucose, ≥99,5%	Roth

L-Glutamic acid monosodium salt hydrate	Sigma
Glycerol	Roth
HEPES, PUFFERAN ≥99,5%	Roth
Potassium chloride	Roth
Magnesium chloride	Roth
Sodium chloride	Roth
Magnesium sulfate	Roth
Mowiol 4-88	Roth
Paraformaldehyde	Roth
TRIS, PUFFERAN ≥99,9%	Roth
Triton X 100	Roth
Trypan blue	Roth
Topical tissue adhesive	World precision instruments
LB-Agar (Lennox)	Roth
LB-Medium (Luria/Miller)	Roth
DNA Ladder 1kb	Promega
DNA Ladder 100bp	Promega
DNA Polymerase I Large (Klenow) Fragment Mini Kit	Promega

Table 4: Primary antibodies

Primary Antibodies	
Anti-MAP2	Sigma/Santa Cruz
Anti-Synapsin I	Synaptic Systems

Table 5: Secondary antibodies

Secondary Antibodies	
Cy™3-conjugated AffiniPure F(ab´)$_2$ fragment goat anti-mouse IgG	Jackson Immuno Research Laboratories Inc.
Cy™3-conjugated AffiniPure F(ab´)$_2$ fragment goat anti-rabbit IgG	Jackson Immuno Research Laboratories Inc.
Fluorescein (FITC)-conjugated AffiniPure F(ab´)$_2$ fragment goat anti-mouse IgG	Jackson Immuno Research Laboratories Inc.
Fluorescein (FITC)-conjugated AffiniPure F(ab´)$_2$ fragment goat anti-mouse IgG	Jackson Immuno Research Laboratories Inc.

Table 6: Software used for experiments and data evaluation

Software	Application
IonWizard 6.1, Cairn research	Calcium imaging
GraphPad prism	Data analysis, statistics
LAS-AF	Imaging analysis (confocal microscope)
ImageJ	Imaging analysis

Table 7: Commercial kits used for experiments

Commercial kits	
Quiagen Quiaprep Spin Miniprep Kit	Quiagen
Quiagen MinElute Gel extraction Kit	Quiagen
Quiagen MinElute Reaction Cleanup Kit	Quiagen
Glutamate Assay Kit	BioVision
LDH Cytotoxicity Detection Kit	Clontech
Limulus Amebocyte Lysate Kit	Lonza
Magnetofection™ NeuroMag	Oz Biosciences

4.2 Buffers and solutions

Artificial cerebrospinal fluid (ACSF)

- 124 mM NaCl
- 2,5 mM KCl
- 2,0 mM $MgSO_4$
- 1,25 mM KH_2PO_4
- 26 mM $NaHCO_3$
- 10 mM glucose
- 4 mM sucrose
- 2,5 mM $CaCl_2$
- Adjust pH to 7.4 by aerating with 95 % O_2, 5 % CO_2 (carbogen)

Mowiol 4-88 mounting medium:

- 2.4 g Mowiol 4-88 are mixed in 6 g Glycerol (in small vial)
- Add 6 ml aqua destillata and leave stirring for approximately 3 hrs on RT
- Add 12 ml Tris-Buffer, 0,2 M, pH 8.5
- Heat up 10 minutes on 50 °C, agitate occasionally
- Add 1,4-Diazobicyclo-(2,2,2)-octan (DABCO) up to 2,5 % to reduce fading
- Centrifuge 15 min at 4 °C and 5000 g
- Aliquot and store at -20 °C

Paraformaldehyde fixative, 4 %

- Heat 450 ml Aqua destillata in a glass beaker to 60 °C while stirring
- Add 20 g paraformaldehyde powder
- Cover and maintain at 60 °C
- Add 5 drops of 2 N NaOH
- Remove from heat and add 50 ml of 10X PBS
- Adjust pH to 7.2
- Aliquot and store at -20 °C

Poly-L-Ornithine (PLO) solution for coating of dishes

- Solve 3,71 g boric acid in 400 ml aqua bidest.
- Add 100 mg PLO
- Filtrate sterile
- Aliquot and store at -20 °C

Phosphate buffered saline (10x; PBS)

- 1,37 M NaCl
- 26,8 mM KCl
- 101,4 mM Na_2HPO4
- 17,6 mM KH_2PO_4
- Adjust pH to 7,3

Modified artificial cerebrospinal fluid (mACSF) for calcium imaging

- 133 mM NaCl
- 3 mM KCl
- 1,5 mM $CaCl_2$
- 1,2 mM NaH_2PO_4
- 1 mM $MgCl_2$
- 10 mM D-glucose
- 10 mM HEPES
- Filtrate sterile, store at 4 °C until use

Live cell imaging buffer

- 135 mM NaCl
- 2 mM $MgCl_2$
- 2 mM $CaCl_2$
- 4 mM KCl
- 5 mM HEPES
- Adjust pH to 7,4

Calcium-free live cell imaging buffer

- 135 mM NaCl
- 2 mM $MgCl_2$
- 4 mM KCl
- 5 mM HEPES
- Adjust pH to 7,4

5 Results

5.1 Live cell imaging of primary neurons

To investigate the effects of pneumolysin on brain cells, we used a primary culture of hippocampal neurons, seeded onto PLO-coated chamberslides, transfected with GFP (as described in 3.4.2). Prior to each experiment, one healthy neuron (healthy neurons display a multiple branched dendritic tree, the GFP signal is strong, the cells don´t move upon shaking of the chamberslide) per chamber was chosen for observation (see Figure 14). Cells at the very edge of the chamberslide as well as cells with an unhealthy appearance were excluded from the experiments.

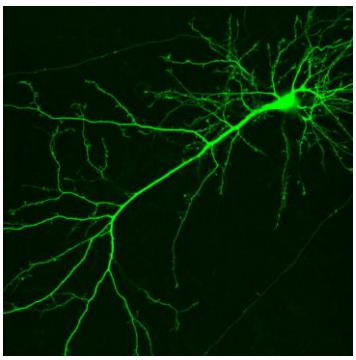

Figure 14: Primary mouse neuron (DIV 14)

For live cell imaging experiments only neurons with a healthy architecture were chosen.

Suitable toxin concentrations for *in vitro* experiments were investigated in our lab by using primary astrocyte culture in a permeabilization assay using propidium iodide staining (Fortsch et al., 2011). Sub-lytic concentrations were considered between 0,05 and 0,2 µg/ml. Thus, in order to achieve proper sub-lytic effects without immediately destroying the cells, we utilized live cell imaging experiments with primary hippocampal neurons using a concentration of 0,1 µg/ml pneumolysin.

5.1.1 Sub-lytic amounts of pneumolysin induce morphological changes in primary neurons

The cells were investigated by using laser scanning confocal microscopy (LSCM), after transfection with green fluorescent protein (GFP). To investigate the cells in an environment close to physiological

conditions, the experiments were set up using a live cell imaging buffer, closely related to the cerebrospinal fluid (CSF), in a heating chamber on top of a heating plate, ensuring a constant temperature of 37 °C.

The neurons were seeded at a density which ensures a proper growth and interconnection. Cells were used at an age of 14 to 21 days *in vitro* (DIV), when they already established cell-to-cell contacts and developed dendritic spines, resembling the synaptic compartments of the neurons. They were challenged with amounts of PLY, comparable to the PLY concentrations measured in the liquor of patients suffering from pneumococcal meningitis (0,1 µg/ml) (Spreer et al., 2003).

All cells were observed for about 30 minutes. Observation of mock-treated control cells revealed no changes in cell shape, size or in the fluorescence of GFP. Even 3 hrs. after the imaging procedure, control cells revealed no damage, as shown in Figure 15. The cells still showed strong GFP fluorescence and a healthy architecture, excluding that phototoxicity damaged the cells significantly during the investigation.

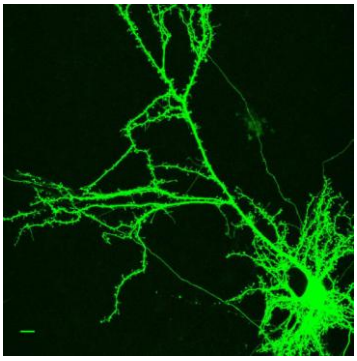

Figure 15: Primary mouse neuron 3 hours after observation

Primary mouse neuron (DIV 19), 3 hrs. after investigation (30 minutes mock-treated live cell imaging, after 3 hrs. pictured again). The neuron still shows a healthy appearance and displays a lot of dendritic spines. Scale bar: 10 µm.

Cells treated with sub-lytic amounts of pneumolysin showed various morphological changes during 30 minutes of observation. The first signs of changes in cell morphology occurred during the first 5 minutes after toxin application. The dendrites of the neurons developed focal swellings, referred to as varicosities (see Figure 16). However, these cells didn´t die, the swellings remained connected to each other, and the GFP signal remained strong. Also, they did not lose the contact to the bottom of the chambered glass slide.

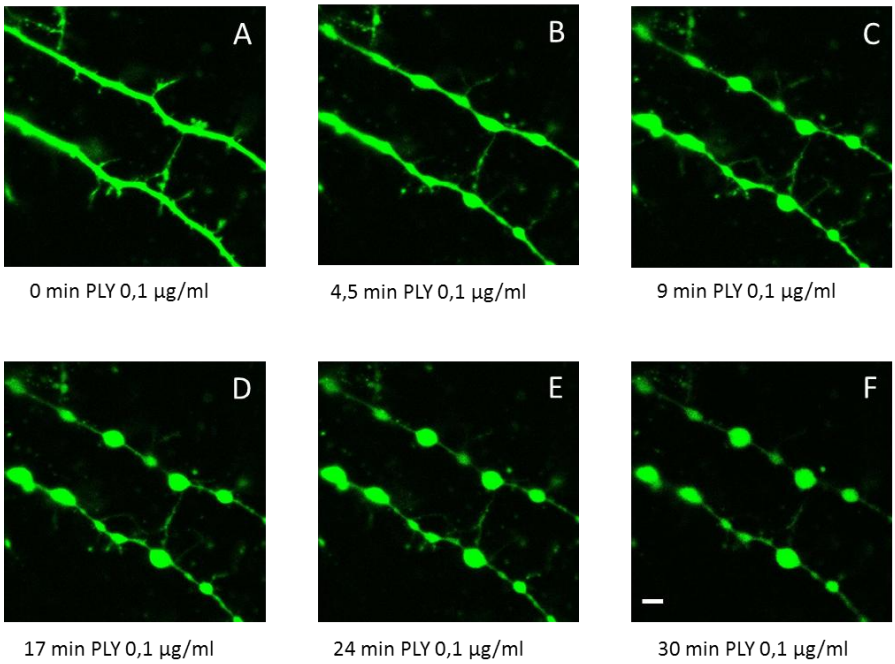

Figure 16: Live cell imaging of primary neurons incubated with PLY

Primary mouse neurons (DIV 14), transfected with a GFP construct. During 30 minutes of live cell imaging, the dendrites of the neurons showed focal swellings; dendritic spines were affected in number and appearance. The neurons stayed alive during the whole investigation. Scale bar: 5 µm.

However, a few observed neurons died during investigation. Dying neurons can be identified easily. They lose contact to the bottom of the chamber slide and the GFP signal gets rapidly lost by protease degradation of the fluorescent protein and due to the breakdown of the neuronal cell membrane (see Figure 17).

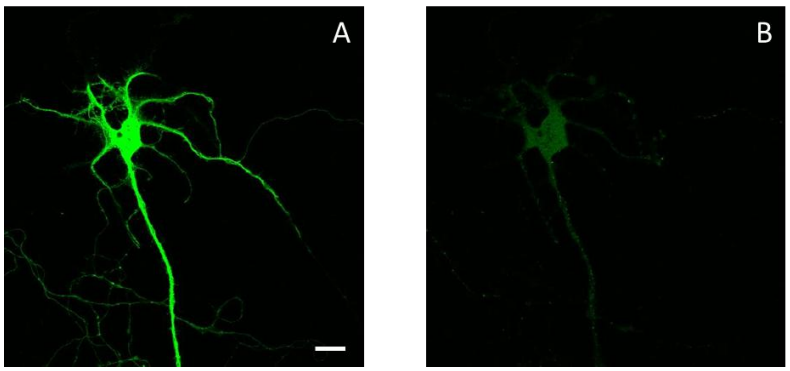

Figure 17: Dying neuron

Dying neurons can be easily identified by a loss of the GFP signal (B) and the detachment from the bottom of the chamberslide. Scale bar: 10 µm.

From all the observed cells, 55 % remained unchanged, 15 % died, and about 30 % of all the neurons observed showed the formation of varicosities during the imaging process. Dying neurons were excluded from the statistics.

Pneumolysin is known to produce extracellular calcium influx into the cells (Stringaris et al., 2002). To clarify the role of calcium influx in the changes we observed, we analyzed the role of pneumolysin in ca-free buffer conditions. The live cell imaging experiments carried out in calcium free buffer showed the same effects on dendrites and dendritic spines as experiments carried out in buffer with physiological calcium levels.

As the formation of varicosities mostly refers to the injury of neurons induced by an over-stimulation of glutamate receptors, referred to as excitotoxicity (see 2.2), we investigated if an inhibitor of glutamate receptors is capable of reducing injuries. The neurons in hippocampus and cortex are in large part glutamatergic neurons (Megias et al., 2001). As these cells express NMDA receptors as main glutamate receptors, we used an inhibitor of the NMDA receptor (MK-801) to address our questions (see chapter 5.2.4.2).

5.2 Establishing an acute brain slice culture

In order to study the morphological changes arising during the incubation with pneumolysin in a more detailed way and in a more complex system, close to the *in vivo* situation, a suitable brain slice culture was developed. Aim of this application was to develop a method, with which it is possible to incubate acute brain slices with pneumolysin (and, for the future, with other toxins and compounds, too) while keeping them alive for several hours, and a reproducible staining method, allowing to stain and investigate single neurons in their natural environment.

There are several brain slice culturing methods described in literature. First, we applied a method, where the brain slices were incubated on an orbital shaker using cell nets inserted in 6 well plates. The plates were kept in a cell culture incubator at 37 °C and 5 % CO_2 during the whole toxin challenge. The cytotoxicity (measured LHD, released into the supernatant) of this approach was about 10 - 12 %. This led us to the implementation of a second approach, where we replaced the orbital shaker and accommodated the brain slices with oxygen by direct admission of carbogen into the culture medium through needles.

By the addition of carbogen to the brain slice culture, we were able to scale down the relative LDH release (directly correlated with cell death) for more than 50 % (see Figure 18).

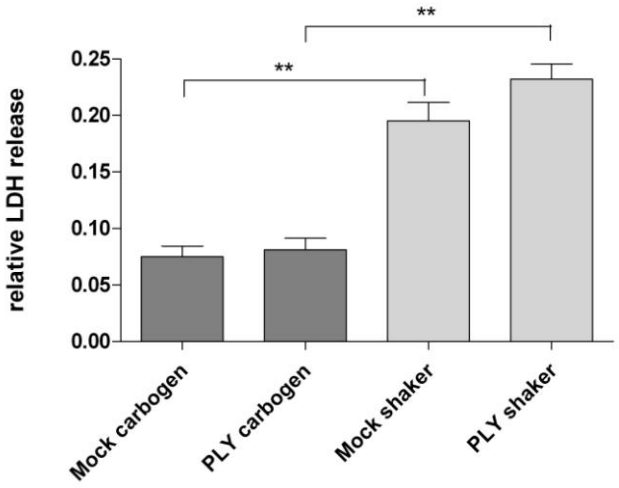

Figure 18: Cytotoxicity of two different brain slice culturing methods

*By improving the culturing method of brain slices with a constant gassing of carbogen, cytotoxicity could be reduced for more than 50 %. PLY treated brain slices were challenged with 0,2 µg/ml PLY for 5 hours. All values represent the mean ± SEM, n=11 for the carbogen method; n=4 for the shaker method; Mann-Whitney-U-Test; **p<0,01*

This method was finally used for all further brain slice experiments. The exact method is described in detail in Figure 19 as well as in 3.3.2.

As a time frame for the incubation, we had chosen 5 hours of incubation. We investigated different time frames for incubation; from 2 to 24 hours. The first manifestations were observed 3 hours after toxin application. We used 5 hours of incubation, because during this time the toxin had the chance of distribution. When the slices were challenged with the toxin for more than 5 hours the effects weren´t aggravated. Additionally, when the time frame of incubation expands, several elements of uncertainty, like pH changes, contaminations, loss of medium, etc. have to be taken into consideration.

As shown in Figure 18, the cytotoxicity of the pneumolysin treated, carbogenated brain slice culturing supernatant is not elevated in comparison to the mock-treated control. A slight elevation of LDH release is due to the slicing process, where it cannot be anticipated that cells get damaged at the very top of the slide, where the razorblade cuts the tissue.

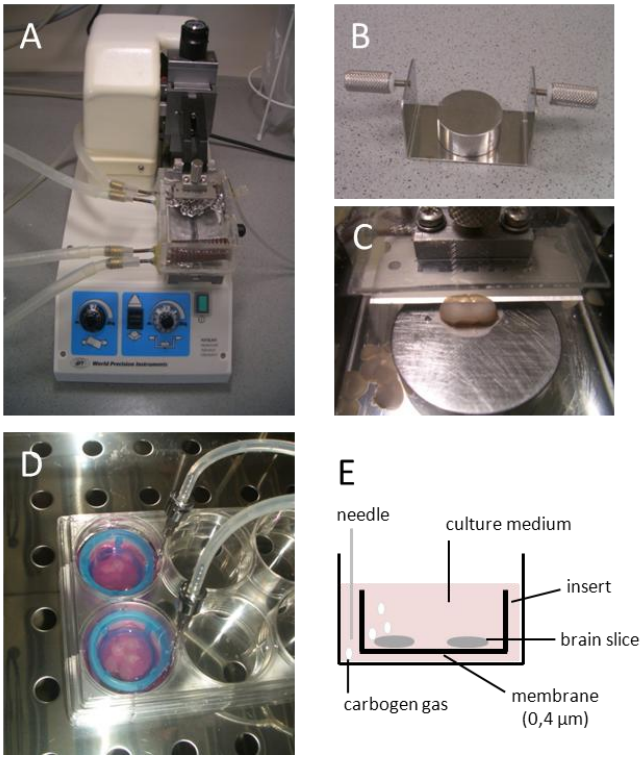

Figure 19: Schematic of the brain slicing process

The mouse brain gets sliced up in carbogenated ACSF (A). After removal of the cerebellum, the brain is glued on a specimen holder (B) and cut into 300 µm thick slices by a vibratome (C). The brain slices get transferred to a 6 well plate, where the slices are constantly gassed with carbogen gas during incubation at 37 °C (D+E).

To ensure an observer-blinded study, we randomly numbered the glass slides the brain slices were mounted on. By constantly gassing the slices with carbogen (Figure 19 D), it was ensured, that the cells had enough oxygen for optimal survival. The medium contained glucose, which is essential for a proper functioning of brain cells. Antibiotics minimize the possibility of contamination during incubation.

5.2.1 C57BL/6 mice (p7) brain slices

First experiments were carried out with C57BL/6 mice at postnatal day 7 (p7). The neurons imaged were all alive prior to fixation with 2 % formalin. DiI is a compound which diffuses along the membrane, thereby staining the whole dendritic tree. This can only function properly, if the membrane is still intact which serves as proof of healthy neurons.

As depicted in Figure 20, after challenge with sub-lytic amounts of pneumolysin, the neurons also showed the same kind of focal swellings seen in the live cell imaging experiments. Although the brain slices represent a much more complex system, close to the *in vivo* situation.

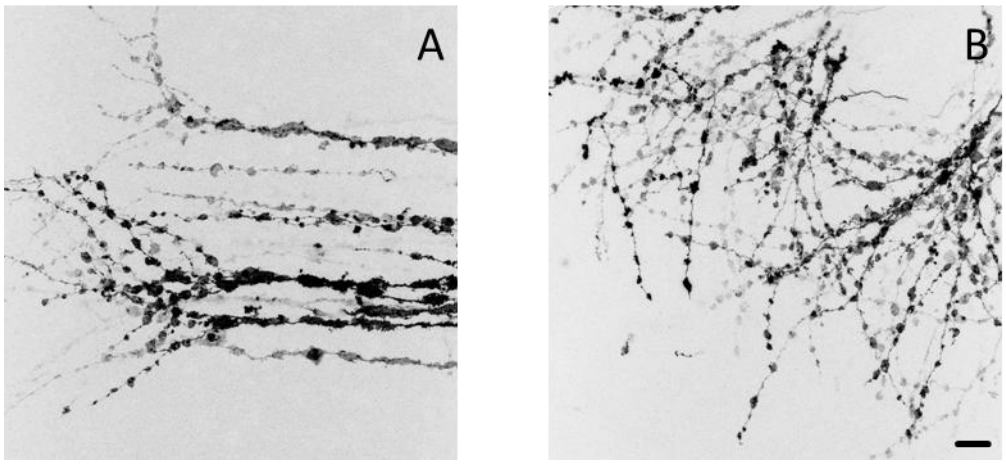

Figure 20: DiI stained neurons in the cortex of brain slices

After 5 hours of incubation with sub-lytic amounts of pneumolysin (0,2 µg/ml), several neurons in the cortex of 300 µm mouse brain slices show focal swellings like they have been observed in the live cell imaging experiments. Scale bar: 20 µm

By counting both varicosities and dendritic spines in the depicted dendrites, we could show an increase in the formation of focal swelling, as well as a slight reduction of dendritic spines (Figure 21).

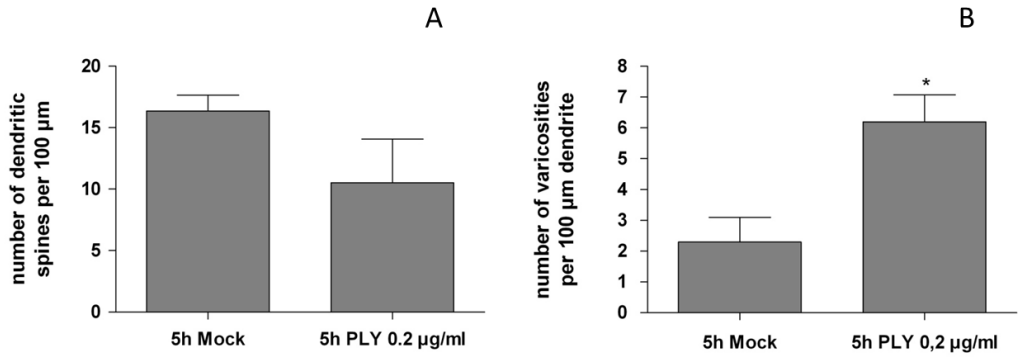

Figure 21: Reduction of dendritic spines and number of varicosities in p7 mouse brain slices

*The slides were randomly numbered, blinding the experiments/conditions. Per each experiment, 4 brain slices per condition were incubated. After staining, 4 randomly chosen neurons per brain slice were depicted by confocal imaging, using z-stacks to picture the whole neuron. Per neuron, all the dendrites which could be clearly seen in the picture, were chosen for investigation of dendritic spines/varicosities. All values represent the mean ± SEM, n = 3 experiments (4 slices/condition/experiment); Mann-Whitney-U-Test; *p<0,05.*

The varicosities ranged between 5-7 varicosities per 100 µm of the dendrite. The number of dendritic spines per 100 µm dendrite ranged between ~15 (mock) and ~10 (PLY).

5.2.2 C57BL/6 mice (p14) brain slices

Because of the fact, that at the age of 7 days, the mouse brain has not established that much spines and dendrite branching, we investigated the effects of PLY also in brain slices of p14 mice.

5.2.2.1 Ctrl vs. PLY

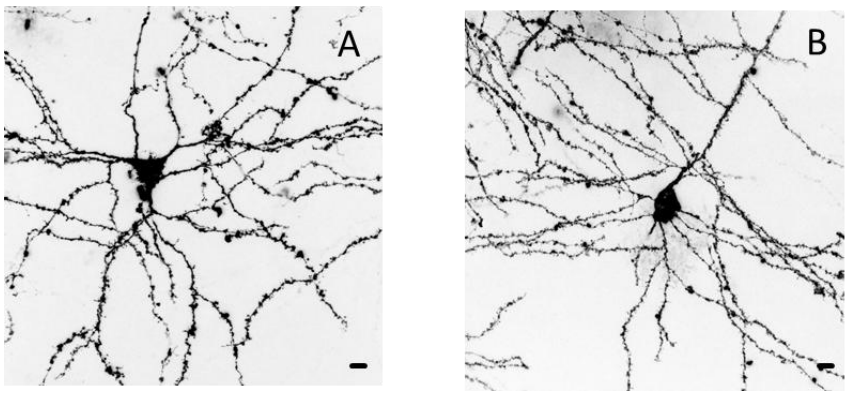

Figure 22: DiI stained neurons in the cortex of 300 µm mouse brain slices

Control neurons in the cortex of brain slices of p14 C57BL/6 mice show an established complex network of dendrites. Also the dendritic spines, representing the postsynapse, have established properly. Scale bar: 10 µm

In brain slices of p14 mice, the control cells showed the typical morphology of healthy neurons in their natural environment (Figure 22), the dendrite morphology remained unchanged under control conditions (mock-treated brain slices; 5 hours incubation at 37 °C with the carbogen method, described in 3.3.2).

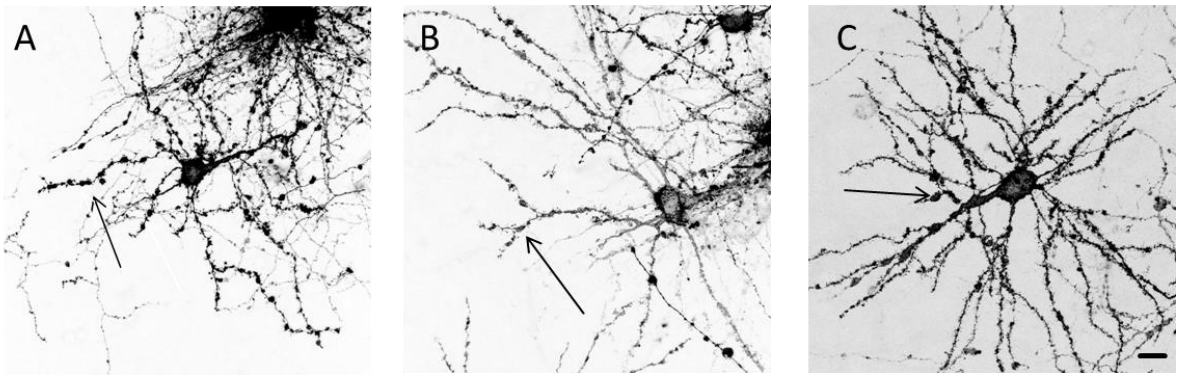

Figure 23: Dendrites of neurons in brain slices show morphological changes upon PLY challenge

After challenge with pneumolysin, the dendrites show clear signs of varicosity formation (arrows). Scale bar: 10 µm

In this model, pneumolysin also caused a significant reduction of dendritic spines as well as an increase in varicosities (see Figure 23 and Figure 24).

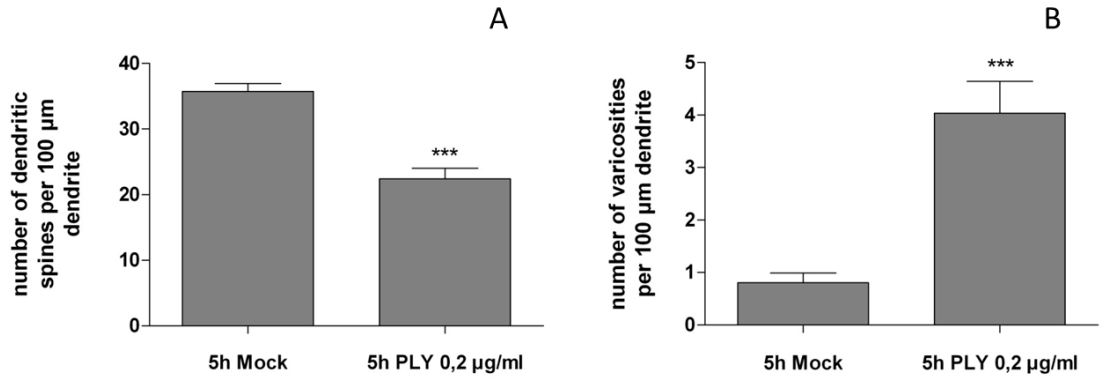

Figure 24: Reduction of dendritic spines and induction of varicosities in brain slices incubated with sub lytic amounts of pneumolysin

*After 5 hrs. incubation with 0,2 µg/ml pneumolysin, brain slices of C57BL/6 mice, 14 days postnatal, show a significant reduction of dendritic spines and an increase in the formation of varicosities. All values represent the mean ± SEM, n = 4 experiments (4 slices/condition/experiment); Mann-Whitney-U-Test; ***p<0,001.*

As shown in Figure 24, the dendrites in the older brain slices show more dendritic spines in general (about 35 per 100 µm dendrite). Upon PLY challenge, the spines get reduced for about 30 %. The varicosities range between 3 and 5 per 100 µm dendrite. The number of varicosities in the older brain slices is slightly increased in comparison to the number of varicosities in the p7 brain slices.
The reduction of dendritic spines as well as the formation of varicosities over time is statistically highly relevant.
To visualize dendrite morphology, we also used an immunofluorescence method with a monoclonal antibody against the dendrite-specific microtubule-associated protein MAP2. As shown in
Figure 25, mock-treated brain slices exhibit regular, healthy neurite architecture.

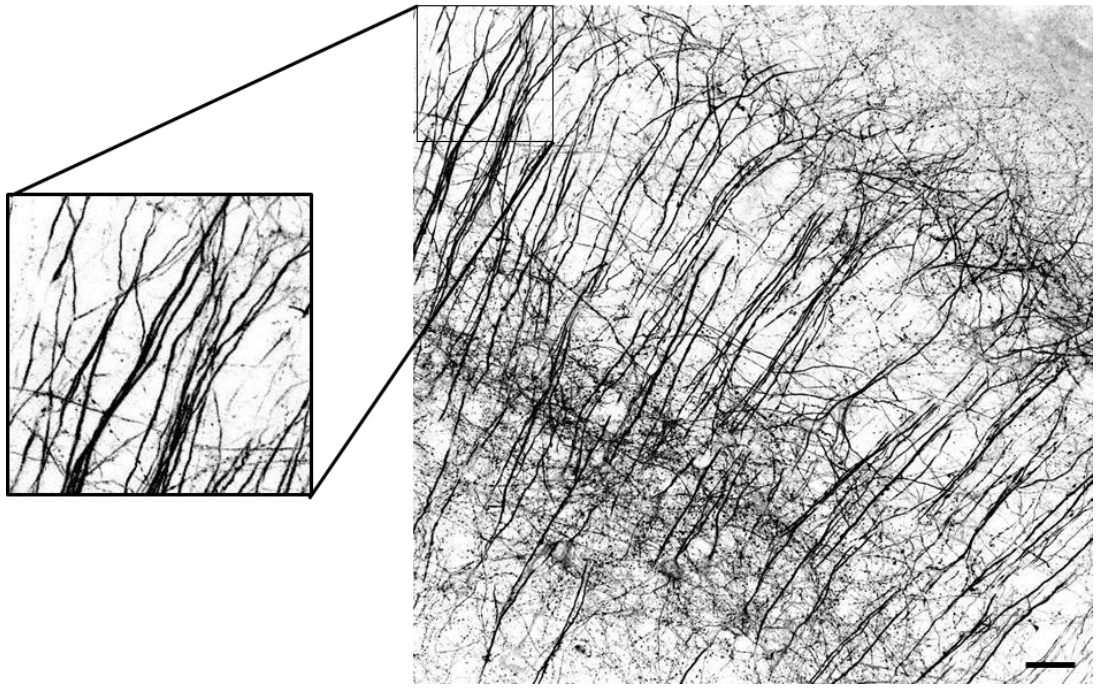

Figure 25: MAP2 immunostaining of neurons in the cortex of C57BL/6 mice

MAP2 immunostaining of cortical neurons in a brain slice of p14 C57BL/6 mice. 5h mock-treated. The architecture of the dendrites is intact, they show a regular morphology. Scale bar: 30 µm

Upon PLY challenge, the development of varicosities can be visualized with MAP2 immunohistochemistry, too (see Figure 26). Some of the depicted dendrites show irregular beadings.

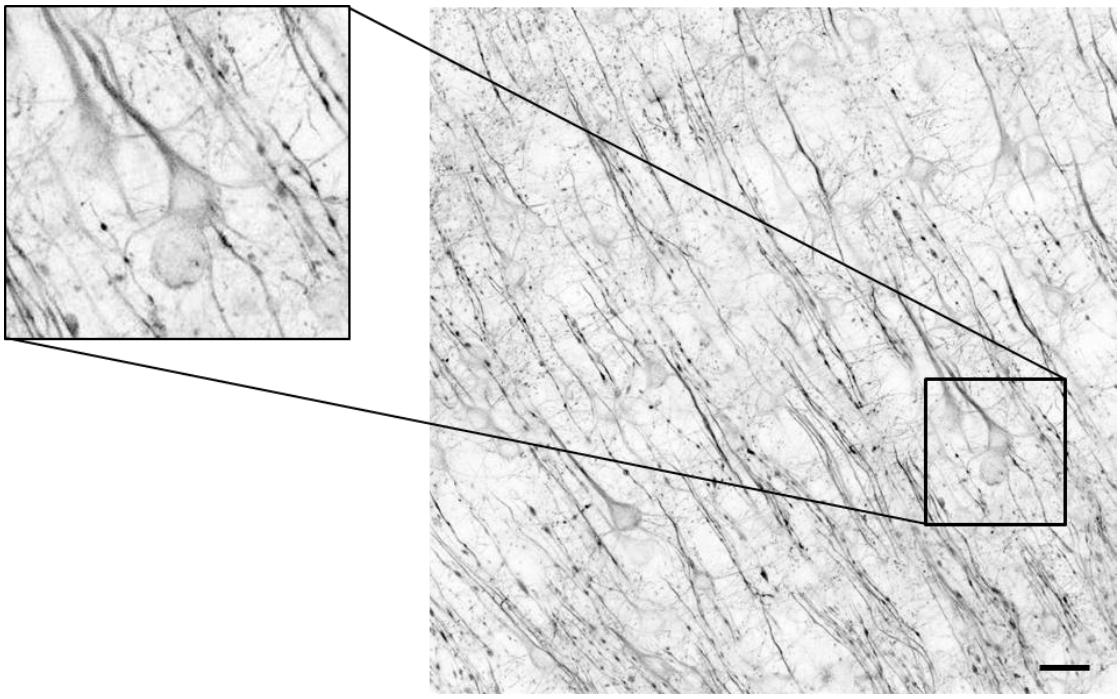

Figure 26: MAP2 immunostaining brain slices after PLY challenge

After challenge with 0,2 µg/ml PLY for 5 hours, the cytoskeletal architecture of cortical mouse neurons is altered. Scale bar: 30 µm

5.2.3 Cell culture conditions modulating the toxicity of pneumolysin

As brain cell homeostasis is altered in the course of bacterial meningitis, we also investigated the toxicity of pneumolysin under disease-relevant conditions.

If the brain slices are incubated on a shaker in the incubator, without a constant source of oxygen, pneumolysin leads to a higher cell death rate compared to the mock-treated brain slices (see Figure **27**). This deprivation of oxygen mimics dramatic conditions during pneumococcal meningitis, where some brain areas are affected by ischemia (Gerber and Nau, 2010).

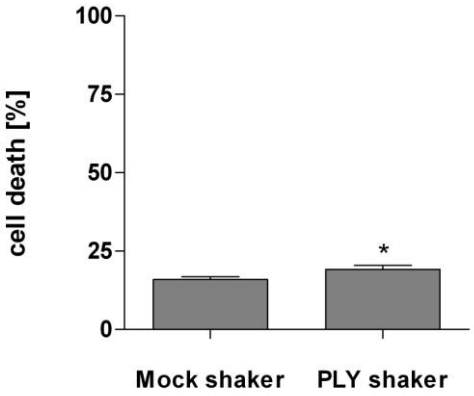

Figure 27: Cell death induced by PLY (brain slice shaker method)

*All values represent the mean ± SEM; n = 4; Mann-Whitney-U-Test; *p<0,05*

The reduction of extracellular calcium levels is often correlated with an aggravated course of different systemic bacterial diseases (Ben-Abraham et al., 2002; Cooper and Morganelli, 1998). The incubation of mouse brain slices with PLY in two different extracellular calcium concentrations revealed a higher LDH release in a low-calcium extracellular milieu (see Figure 28).

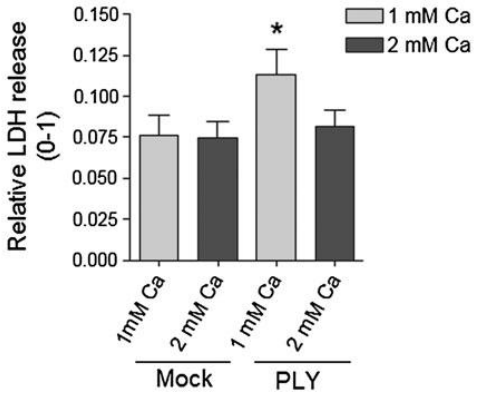

Figure 28: LDH release brain slices with differing calcium concentrations

*Brain slices incubated for 4 hours with or without 0.2 µg/ml PLY in the presence of 1 and 2 mM extracellular calcium. All values represent the mean ± SEM; n = 6 experiments (5 slices/condition/experiment) ; Mann-Whitney-U-Test; *p<0,05*

5.2.4 Brain slices of mice with pneumococcal meningitis

Brain slices of mice suffering from pneumococcal meningitis were kindly provided by Prof. Roland Nau and Prof. Wolfgang Brück from the Department of Neuropathology, University of Göttingen. The slices stem from C57BL/6 mice, ca. 2 months old, infected with *S. pneumoniae.* Two different

pathogen strains were used for infection. One strain was capable of producing pneumolysin, the other strain was a PLY-deficient one. For control, we were provided with brain slices from healthy mice at the same stage of development. By immunohistochemistry for both MAP2 (a dendritic protein) and synapsin (a presynaptic marker), we were able to measure the relative synaptic density in the cortex of these brain slices, comparing the fluorescence intensities for synapsin, normalized to the MAP2 signal in the same region in order to compensate sectioning differences. The analysis was limited to the layers I-III of the parietal cortex, positioned in adjacent vicinity to the CSF space, populated by the pneumococci.

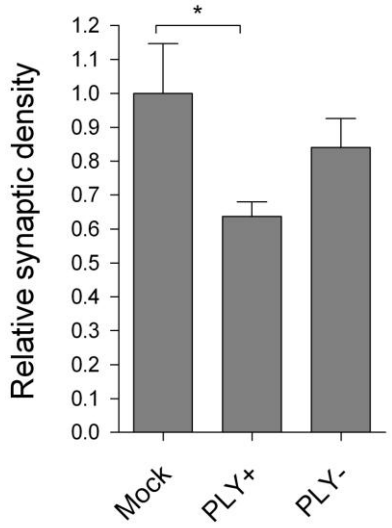

Figure 29: Relative synaptic density in the cortex of C57BL/6 mice suffering from pneumococcal meningitis

*Brain slices from mice infected with PLY+ or PLY- strains of Streptococcus pneumoniae. Immunohistochemistry for MAP2 and Synapsin. All values represent the mean ± SEM; Mann-Whitney-U-Test; *p<0,05*

As shown in Figure 29, there is a significant decrease in the synaptic density in the cortices of mice suffering from pneumococcal meningitis with PLY production in comparison to the mock-treated control mice as well as in comparison to the mice infected with a PLY-deficient mutant of the pathogen.

5.2.4.1 Delta6 mutant

Challenge of brain slices with different concentrations of the delta6 mutant (unable to form pores) showed no effects in the number and appearance of dendritic spines, as well as in the formation of varicosities (data not shown).

5.2.4.2 MK-801 – role in primary neuronal culture

To investigate the effects of an inhibitor of NMDA receptors on the morphological cell shape changes observed after PLY treatment, we used MK-801 as a potent, non-competitive inhibitor of the NMDA receptor (Wong et al., 1986). The inhibitor was used in live cell imaging experiments and got added in a final concentration of 10 µM immediately after the first signs of varicosity formation. The whole imaging process took 30 minutes.

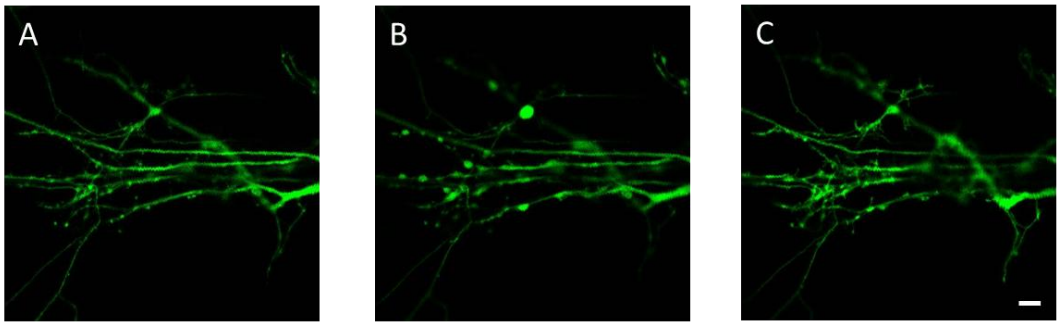

Figure 30: Live cell imaging of primary mouse neurons (DIV 14) incubated with PLY and MK-801
Primary hippocampal neurons, transfected with a GFP construct. Scale bar: 10 µm

As shown in Figure 30, the addition of MK-801 led to a reversion of the morphological changes; almost to the original state. The same experiment was accomplished with neurons at DIV 21, as shown in Figure 31. Even at this stage of development, the inhibitor was capable of reverting the formation of varicosities.

As depicted in Figure 30 and Figure 31, the addition of MK-801, applied to the cells after they showed the first signs of alteration, was capable to reduce the focal swellings induced by the toxin.

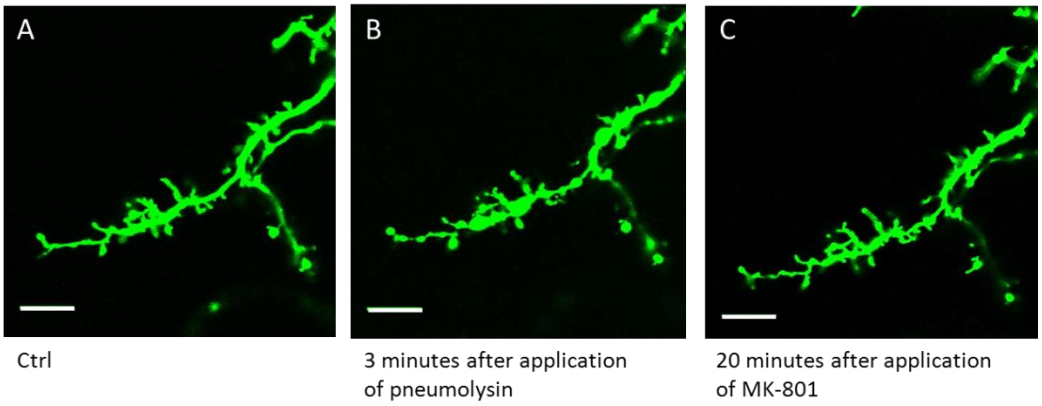

Figure 31: Live cell imaging of primary neurons (DIV 21) incubated with PLY and MK-801

In live cell imaging experiments with primary hippocampal mouse neurons, the first signs of morphological alterations occurred 3 – 5 minutes after pneumolysin challenge (B). By immediate application of the inhibitor, the formation of varicosities could be reversed (C). Scale bar: 10 µm

5.2.4.3 MK-801 – role in brain slice culture

As the addition of MK-801 was capable of reverting the formation of varicosities in primary neuronal culture, we investigated if the inhibitor effects the formation of varicosities also in a more complex system like brain slices. As shown in Figure 32, incubation with 10 µM MK-801 concurrently with pneumolysin significantly reduced the number of varicosities.

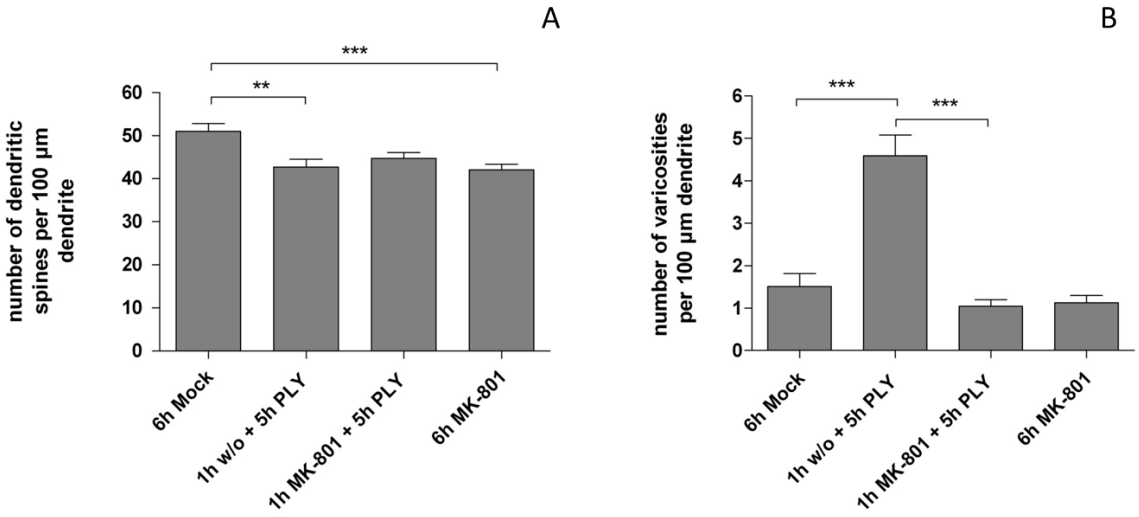

Figure 32: Dendritic spines and varicosities per 100 µm dendrite in mouse brain slices (p14)

*Brain slices incubated for 5 hours with 0.2 µg/ml PLY and MK-801. All values represent the mean ± SEM; n = 4 experiments (4 slices/condition/experiment); Mann-Whitney-U-Test; **p<0,01; ***p<0,001*

As previously, PLY led to a decrease in the number of dendritic spines. 6 hours incubation with 10 µM MK-801 led to a significant decrease in the number of dendritic spines per 100 µm dendrite.
The MAP2 immunohistochemical staining of brain slices that were preincubated with 10 µM MK-801 prior to pneumolysin incubation showed a normal architecture of the dendrites in the cortex (see Figure 33).

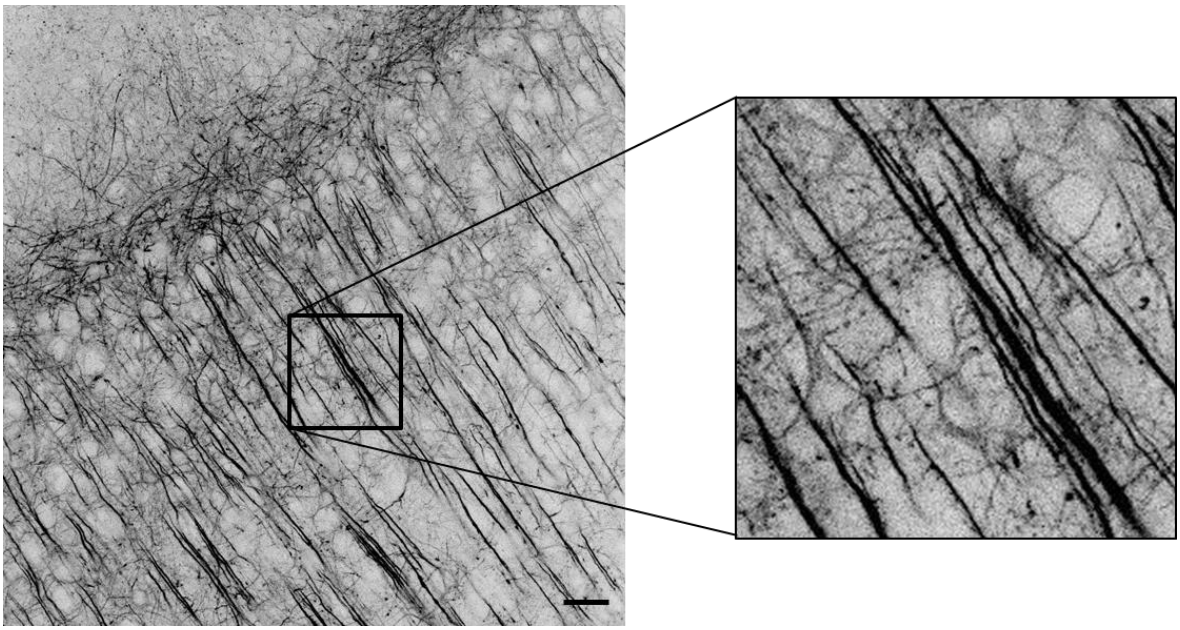

Figure 33: MAP2 immunostaining

Brain slices incubated with 10 µM MK-801 one hour prior to 5 hrs. PLY incubation. Preincubation with 10 µM MK-801 leads to a preserved structure of dendrites. Scale bar: 30 µm.

5.2.4.4 AP5 brain slice experiments

We also investigated, if another inhibitor of NMDA receptors (AP5) is capable to reduce the focal swellings, induced by pneumolysin. Thereby it should be investigated, if the observed effects are due to a possible interference of MK-801 directly with the PLY pores, or if the effects are glutamate receptor specific. AP5, in contrast to MK-801, is a competitive inhibitor of NMDA receptors. It blocks the receptor by binding at the same binding site as glutamate.
As shown in Figure 34, AP5 also leads to a significant reduction in the number of varicosities, caused by pneumolysin.

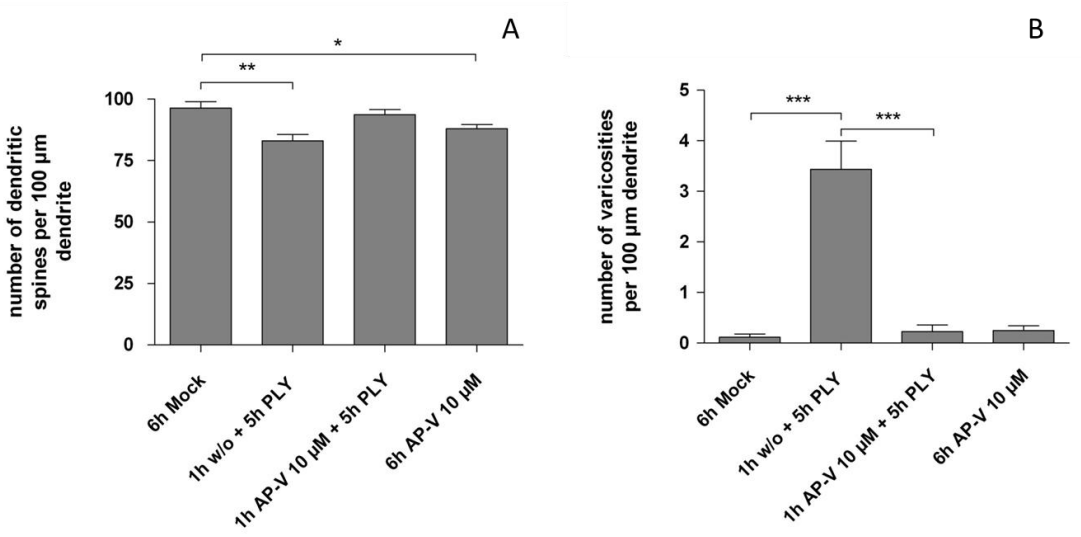

Figure 34: AP5 (10 µM) effects of the number of spines and varicosities

*All values represent the mean ± SEM. n = 3 experiments (4 slices/condition/experiment); Mann-Whitney-U-Test; *p<0,05; **p<0,01; ***p<0,001*

As several publications mention that the AP5 inhibitor is more effective in concentrations of about 50 µM, we incubated the brain slices with this higher concentration of AP5 and revealed the same results; a significant reduction of varicosities caused by pneumolysin (see Figure 35).

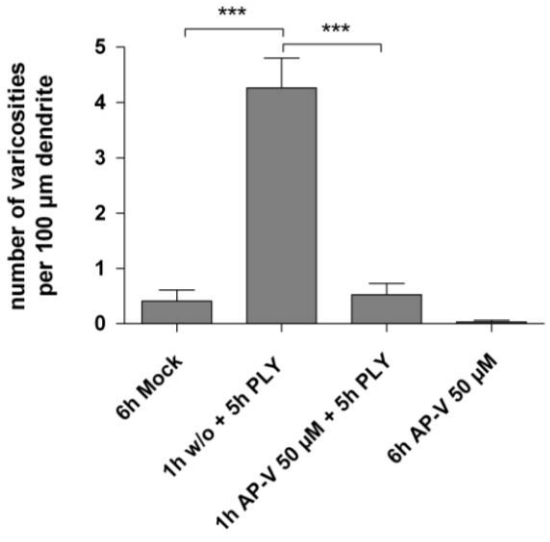

Figure 35: Number of varicosities (50 µM AP5)

*All values represent the mean ± SEM. n = 1 experiment (4 slices/condition/experiment); Mann-Whitney-U-Test; ***p<0,001*

5.3 Glutamate measurement

To investigate if the observed effects on neuronal dendrites refer to a discharge of glutamate, we measured glutamate levels in the supernatant of the brain slice culture (for the exact method, see 3.6.2). With this method, no changes in the glutamate levels of brain slice culture could be observed (see Figure 36).

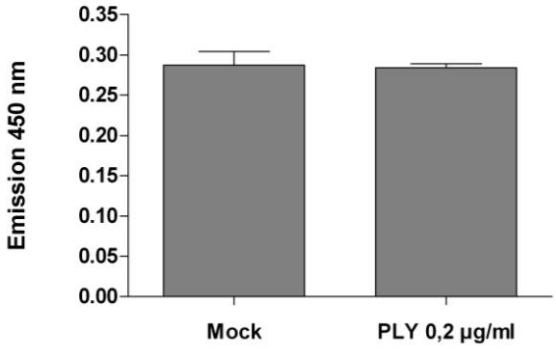

Figure 36: Glutamate levels in the supernatant of brain slice culture

An enzymatic glutamate assay did not observe any changes in glutamate levels in the supernatant of brain slice culture. All values represent the mean ± SEM. n = 3 experiments (4 slices/condition/experiment).

Next, we investigated, if the reuptake of glutamate into brain tissue is affected after challenge with PLY. Therefore, brain slices were treated with 0,4 µg/ml pneumolysin for 4 hours. Afterwards, the slices got challenged with 100 µM glutamate for one additional hour. Subsequently, supernatant was taken to perform a glutamate assay.

Figure 37 shows, that the uptake of glutamate into brain tissue was not altered after four hours of PLY incubation.

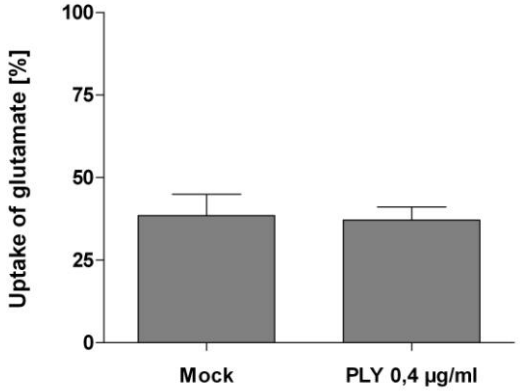

Figure 37: Reuptake of glutamate into brain slices

The glutamate assay did not observe changes in the capacity to take up glutamate from the supernatant back into brain tissue. All values represent the mean ± SEM. n = 3 experiments (4 slices/condition/experiment).

To investigate glutamate levels in brain slice culture over time, slices were challenged with 0,2 µg/ml pneumolysin for a time period of 5 hours. Every 30 minutes, 50 µl of supernatant were taken for the enzymatic glutamate assay.

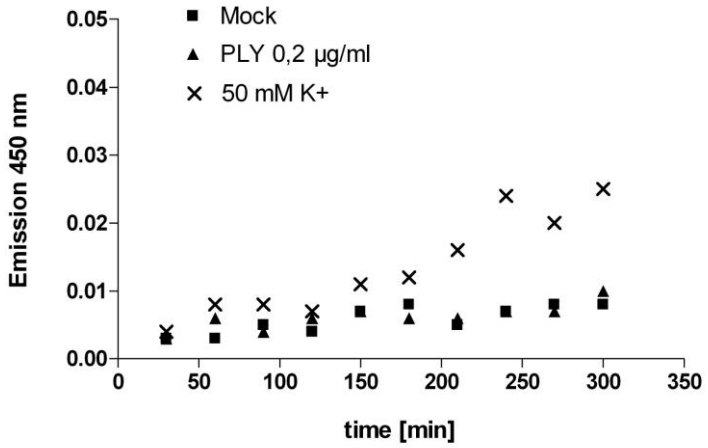

Figure 38: Glutamate levels in brain slice culture over time

Over a time period of 5 hours, the glutamate concentrations in the supernatant of the brain slice culture rises slightly in control and PLY-treated experiments. In the culture, treated with high potassium levels, glutamate is elevated to a higher extent.

As shown in Figure 38, the glutamate levels were elevated, when the slices were treated with high potassium levels. That is so far no surprise, as high levels of potassium lead to a prolonged depolarization of neurons (Jing et al., 1991).

The supernatant of the mock-treated tissue as well as the supernatant of the PLY-treated brain slices shows nearly no elevation of glutamate levels. All the slices from this experiment were stained with the help of a MAP2 antibody.

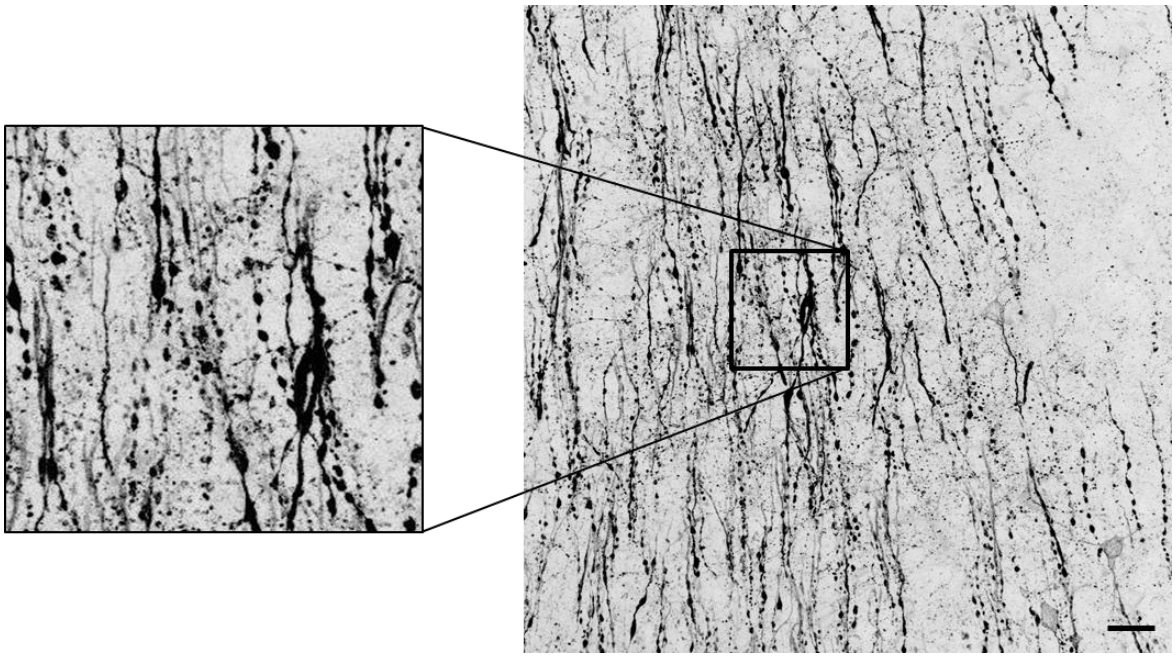

Figure 39: MAP2 immunostaining of brain slices

MAP2 immunostaining of neurons in the cortex of C57BL/6 mice (p14) after challenge with 50 mM potassium for 5 hours. Scale bar: 30 µm

As depicted in Figure 39, brain slices which were challenged with a high concentration of potassium, known to lead to excessive depolarization of neurons, showed neurons with a high amount of varicosities in the dendrites. Nearly none of the observed neurons showed an intact architecture.

5.4 Calcium imaging

It is known, that pneumolysin leads to a calcium influx *in vitro* (Stringaris et al., 2002). To investigate, if this calcium influx may be blocked by the application of MK-801 (and thus indicate a provisional direct interaction of MK-801 with the PLY pores), we used primary astrocytic culture, loaded with fura-2. To measure elevated intracellular calcium, we used the IonOptix setup. With the help of this setup, it is possible to calculate the elevated intracellular calcium by measuring the increasing fluorescence of fura-2 AM (see 3.8.2). An example of such a calcium chart is shown in Figure 40.

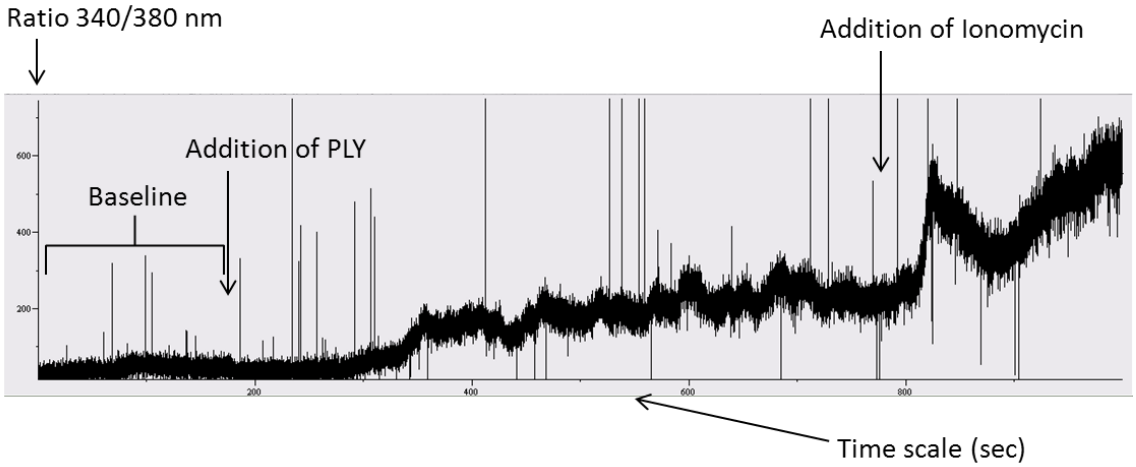

Figure 40: Example of a calcium chart

After addition of pneumolysin, the intracellular calcium concentration rises. Addition of ionomycin at the end of each experiment serves as positive control.

The addition of Ionomycin (10 µM) at the end of each experiment served as a positive control, presumably equalizing the level of calcium inside and outside the cells.

PLY led, as expected, to an increase in intracellular calcium levels after round about one minute. MK-801, which has been applied concurrently with pneumolysin, delayed the beginning of the rise of intracellular calcium for ca. 2 minutes (see Figure 41), without affecting the calcium level in the cytosol.

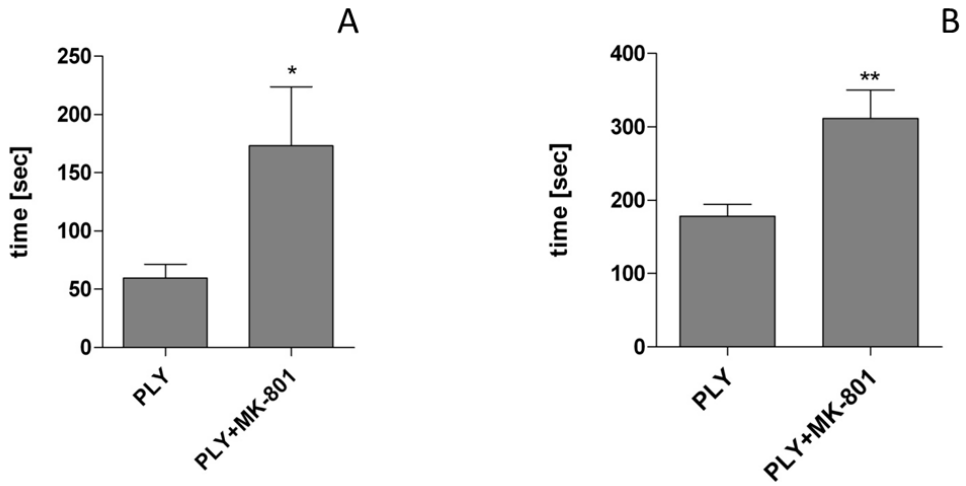

Figure 41: Evaluation of the calcium experiments

A: Time span till the beginning of the intracellular calcium rise
B: Time span till the maximum calcium increase is reached
*All values represent the mean ± SEM; n = 6; Mann-Whitney-U-Test ; *p<0,05; **p<0,01*

Additionally, MK-801 was able to delay the point of time, when the peak of calcium increase was reached for about 2 minutes (Figure 41 B).

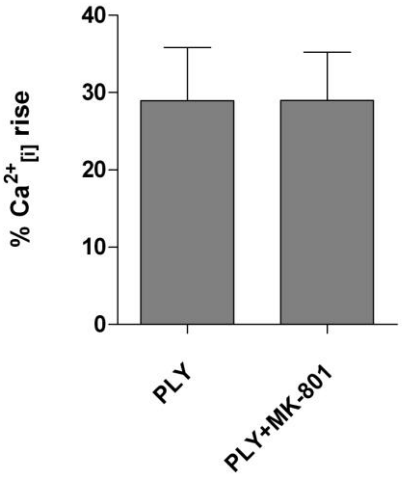

Figure 42: Rise of intracellular calcium

No change in the percental rise of intracellular calcium was observed. All values represent the mean ± SEM; n = 6.

As shown in Figure 42, intracellular calcium levels were elevated for about 30 % after PLY challenge. The application of MK-801 was not capable of reducing the rise in intracellular calcium levels.

6 Discussion

Bacterial meningitis induced by the pathogen S*treptococcus pneumoniae* is still a devastating disease with high mortality rates, especially among little children and elderly people in developing countries. One major virulence factor of *S. pneumoniae* is the CDC pneumolysin. It has been shown that strains of *S. pneumoniae* which are not capable of producing pneumolysin, exhibit a reduced virulence (Hirst et al., 2008). The contribution of pneumolysin to a severe outcome of pneumococcal meningitis has recently been shown by Wall et al., who found out that PLY persists in the CSF of meningitis patients, even when the number of bacteria is lowered due to antibiotic therapy. The amount of PLY during suffering was higher in the CSF of non-survivors compared to the CSF levels of patients who survived the disease (Wall et al., 2012).
There are several publications dealing with the effects of pneumolysin. However, most of these experiments were carried out with concentrations above the toxin levels found in the CSF of patients suffering from pneumococcal meningitis, as lytic pore formation occurs with higher concentrations of the toxin, milder effects and apoptosis in lower concentrations (Braun et al., 2002). Thus, we investigated toxin effects with concentrations ranging from 0,1 to 0,2 µg/ml, corresponding to the toxin levels found in the CSF of meningitis patients (Spreer et al., 2003).

Brain damage in pneumococcal meningitis leads to long-term neurologic sequelae in 30 % of the survivors, manifested especially in hearing loss along with learning and memory deficits (Schmidt et al., 2006; Wellmer et al., 2000). Another manifestation of neurological impairment is the occurrence of seizures during childhood meningitis (Chao et al., 2008). Grimwood et al. found out that even 12 years after recovery from bacterial meningitis, many of the intellectual and cognitive impairments still persisted (Grimwood et al., 2000). The risk of long-term neurological sequelae is highest in low-income countries, where the burden of meningitis is highest (Edmond et al., 2010).

As several mechanisms seem to be involved in the processes leading to such a severe outcome of this form of meningitis, the aim of this thesis was to clarify the role of pneumolysin in the establishment of neurological deficits during and after recovery from pneumococcal meningitis.

During the work on this thesis, the effect of pneumolysin onto primary neurons was investigated. Therefore, a primary neuronal culture as well as a newly established acute brain slice model was used. Cells as well as slices were treated with sub-lytic amounts of pneumolysin, proven to be sub-

lytic with the help of different methods in our lab (Fortsch et al., 2011). The effects were investigated by using two different staining methods and laser scanning confocal microscopy. Further insight was provided with the help of calcium imaging using primary mouse astrocytes. Modulations of the toxin induced effects were carried out with two different antagonists of the NMDA receptor.

Because pneumococcal meningitis represents the greatest burden in children aged 0-5 (see Figure 2), we used mice at the age of 7 to 14 days for brain slice culture, when the brain architecture of mice is still developing and thus comparable to the brain architecture of infants. Additionally, brain slices of younger mice show a better survival during culturing than those of adult mice (Lipton et al., 1995).

The very first findings we got by using primary neuronal culture, transfected with a GFP construct and investigated via confocal time-lapse imaging. We observed the induction of focal swellings along the dendrites of primary hippocampal neurons as well as the collapse of dendritic spines, starting approximately 3 minutes after sub-lytic pneumolysin challenge.

The formation of regular dendritic beadings is well described in literature. In 1982, Purpura et al. examined the brain biopsies of 5 young children, suffering from severe neurobehavioral retardation of unknown etiology. In this brain tissue, over 90 % of neurons were affected by varicosity formation and loss of dendritic spines (Purpura et al., 1982).

As 30 % survivors of pneumococcal meningitis suffer from neurological deficits like seizures or memory and learning disabilities, it appears obvious that our findings might be related to these deficits. Purpura et al. already proposed that the alterations in the dendritic structure of neuronal cells may represent a primary target in the pathobiological process underlying neurobehavioral failure (Purpura et al., 1982).

Later studies more and more related the formation of varicosities to excitotoxic events, meaning the excessive or prolonged activation of glutamate receptors (Olney, 1990). These dendrite beadings occur after NMDA challenge (Ikegaya et al., 2001; McDonald and Johnston, 1993; Olney, 1969) as well as after application of kainic acid (Al-Noori and Swann, 2000; Oliva et al., 2002), which is commonly used in the field of epilepsy research to evoke seizures. These facts lead to the hypothesis that the dendritic beadings, occurring after challenge with sub-lytic concentrations of pneumolysin, are caused by a non-physiological activation of glutamate receptors.

Concurrently with the regular beading of the dendrites, we observed a decrease in the number of dendritic spines in the areas of the beadings. The formation of varicosities is often accompanied with the loss of dendritic spines:
In 2001, Hasbani et al. used cultured cortical neurons, either expressing yellow fluorescent protein or stained with DiI, for sublethal excitotoxic exposure (NMDA, kainate or oxygen-glucose deprivation). With the help of time-lapse microscopy, they tracked the fates of dendritic spines. The neurons underwent dendritic beading and the loss of approximately 50 % of dendritic spines. Consistent with our findings, they observed most spine loss in regions of local dendrite swelling. They also investigated the recovery of dendritic spines along the dendritic shafts (Hasbani et al., 2001). If the dendritic spines reemerge after washout of pneumolysin (or inactivation with cholesterol) should be investigated with the help of further experiments.

To shed a bit more light on the disappearance of the dendritic spines, we were provided with brain slices from adult mice, suffering from pneumococcal meningitis. With synapsin I as a marker for the presynapse, we could show that the synaptic density is decreased in the cortex of mice suffering from pneumococcal meningitis with a *Streptococcus pneumoniae* strain, capable of producing pneumolysin. The fact, that the synaptic density was not decreased to that extend in mice which are infected with a strain of *Streptococcus pneumoniae* lacking the ability to produce pneumolysin, leads to the conclusion, that pneumolysin is directly involved in the seen effects.
In 1993, Rosahl et al. showed that a synapsin I knockout in mice leads to learning and memory deficits (Rosahl et al., 1993). Pneumolysin leads to a reduction in synapsin I, which might be an additional explanation for the cognitive impairment after recovery from pneumococcal meningitis.

However, additional experiments should be performed, testing if the morphological changes observed really correlate with functional impairment. During cerebral ischemia, neurons undergo rapid alterations in their dendritic structure consisting of focal swelling and spine loss. Hasbani et al. could show that presynaptic and postsynaptic elements remained in physical proximity throughout spine loss and recovery (Hasbani et al., 2001). These results suggest that an elimination of dendritic spines is not necessarily associated with the loss of synaptic contacts.

None of the effects mentioned above were observed after incubation with the delta6 mutant of pneumolysin (a completely non-pore-forming mutant), neither in primary culture, nor in acute brain

slice culture. This leads to the hypothesis that membrane-binding and the formation of pores are required for the induction of excitotoxic events through pneumolysin.

Several publications mention that neurotoxicity of pneumolysin is dependent on calcium influx through the pore (Stringaris et al., 2002), and excitotoxic events are also related to a calcium influx through activated glutamate receptors (Hoskison et al., 2007). When we investigated time lapse imaging with primary neurons in calcium free buffer the formation of varicosities wasn't abolished. This leads to the hypothesis that neurons not only become damaged by pneumolysin through calcium influx into the cells. The formation of focal swellings seems to be independent of calcium influx.

Several studies mentioned already that varicosity formation is independent of calcium influx into the cell: Swann et al. stated in 2000 that the cellular mechanisms underlying varicosity formation and spine loss appear to be different. They postulated that the loss of dendritic spines is produced by calcium-mediated alterations of the spine cytoskeleton, while dendritic beading is independent of calcium influx, but dependent on intracellular sodium and chloride movement (Swann et al., 2000), which goes along with our findings, that varicosity formation wasn´t abolished in calcium-free buffer. Additionally, it has been postulated that dendritic beading occurs much more rapidly than calcium dependent excitotoxic cell death (Hasbani et al., 1998; Swann et al., 2000).

To investigate the effects we saw with the help of primary neuronal culture in a more complex system, we developed a reproducible acute brain slice culturing method.

There are several brain slice culturing methods described in literature. One prominent method has been described by Stoppini et al. in 1991. For experiments, they placed the slices on top of a membrane at the interface between air and culture medium (Stoppini et al., 1991). This model is suitable to study physiological mechanisms occurring during the first days in culture. A big disadvantage is that upon treatment with different compounds (PLY in our case), only one side of the brain slide gets in contact with the toxin. Another disadvantage is that the top of the slide will be covered with astrocytes over time. That does not refer to the original *in vivo* state and makes analysis of toxin effects more complicated.

Another method described in literature is the roller model. Due to this culturing method, the brain slices are kept in glass bottles and, for incubation, placed on top of a horizontal roller. Thereby, the brain slices are free-floating in medium during toxin challenge, ensuring the toxin to contact all sides

of the brain slice (Victorov et al., 2001). The major disadvantage of this method is the lack of fresh oxygen.
To combine the best properties of both methods, we did some modifications. By placing the whole brain slices in the culture medium, it is ensured, that the toxin has contact to all sides of the slice. By constant gassing with carbogen, it is ensured, that the slices are provided with enough oxygen. Glucose supplement to the culture medium ensures proper functioning of brain cells over time.

Neuronal morphology in the tissue context was visualized using the fluorescent membrane tracer DiI or by immunohistochemistry with an antibody to the dendrite-specific microtubule-associated protein MAP2.
DiI is widely used as a retrograde or antegrade neuronal tracer. The dye is suitable for the staining of neurons in dissociated cultures (Honig and Hume, 1986, 1989) as well as for tracing neurons in brain slices by focal application of single crystals (Hosokawa et al., 1992; Seabold et al., 2010) or by using a suspension of DiI in PBS (Park et al., 1996). Especially for the staining of dendritic spines, which are near the resolution limit for optical microscopy, DiI tracers represent a simple but effective staining method. In our case, we applied single crystals directly to several cortex areas, to ensure a proper staining of single neurons in these brain regions. DiI does not spread from labeled to unlabeled neurons, ensuring single stained neurons in the complex network of brain tissue (Honig and Hume, 1986).
As it has been shown that brain slices, fixed with lower concentrations of paraformaldehyde solution than typically used (4 %), show a better distribution of the DiI compound, we used a 2 % PFA solution for fixation (Kim et al., 2007). It is important to use preheated PFA for the fixation process, as it has been shown that chilled solutions can cause a reduction of dendritic spines in brain slices (Kirov et al., 2004). The medium should contain a certain amount of glucose, as oxygen-glucose deprivation is known to induce varicosities in the dendrites of cultured cortical neurons (Park et al., 1996).

By using the shaker method for the incubation of brain tissue, the leakage of LDH into the supernatant is enhanced in comparison to the carbogenated brain slice culturing model. This might be due to the fact that the brain tissue is not sufficiently provided with oxygen. It should be taken into consideration, to use this method as a model for ischemic tissue insults; to examine the pathophysiology of brain diseases with the help of a model of an ischemic tissue context.
In our case, this brain slice culturing method does not make much sense, because it has been shown that ischemia causes varicosity formation itself (Hori and Carpenter, 1994). The aim of this work was

to identify the effects directly mediated by pneumolysin. Therefore, we had to abolish all other mediators of changes.

By reducing the extracellular calcium levels during PLY challenge in brain slice culture from 2 mM to 1 mM, we observed a higher LDH release, corresponding to a higher cytotoxicity. This means that PLY concentrations, which were proven to be sub-lytic, can become lytic in consequence of decreased extracellular calcium levels (Wippel et al., 2011). The reduction of extracellular calcium levels is often correlated with an aggravated course of different systemic bacterial diseases. Hypocalcemia is especially observed in patients suffering from streptococcus group A bacteremia and sepsis (Ben-Abraham et al., 2002; Cooper and Morganelli, 1998). However, it should be taken into consideration, that lower calcium levels in the serum are not necessarily correlated with decreased calcium levels in the CSF of the patients. Interesting about these findings is, that streptolysin O (a protein toxin produced by group A streptococci) belongs to the family of cholesterol-dependent cytolysins, too (Johnson et al., 1980). Another point to consider is that the experiments were performed with calcium levels which correspond to the calcium levels in the CSF of rodents (Jones and Keep, 1988). In humans, CFS calcium levels are round about 0,6 mM (Bereczki et al., 2000), which might be due to a higher lytic capacity of pneumolysin in human patients.

As previously mentioned, we used a second method to visualize the dendrites in brain slices besides DiI: immunohistochemistry with an antibody against MAP2. MAP2 is a neuron-specific protein, selectively localized in the dendrites and somata of neurons. This protein is thought to be involved in the assembly of microtubules by crosslinking microtubules with other microtubules and intermediate filaments (Bernhardt and Matus, 1984). With the help of this staining method, we were also able to visualize the dendritic beadings, suggesting that the observed effect is not only dependent on osmotic changes or malformation of the plasma membrane, but also dependent on changes in the cytoskeleton of the depicted neurons.

Swann et al. described in 2000 the same dendritic abnormalities in studies with human epilepsy tissue and comparable animal models of focal epilepsy. Like several studies before, they connected the excessive release of glutamate during seizures to the occurrence of these abnormalities (Swann et al., 2000). Focal swellings or varicosity formation in dendrites and loss of dendritic spines are the earliest indications of glutamate-induced excitotoxicity (Tseng and Firestein, 2011). In 2005, Takeuchi et al. mentioned that dendritic beading can be induced by activated microglia and occurs through

NMDA receptor signaling. They stated that blockage of NMDA receptors may be an effective therapeutic approach for neurodegenerative diseases (Takeuchi et al., 2005).
Thus, we decided to investigate, if an inhibitor of the NMDA receptor is capable of anticipating the effects mediated by pneumolysin. With the help of MK-801 we could reverse the formation of varicosities in some of the experiments. This finding leads to the hypothesis, that pneumolysin-mediated neurotoxicity directly involves the activation of NMDA receptors.
However, blocking the NMDA receptors is a double-edged sword as it can lead to neuronal death, too. Normal activation patterns of the NMDA receptor have been shown to be neuroprotective against both apoptotic and excitotoxic events (Hardingham, 2009). Additionally, many clinical trials using NMDA receptor antagonists in the field of stroke, traumatic brain injury and dementia have failed due to poor tolerance and efficiency. These trials involved more than 9000 patients, but none of the agents used revealed therapeutically relevant. The only exception was magnesium, which showed benefits in the treatment of subarachnoid haemorrhage (Muir, 2006).
Ikonomidou and Turski proposed, that NMDA receptor antagonists failed in stroke and traumatic brain injury trials in human beings because blocking the NMDARs, and thereby synaptic transmission, hinders neuronal survival (Ikonomidou and Turski, 2002).
In our experiments, MK-801 significantly reduced the number of dendritic spines itself; an effect that is already known (Butler et al., 1999) and also exhibits MK-801 as an inappropriate compound for the implementation in clinical trials.

AP5 serves as another inhibitor of the NMDA receptor. In contrast to MK-801, it competitively inhibits the glutamate binding site of the receptor (Morris et al., 1986). In our experiments, AP5 showed the same effects concerning the suppression of varicosity formation. This is a hint that MK-801 abolished dendrite beading really by blocking the NMDAR and not via direct interaction with pneumolysin or the PLY pores. Unfortunately, AP5 is not really a good alternative to MK-801 as it has been shown that it inhibits learning and memory processes (Davis et al., 1992). This is consistent with our findings that AP5 reduced the number of dendritic spines itself.

It is known that microtubule dynamics are involved in varicosity formation. Disintegrated microtubules and a reduction in the immunoreactivity against MAP2 have been found in swollen dendrites (Tomimoto and Yanagihara, 1992). In 2006, Hoskison and Shuttleworth observed an aggregation of MAP2 into dendritic beadings after a brief exposure to excitotoxic agents, referring to a depolymerization of microtubules (Hoskison and Shuttleworth, 2006). In 2003, Buddle et al. found

out that the NMDA receptor resides in a complex with MAP2 and that the activation of the NMDA receptor plays a prominent role in the breakdown of MAP2 (Buddle et al., 2003). This goes along with our findings, where pneumolysin leads to an altered MAP2 signal in immunohistochemistry that can be blocked with an inhibitor of the NMDA receptor.
Tseng and Firestein proposed a mechanism, where the post-synaptic density-95 protein (PSD-95) is involved in the modulations of the microtubule cytoskeleton during exposure to sublethal excitotoxic events (Tseng and Firestein, 2011). PSD-95 is a postsynaptic neuronal scaffolding protein, located in dendritic spines. It associates with N-methyl-D-aspartate receptors and links them to intracellular signaling molecules (Watanabe et al., 2003). Additionally, Morales and Fifkova postulated that MAP2 may organize actin filaments in dendritic spines and endow the actin network of the spines with dynamic properties that are necessary for synaptic plasticity (Morales and Fifkova, 1989). Thus, it seems possible that the formation of varicosities is indirectly related to the loss of dendritic spines.

As several studies mention that the morphological changes after excitotoxic insults disappear within 2 hours after the excitotoxic agents have been removed (Faddis et al., 1997; Hasbani et al., 1998; Park et al., 1996), it should be taken into consideration if it is more reasonable to work on the reduction of the compounds which lead to excitotoxicity (pneumolysin, in our case) than to block the receptors directly.

Despite the finding that varicosity formation is independent of calcium influx, we performed some experiments, measuring the elevation of intracellular calcium levels with the help of primary mouse astrocytes. These cells are easier to handle, less vulnerable and since the cells have to be rinsed several times during the fura-2 loading process, a good alternative. Due to the fact that NMDARs are also present in mouse astrocytes (Verkhratsky and Kirchhoff, 2007) and even in human astrocytes (Lee et al., 2010), they represent a good model for the investigation, if MK-801 is capable of altering calcium influx patterns, as it has been postulated that glutamate excitotoxicity is strongly dependent on calcium influx (Manev et al., 1989). The elevation of intracellular calcium levels for about 30 % could not be dropped down after addition of MK-801, which is no surprise, as pneumolysin arouses calcium influx itself. The delay of the time span till the rise of intracellular calcium begins and the time span till the calcium peak is reached, might be due to the fact that MK-801 blocks calcium influx through the NMDA receptor and thus, calcium mainly rushes into the cell through the pneumolysin pore itself.

Another interesting point concerning the calcium influx into astrocytes is that several studies found out, that astrocytes release glutamate themselves in response to elevated intracellular calcium levels (Bonansco et al., 2011; Perea and Araque, 2007). The release of glutamate by astrocytes after pneumolysin challenge might be another reason for overexcited neurons and the development of excitotoxic insults.

Glutamatergic transmission is central for diverse brain functions, being particularly important for learning, memory, and cognition. In normal brain homeostasis, glutamate, released by neurons during synaptic transmission, gets cleared up from the synaptic cleft via uptake by astrocytes. As it is known that astrocytes get damaged upon challenge with pneumolysin (Fortsch et al., 2011; Hupp et al., 2012) we investigated if the capacity of glutamate uptake into brain tissue is affected.
Surprisingly, we could not observe any changes in glutamate levels; neither in the glutamate reuptake capacity of brain tissue nor in the discharge of glutamate from brain tissue into the supernatant.
In 2007, Braun et al. linked the neurotoxicity of pneumolysin to the damage of mitochondria (Braun et al., 2007). It is known, that mitochondrial dysfunction increases the vulnerability of neurons towards dendritic beading during normal physiological activity (Greenwood et al., 2007). This might be an explanation why we could not observe any changes in the glutamate status of brain tissue. Maybe pneumolysin damages mitochondria and thus makes the neurons more vulnerable to physiological glutamate concentrations. However, Braun et al. used the toxin in concentrations of 0,2 to 0,5 µg/ml for an incubation time of up to 6 hours, which are relatively tough conditions for primary neurons. It should be taken into consideration to investigate, if there is any damage of mitochondria induced by sub-lytic amounts of pneumolysin.

7 Concluding remarks and perspectives

This is the first time, a study connected pneumolysin not only to cell damage, cell death and apoptosis in brain cells, but to excitotoxicity.

Future research, based on the findings of this thesis, will focus on a further clarification of the glutamate effects induced by pneumolysin. First follow-up experiments with a highly sensitive glutamate probe will check if the enzymatic assay used in our experimental setup wasn´t just sensitive enough or if there is really no change in the glutamate status of brain tissue upon pneumolysin challenge.

To ensure, that only pyramidal neurons are observed in the brain slices, a genetically modified mouse model will be introduced. These mice express GFP in a small amount of their cortical, pyramidal neurons. By studying the effects of pneumolysin with the help of brain slices from these mice, it is possible to diminish one error source: the staining process. Additionally, it ensures a random staining of neurons and is also time-saving.

As the NMDAR antagonists MK-801 and AP5 exhibited severe side-effects (such as cognitive disruption) in clinical trials, other options for the prevention of excitotoxic insults should be taken into consideration.

The introduced brain slice culturing method represents an easy, cheap and very good reproducible method. With this application, it is possible to maintain brain slices for several hours (in our experiments up to 24 hours) alive. For further experiments, it is possible to adopt these *ex vivo* models for the screening of therapeutic molecules as well as for the testing of different compounds with regard to their neurotoxic potentials.

As the loss of dendritic spines is not necessarily associated with the loss of synaptic contacts (Hasbani et al., 2001), this question should be addressed in further experiments, searching for a possible connection between morphological and functional alterations. One possibility could be electrophysiological measurements in brain slices.
All in all it should be taken into consideration to develop agents that directly inhibit pneumolysin, as this may represent an additional useful therapy for pneumococcal meningitis.

8 References

Al-Noori, S., and Swann, J.W. (2000). A role for sodium and chloride in kainic acid-induced beading of inhibitory interneuron dendrites. *Neuroscience* **101**, 337-348.

Albers, G.W., Goldberg, M.P., and Choi, D.W. (1989). N-methyl-D-aspartate antagonists: ready for clinical trial in brain ischemia? *Annals of neurology* **25**, 398-403.

Allen, N.J., and Barres, B.A. (2009). Neuroscience: Glia - more than just brain glue. *Nature* **457**, 675-677.

AlonsoDeVelasco, E., Verheul, A.F., Verhoef, J., and Snippe, H. (1995). Streptococcus pneumoniae: virulence factors, pathogenesis, and vaccines. *Microbiological reviews* **59**, 591-603.

Anderson, W.M., and Trgovcich-Zacok, D. (1995). Carbocyanine dyes with long alkyl side-chains: broad spectrum inhibitors of mitochondrial electron transport chain activity. *Biochemical pharmacology* **49**, 1303-1311.

Andersson, B., Dahmen, J., Frejd, T., Leffler, H., Magnusson, G., Noori, G., and Eden, C.S. (1983). Identification of an active disaccharide unit of a glycoconjugate receptor for pneumococci attaching to human pharyngeal epithelial cells. *The Journal of experimental medicine* **158**, 559-570.

Arditi, M., Mason, E.O., Jr., Bradley, J.S., Tan, T.Q., Barson, W.J., Schutze, G.E., Wald, E.R., Givner, L.B., Kim, K.S., Yogev, R*., et al.* (1998). Three-year multicenter surveillance of pneumococcal meningitis in children: clinical characteristics, and outcome related to penicillin susceptibility and dexamethasone use. *Pediatrics* **102**, 1087-1097.

Baba, H., Kawamura, I., Kohda, C., Nomura, T., Ito, Y., Kimoto, T., Watanabe, I., Ichiyama, S., and Mitsuyama, M. (2001). Essential role of domain 4 of pneumolysin from Streptococcus pneumoniae in cytolytic activity as determined by truncated proteins. *Biochemical and biophysical research communications* **281**, 37-44.

Bak, L.K., Schousboe, A., and Waagepetersen, H.S. (2006). The glutamate/GABA-glutamine cycle: aspects of transport, neurotransmitter homeostasis and ammonia transfer. *Journal of neurochemistry* **98**, 641-653.

Balachandran, P., Hollingshead, S.K., Paton, J.C., and Briles, D.E. (2001). The autolytic enzyme LytA of Streptococcus pneumoniae is not responsible for releasing pneumolysin. *Journal of bacteriology* **183**, 3108-3116.

Ben-Abraham, R., Keller, N., Vered, R., Harel, R., Barzilay, Z., and Paret, G. (2002). Invasive group A streptococcal infections in a large tertiary center: epidemiology, characteristics and outcome. *Infection* **30**, 81-85.

Benarroch, E.E. (2011). NMDA receptors: recent insights and clinical correlations. *Neurology* **76**, 1750-1757.

Bereczki, D., Fekete, I., Loof, I., Kobberling, W., Valikovics, A., Nemeth, G., Fulesdi, B., and Csiba, L. (2000). Cations of cisternal cerebrospinal fluid in humans and the effect of different doses of nimodipine on CSF calcium after stroke. *Clinical neuropharmacology* **23**, 318-323.

Berliocchi, L., Bano, D., and Nicotera, P. (2005). Ca2+ signals and death programmes in neurons. *Philosophical transactions of the Royal Society of London Series B, Biological sciences* **360**, 2255-2258.

Bernhardt, R., and Matus, A. (1984). Light and electron microscopic studies of the distribution of microtubule-associated protein 2 in rat brain: a difference between dendritic and axonal cytoskeletons. *The Journal of comparative neurology* **226**, 203-221.

Bittigau, P., and Ikonomidou, C. (1997). Glutamate in neurologic diseases. *Journal of child neurology* **12**, 471-485.

Bonansco, C., Couve, A., Perea, G., Ferradas, C.A., Roncagliolo, M., and Fuenzalida, M. (2011). Glutamate released spontaneously from astrocytes sets the threshold for synaptic plasticity. *The European journal of neuroscience* **33**, 1483-1492.

Braun, J.S., Hoffmann, O., Schickhaus, M., Freyer, D., Dagand, E., Bermpohl, D., Mitchell, T.J., Bechmann, I., and Weber, J.R. (2007). Pneumolysin causes neuronal cell death through mitochondrial damage. *Infection and immunity* **75**, 4245-4254.

Braun, J.S., Sublett, J.E., Freyer, D., Mitchell, T.J., Cleveland, J.L., Tuomanen, E.I., and Weber, J.R. (2002). Pneumococcal pneumolysin and H(2)O(2) mediate brain cell apoptosis during meningitis. *The Journal of clinical investigation* **109**, 19-27.

Brouwer, M.C., Tunkel, A.R., and van de Beek, D. (2010). Epidemiology, diagnosis, and antimicrobial treatment of acute bacterial meningitis. *Clinical microbiology reviews* **23**, 467-492.

Buddle, M., Eberhardt, E., Ciminello, L.H., Levin, T., Wing, R., DiPasquale, K., and Raley-Susman, K.M. (2003). Microtubule-associated protein 2 (MAP2) associates with the NMDA receptor and is spatially redistributed within rat hippocampal neurons after oxygen-glucose deprivation. *Brain research* **978**, 38-50.

Buerli, T., Pellegrino, C., Baer, K., Lardi-Studler, B., Chudotvorova, I., Fritschy, J.M., Medina, I., and Fuhrer, C. (2007). Efficient transfection of DNA or shRNA vectors into neurons using magnetofection. *Nature protocols* **2**, 3090-3101.

Butler, A.K., Uryu, K., Rougon, G., and Chesselet, M.F. (1999). N-methyl-D-aspartate receptor blockade affects polysialylated neural cell adhesion molecule expression and synaptic density during striatal development. *Neuroscience* **89**, 1169-1181.

Chao, Y.N., Chiu, N.C., and Huang, F.Y. (2008). Clinical features and prognostic factors in childhood pneumococcal meningitis. *Journal of microbiology, immunology, and infection = Wei mian yu gan ran za zhi* **41**, 48-53.

Cho, S., Wood, A., and Bowlby, M.R. (2007). Brain slices as models for neurodegenerative disease and screening platforms to identify novel therapeutics. *Current neuropharmacology* **5**, 19-33.

Cooper, B.W., and Morganelli, E. (1998). Group B streptococcal bacteremia in adults at Hartford Hospital 1991-1996. *Connecticut medicine* **62**, 515-517.

Cundell, D.R., Gerard, N.P., Gerard, C., Idanpaan-Heikkila, I., and Tuomanen, E.I. (1995). Streptococcus pneumoniae anchor to activated human cells by the receptor for platelet-activating factor. *Nature* **377**, 435-438.

Davis, S., Butcher, S.P., and Morris, R.G. (1992). The NMDA receptor antagonist D-2-amino-5-phosphonopentanoate (D-AP5) impairs spatial learning and LTP in vivo at intracerebral concentrations comparable to those that block LTP in vitro. *The Journal of neuroscience : the official journal of the Society for Neuroscience* **12**, 21-34.

Dong, X.X., Wang, Y., and Qin, Z.H. (2009). Molecular mechanisms of excitotoxicity and their relevance to pathogenesis of neurodegenerative diseases. *Acta pharmacologica Sinica* **30**, 379-387.

Edmond, K., Clark, A., Korczak, V.S., Sanderson, C., Griffiths, U.K., and Rudan, I. (2010). Global and regional risk of disabling sequelae from bacterial meningitis: a systematic review and meta-analysis. *The Lancet infectious diseases* **10**, 317-328.

Emptage, N.J. (2001). Fluorescent imaging in living systems. *Current opinion in pharmacology* **1**, 521-525.

Faddis, B.T., Hasbani, M.J., and Goldberg, M.P. (1997). Calpain activation contributes to dendritic remodeling after brief excitotoxic injury in vitro. *The Journal of neuroscience : the official journal of the Society for Neuroscience* **17**, 951-959.

Fortsch, C., Hupp, S., Ma, J., Mitchell, T.J., Maier, E., Benz, R., and Iliev, A.I. (2011). Changes in astrocyte shape induced by sublytic concentrations of the cholesterol-dependent cytolysin pneumolysin still require pore-forming capacity. *Toxins* **3**, 43-62.

Gerber, J., and Nau, R. (2010). Mechanisms of injury in bacterial meningitis. *Current opinion in neurology* **23**, 312-318.

Gilbert, R.J., Heenan, R.K., Timmins, P.A., Gingles, N.A., Mitchell, T.J., Rowe, A.J., Rossjohn, J., Parker, M.W., Andrew, P.W., and Byron, O. (1999a). Studies on the structure and mechanism of a bacterial protein toxin by analytical ultracentrifugation and small-angle neutron scattering. *Journal of molecular biology* **293**, 1145-1160.

Gilbert, R.J., Jimenez, J.L., Chen, S., Tickle, I.J., Rossjohn, J., Parker, M., Andrew, P.W., and Saibil, H.R. (1999b). Two structural transitions in membrane pore formation by pneumolysin, the pore-forming toxin of Streptococcus pneumoniae. *Cell* **97**, 647-655.

Gilbert, R.J., Rossjohn, J., Parker, M.W., Tweten, R.K., Morgan, P.J., Mitchell, T.J., Errington, N., Rowe, A.J., Andrew, P.W., and Byron, O. (1998). Self-interaction of pneumolysin, the pore-forming protein toxin of Streptococcus pneumoniae. *Journal of molecular biology* **284**, 1223-1237.

Goetghebuer, T., West, T.E., Wermenbol, V., Cadbury, A.L., Milligan, P., Lloyd-Evans, N., Adegbola, R.A., Mulholland, E.K., Greenwood, B.M., and Weber, M.W. (2000). Outcome of meningitis caused by Streptococcus pneumoniae and Haemophilus influenzae type b in children in The Gambia. *Tropical medicine & international health : TM & IH* **5**, 207-213.

Greenwood, S.M., Mizielinska, S.M., Frenguelli, B.G., Harvey, J., and Connolly, C.N. (2007). Mitochondrial dysfunction and dendritic beading during neuronal toxicity. *The Journal of biological chemistry* **282**, 26235-26244.

Griffith, F. (1928). The Significance of Pneumococcal Types. *The Journal of hygiene* **27**, 113-159.

Grimwood, K., Anderson, P., Anderson, V., Tan, L., and Nolan, T. (2000). Twelve year outcomes following bacterial meningitis: further evidence for persisting effects. *Archives of disease in childhood* **83**, 111-116.

Grynkiewicz, G., Poenie, M., and Tsien, R.Y. (1985). A new generation of Ca2+ indicators with greatly improved fluorescence properties. *The Journal of biological chemistry* **260**, 3440-3450.

Hardingham, G.E. (2009). Coupling of the NMDA receptor to neuroprotective and neurodestructive events. *Biochemical Society transactions* **37**, 1147-1160.

Hasbani, M.J., Hyrc, K.L., Faddis, B.T., Romano, C., and Goldberg, M.P. (1998). Distinct roles for sodium, chloride, and calcium in excitotoxic dendritic injury and recovery. *Experimental neurology* **154**, 241-258.

Hasbani, M.J., Schlief, M.L., Fisher, D.A., and Goldberg, M.P. (2001). Dendritic spines lost during glutamate receptor activation reemerge at original sites of synaptic contact. *The Journal of neuroscience : the official journal of the Society for Neuroscience* **21**, 2393-2403.

Hayashi, H., and Miyata, H. (1994). Fluorescence imaging of intracellular Ca2+. *Journal of pharmacological and toxicological methods* **31**, 1-10.

Herron, C.E., Lester, R.A., Coan, E.J., and Collingridge, G.L. (1986). Frequency-dependent involvement of NMDA receptors in the hippocampus: a novel synaptic mechanism. *Nature* **322**, 265-268.

Hertz, L., Dringen, R., Schousboe, A., and Robinson, S.R. (1999). Astrocytes: glutamate producers for neurons. *Journal of neuroscience research* **57**, 417-428.

Hirst, R.A., Gosai, B., Rutman, A., Guerin, C.J., Nicotera, P., Andrew, P.W., and O'Callaghan, C. (2008). Streptococcus pneumoniae deficient in pneumolysin or autolysin has reduced virulence in meningitis. *The Journal of infectious diseases* **197**, 744-751.

Hirst, R.A., Rutman, A., Sikand, K., Andrew, P.W., Mitchell, T.J., and O'Callaghan, C. (2000a). Effect of pneumolysin on rat brain ciliary function: comparison of brain slices with cultured ependymal cells. *Pediatric research* **47**, 381-384.

Hirst, R.A., Sikand, K.S., Rutman, A., Mitchell, T.J., Andrew, P.W., and O'Callaghan, C. (2000b). Relative roles of pneumolysin and hydrogen peroxide from Streptococcus pneumoniae in inhibition of ependymal ciliary beat frequency. *Infection and immunity* **68**, 1557-1562.

Hoban, D.J., Doern, G.V., Fluit, A.C., Roussel-Delvallez, M., and Jones, R.N. (2001). Worldwide prevalence of antimicrobial resistance in Streptococcus pneumoniae, Haemophilus influenzae, and Moraxella catarrhalis in the SENTRY Antimicrobial Surveillance Program, 1997-1999. *Clinical infectious diseases : an official publication of the Infectious Diseases Society of America* **32 Suppl 2**, S81-93.

Honig, M.G., and Hume, R.I. (1986). Fluorescent carbocyanine dyes allow living neurons of identified origin to be studied in long-term cultures. *The Journal of cell biology* **103**, 171-187.

Honig, M.G., and Hume, R.I. (1989). Dil and diO: versatile fluorescent dyes for neuronal labelling and pathway tracing. *Trends in neurosciences* **12**, 333-335, 340-331.

Hori, N., and Carpenter, D.O. (1994). Functional and morphological changes induced by transient in vivo ischemia. *Experimental neurology* **129**, 279-289.

Hoskison, M.M., and Shuttleworth, C.W. (2006). Microtubule disruption, not calpain-dependent loss of MAP2, contributes to enduring NMDA-induced dendritic dysfunction in acute hippocampal slices. *Experimental neurology* **202**, 302-312.

Hoskison, M.M., Yanagawa, Y., Obata, K., and Shuttleworth, C.W. (2007). Calcium-dependent NMDA-induced dendritic injury and MAP2 loss in acute hippocampal slices. *Neuroscience* **145**, 66-79.

Hosokawa, T., Bliss, T.V., and Fine, A. (1992). Persistence of individual dendritic spines in living brain slices. *Neuroreport* **3**, 477-480.

Hupp, S., Heimeroth, V., Wippel, C., Fortsch, C., Ma, J., Mitchell, T.J., and Iliev, A.I. (2012). Astrocytic tissue remodeling by the meningitis neurotoxin pneumolysin facilitates pathogen tissue penetration and produces interstitial brain edema. *Glia* **60**, 137-146.

Ihekweazu, C., Basarab, M., Wilson, D., Oliver, I., Dance, D., George, R., and Pebody, R. (2010). Outbreaks of serious pneumococcal disease in closed settings in the post-antibiotic era: a systematic review. *The Journal of infection* **61**, 21-27.

Ikegaya, Y., Kim, J.A., Baba, M., Iwatsubo, T., Nishiyama, N., and Matsuki, N. (2001). Rapid and reversible changes in dendrite morphology and synaptic efficacy following NMDA receptor activation: implication for a cellular defense against excitotoxicity. *Journal of cell science* **114**, 4083-4093.

Ikonomidou, C., and Turski, L. (2002). Why did NMDA receptor antagonists fail clinical trials for stroke and traumatic brain injury? *Lancet neurology* **1**, 383-386.

Jing, J., Aitken, P.G., and Somjen, G.G. (1991). Lasting neuron depression induced by high potassium and its prevention by low calcium and NMDA receptor blockade. *Brain research* **557**, 177-183.

Johnson, M.K., Geoffroy, C., and Alouf, J.E. (1980). Binding of cholesterol by sulfhydryl-activated cytolysins. *Infection and immunity* **27**, 97-101.

Jones, H.C., and Keep, R.F. (1988). Brain fluid calcium concentration and response to acute hypercalcaemia during development in the rat. *The Journal of physiology* **402**, 579-593.

Kim, B.G., Dai, H.N., McAtee, M., Vicini, S., and Bregman, B.S. (2007). Labeling of dendritic spines with the carbocyanine dye DiI for confocal microscopic imaging in lightly fixed cortical slices. *Journal of neuroscience methods* **162**, 237-243.

Kim, K.S. (2010). Acute bacterial meningitis in infants and children. *The Lancet infectious diseases* **10**, 32-42.

Kirov, S.A., Petrak, L.J., Fiala, J.C., and Harris, K.M. (2004). Dendritic spines disappear with chilling but proliferate excessively upon rewarming of mature hippocampus. *Neuroscience* **127**, 69-80.

Koedel, U., Klein, M., and Pfister, H.W. (2010). New understandings on the pathophysiology of bacterial meningitis. *Current opinion in infectious diseases* **23**, 217-223.

Koedel, U., Scheld, W.M., and Pfister, H.W. (2002). Pathogenesis and pathophysiology of pneumococcal meningitis. *The Lancet infectious diseases* **2**, 721-736.

Koek, W., Woods, J.H., and Winger, G.D. (1988). MK-801, a proposed noncompetitive antagonist of excitatory amino acid neurotransmission, produces phencyclidine-like behavioral effects in pigeons, rats and rhesus monkeys. *The Journal of pharmacology and experimental therapeutics* **245**, 969-974.

Kornelisse, R.F., Westerbeek, C.M., Spoor, A.B., van der Heijde, B., Spanjaard, L., Neijens, H.J., and de Groot, R. (1995). Pneumococcal meningitis in children: prognostic indicators and outcome. *Clinical infectious diseases : an official publication of the Infectious Diseases Society of America* **21**, 1390-1397.

Lau, A., and Tymianski, M. (2010). Glutamate receptors, neurotoxicity and neurodegeneration. *Pflugers Archiv : European journal of physiology* **460**, 525-542.

Lee, M.C., Ting, K.K., Adams, S., Brew, B.J., Chung, R., and Guillemin, G.J. (2010). Characterisation of the expression of NMDA receptors in human astrocytes. *PloS one* **5**, e14123.

Lipton, P., Aitken, P.G., Dudek, F.E., Eskessen, K., Espanol, M.T., Ferchmin, P.A., Kelly, J.B., Kreisman, N.R., Landfield, P.W., Larkman, P.M.*, et al.* (1995). Making the best of brain slices: comparing preparative methods. *Journal of neuroscience methods* **59**, 151-156.

Lynch, J.P., 3rd, and Zhanel, G.G. (2010). Streptococcus pneumoniae: epidemiology and risk factors, evolution of antimicrobial resistance, and impact of vaccines. *Current opinion in pulmonary medicine* **16**, 217-225.

Manev, H., Favaron, M., Guidotti, A., and Costa, E. (1989). Delayed increase of Ca2+ influx elicited by glutamate: role in neuronal death. *Molecular pharmacology* **36**, 106-112.

McDonald, J.W., and Johnston, M.V. (1993). Excitatory amino acid neurotoxicity in the developing brain. *NIDA research monograph* **133**, 185-205.

McIntyre, P. (2010). Adjunctive dexamethasone in meningitis: does value depend on clinical setting? *Lancet neurology* **9**, 229-231.

Megias, M., Emri, Z., Freund, T.F., and Gulyas, A.I. (2001). Total number and distribution of inhibitory and excitatory synapses on hippocampal CA1 pyramidal cells. *Neuroscience* **102**, 527-540.

Mitchell, A.M., and Mitchell, T.J. (2010). Streptococcus pneumoniae: virulence factors and variation. *Clinical microbiology and infection : the official publication of the European Society of Clinical Microbiology and Infectious Diseases* **16**, 411-418.

Mitchell, T.J., and Andrew, P.W. (1997). Biological properties of pneumolysin. *Microb Drug Resist* **3**, 19-26.

Mitchell, T.J., Andrew, P.W., Saunders, F.K., Smith, A.N., and Boulnois, G.J. (1991). Complement activation and antibody binding by pneumolysin via a region of the toxin homologous to a human acute-phase protein. *Molecular microbiology* **5**, 1883-1888.

Mitchell, T.J., Walker, J.A., Saunders, F.K., Andrew, P.W., and Boulnois, G.J. (1989). Expression of the pneumolysin gene in Escherichia coli: rapid purification and biological properties. *Biochimica et biophysica acta* **1007**, 67-72.

Morales, M., and Fifkova, E. (1989). Distribution of MAP2 in dendritic spines and its colocalization with actin. An immunogold electron-microscope study. *Cell and tissue research* **256**, 447-456.

Moran, J.H., and Schnellmann, R.G. (1996). A rapid beta-NADH-linked fluorescence assay for lactate dehydrogenase in cellular death. *Journal of pharmacological and toxicological methods* **36**, 41-44.

Morgan, P.J., Hyman, S.C., Byron, O., Andrew, P.W., Mitchell, T.J., and Rowe, A.J. (1994). Modeling the bacterial protein toxin, pneumolysin, in its monomeric and oligomeric form. *The Journal of biological chemistry* **269**, 25315-25320.

Morgan, P.J., Hyman, S.C., Rowe, A.J., Mitchell, T.J., Andrew, P.W., and Saibil, H.R. (1995). Subunit organisation and symmetry of pore-forming, oligomeric pneumolysin. *FEBS letters* **371**, 77-80.

Morris, R.G. (1989). Synaptic plasticity and learning: selective impairment of learning rats and blockade of long-term potentiation in vivo by the N-methyl-D-aspartate receptor antagonist AP5. *The Journal of neuroscience : the official journal of the Society for Neuroscience* **9**, 3040-3057.

Morris, R.G., Anderson, E., Lynch, G.S., and Baudry, M. (1986). Selective impairment of learning and blockade of long-term potentiation by an N-methyl-D-aspartate receptor antagonist, AP5. *Nature* **319**, 774-776.

Muhe, L., and Klugman, K.P. (1999). Pneumococcal and Haemophilus influenzae meningitis in a children's hospital in Ethiopia: serotypes and susceptibility patterns. *Tropical medicine & international health : TM & IH* **4**, 421-427.

Muir, K.W. (2006). Glutamate-based therapeutic approaches: clinical trials with NMDA antagonists. *Current opinion in pharmacology* **6**, 53-60.

Musher, D.M. (1992). Infections caused by Streptococcus pneumoniae: clinical spectrum, pathogenesis, immunity, and treatment. *Clinical infectious diseases : an official publication of the Infectious Diseases Society of America* **14**, 801-807.

Nollmann, M., Gilbert, R., Mitchell, T., Sferrazza, M., and Byron, O. (2004). The role of cholesterol in the activity of pneumolysin, a bacterial protein toxin. *Biophysical journal* **86**, 3141-3151.

O'Brien, K.L., Wolfson, L.J., Watt, J.P., Henkle, E., Deloria-Knoll, M., McCall, N., Lee, E., Mulholland, K., Levine, O.S., and Cherian, T. (2009). Burden of disease caused by Streptococcus pneumoniae in children younger than 5 years: global estimates. *Lancet* **374**, 893-902.

Oliva, A.A., Jr., Lam, T.T., and Swann, J.W. (2002). Distally directed dendrotoxicity induced by kainic Acid in hippocampal interneurons of green fluorescent protein-expressing transgenic mice. *The Journal of neuroscience : the official journal of the Society for Neuroscience* **22**, 8052-8062.

Olney, J.W. (1969). Brain lesions, obesity, and other disturbances in mice treated with monosodium glutamate. *Science* **164**, 719-721.

Olney, J.W. (1990). Excitotoxicity: an overview. *Canada diseases weekly report = Rapport hebdomadaire des maladies au Canada* **16 Suppl 1E**, 47-57; discussion 57-48.

Owen, R.H., Boulnois, G.J., Andrew, P.W., and Mitchell, T.J. (1994). A role in cell-binding for the C-terminus of pneumolysin, the thiol-activated toxin of Streptococcus pneumoniae. *FEMS microbiology letters* **121**, 217-221.

Paoletti, P. (2011). Molecular basis of NMDA receptor functional diversity. *The European journal of neuroscience* **33**, 1351-1365.

Park, J.S., Bateman, M.C., and Goldberg, M.P. (1996). Rapid alterations in dendrite morphology during sublethal hypoxia or glutamate receptor activation. *Neurobiology of disease* **3**, 215-227.

Parpura, V., Basarsky, T.A., Liu, F., Jeftinija, K., Jeftinija, S., and Haydon, P.G. (1994). Glutamate-mediated astrocyte-neuron signalling. *Nature* **369**, 744-747.

Paton, J.C. (1996). The contribution of pneumolysin to the pathogenicity of Streptococcus pneumoniae. *Trends in microbiology* **4**, 103-106.

Paton, J.C., Rowan-Kelly, B., and Ferrante, A. (1984). Activation of human complement by the pneumococcal toxin pneumolysin. *Infection and immunity* **43**, 1085-1087.

Perea, G., and Araque, A. (2007). Astrocytes potentiate transmitter release at single hippocampal synapses. *Science* **317**, 1083-1086.

Purpura, D.P., Bodick, N., Suzuki, K., Rapin, I., and Wurzelmann, S. (1982). Microtubule disarray in cortical dendrites and neurobehavioral failure. I. Golgi and electron microscopic studies. *Brain research* **281**, 287-297.

Quagliarello, V.J., Long, W.J., and Scheld, W.M. (1986). Morphologic alterations of the blood-brain barrier with experimental meningitis in the rat. Temporal sequence and role of encapsulation. *The Journal of clinical investigation* **77**, 1084-1095.

Ransom, B., Behar, T., and Nedergaard, M. (2003). New roles for astrocytes (stars at last). *Trends in neurosciences* **26**, 520-522.

Ratner, A.J., Hippe, K.R., Aguilar, J.L., Bender, M.H., Nelson, A.L., and Weiser, J.N. (2006). Epithelial cells are sensitive detectors of bacterial pore-forming toxins. *The Journal of biological chemistry* **281**, 12994-12998.

Regev-Yochay, G., Raz, M., Dagan, R., Porat, N., Shainberg, B., Pinco, E., Keller, N., and Rubinstein, E. (2004). Nasopharyngeal carriage of Streptococcus pneumoniae by adults and children in community and family settings. *Clinical infectious diseases : an official publication of the Infectious Diseases Society of America* **38**, 632-639.

Reiss, A., Braun, J.S., Jager, K., Freyer, D., Laube, G., Buhrer, C., Felderhoff-Muser, U., Stadelmann, C., Nizet, V., and Weber, J.R. (2011). Bacterial pore-forming cytolysins induce neuronal damage in a rat model of neonatal meningitis. *The Journal of infectious diseases* **203**, 393-400.

Ring, A., Weiser, J.N., and Tuomanen, E.I. (1998). Pneumococcal trafficking across the blood-brain barrier. Molecular analysis of a novel bidirectional pathway. *The Journal of clinical investigation* **102**, 347-360.

Roe, M.W., Lemasters, J.J., and Herman, B. (1990). Assessment of Fura-2 for measurements of cytosolic free calcium. *Cell calcium* **11**, 63-73.

Rosahl, T.W., Geppert, M., Spillane, D., Herz, J., Hammer, R.E., Malenka, R.C., and Sudhof, T.C. (1993). Short-term synaptic plasticity is altered in mice lacking synapsin I. *Cell* **75**, 661-670.

Rossjohn, J., Gilbert, R.J., Crane, D., Morgan, P.J., Mitchell, T.J., Rowe, A.J., Andrew, P.W., Paton, J.C., Tweten, R.K., and Parker, M.W. (1998). The molecular mechanism of pneumolysin, a virulence factor from Streptococcus pneumoniae. *Journal of molecular biology* **284**, 449-461.

Rossjohn, J., Polekhina, G., Feil, S.C., Morton, C.J., Tweten, R.K., and Parker, M.W. (2007). Structures of perfringolysin O suggest a pathway for activation of cholesterol-dependent cytolysins. *Journal of molecular biology* **367**, 1227-1236.

Sanacora, G., Zarate, C.A., Krystal, J.H., and Manji, H.K. (2008). Targeting the glutamatergic system to develop novel, improved therapeutics for mood disorders. *Nature reviews Drug discovery* **7**, 426-437.

Scarborough, M., and Thwaites, G.E. (2008). The diagnosis and management of acute bacterial meningitis in resource-poor settings. *Lancet neurology* **7**, 637-648.

Scheld, W.M., Koedel, U., Nathan, B., and Pfister, H.W. (2002). Pathophysiology of bacterial meningitis: mechanism(s) of neuronal injury. *The Journal of infectious diseases* **186 Suppl 2**, S225-233.

Scherer, F., Anton, M., Schillinger, U., Henke, J., Bergemann, C., Kruger, A., Gansbacher, B., and Plank, C. (2002). Magnetofection: enhancing and targeting gene delivery by magnetic force in vitro and in vivo. *Gene therapy* **9**, 102-109.

Schmidt, H., Heimann, B., Djukic, M., Mazurek, C., Fels, C., Wallesch, C.W., and Nau, R. (2006). Neuropsychological sequelae of bacterial and viral meningitis. *Brain : a journal of neurology* **129**, 333-345.

Seabold, G.K., Daunais, J.B., Rau, A., Grant, K.A., and Alvarez, V.A. (2010). DiOLISTIC labeling of neurons from rodent and non-human primate brain slices. *Journal of visualized experiments : JoVE*.

Shatursky, O., Heuck, A.P., Shepard, L.A., Rossjohn, J., Parker, M.W., Johnson, A.E., and Tweten, R.K. (1999). The mechanism of membrane insertion for a cholesterol-dependent cytolysin: a novel paradigm for pore-forming toxins. *Cell* **99**, 293-299.

Siegel, G.J. (2006). Basic neurochemistry : molecular, cellular, and medical aspects, 7th edn (Amsterdam ; Boston: Elsevier).

Simberkoff, M.S., Moldover, N.H., and Rahal, J., Jr. (1980). Absence of detectable bactericidal and opsonic activities in normal and infected human cerebrospinal fluids. A regional host defense deficiency. *The Journal of laboratory and clinical medicine* **95**, 362-372.

Sims, N.R., and Zaidan, E. (1995). Biochemical changes associated with selective neuronal death following short-term cerebral ischaemia. *The international journal of biochemistry & cell biology* **27**, 531-550.

Smith, C.L. (2008). Basic confocal microscopy. *Current protocols in molecular biology / edited by Frederick M Ausubel [et al]* **Chapter 14**, Unit 14 11.

Smith, H., and Bannister, B. (1973). Cerebrospinal-fluid immunoglobulins in meningitis. *Lancet* **2**, 591-593.

Solovyova, A.S., Nollmann, M., Mitchell, T.J., and Byron, O. (2004). The solution structure and oligomerization behavior of two bacterial toxins: pneumolysin and perfringolysin O. *Biophysical journal* **87**, 540-552.

Spreer, A., Kerstan, H., Bottcher, T., Gerber, J., Siemer, A., Zysk, G., Mitchell, T.J., Eiffert, H., and Nau, R. (2003). Reduced release of pneumolysin by Streptococcus pneumoniae in vitro and in vivo after treatment with nonbacteriolytic antibiotics in comparison to ceftriaxone. *Antimicrobial agents and chemotherapy* **47**, 2649-2654.

Squire, L.R. (2008). Fundamental neuroscience, 3rd edn (Amsterdam ; Boston: Elsevier / Academic Press).

Stahel, P.F., Nadal, D., Pfister, H.W., Paradisis, P.M., and Barnum, S.R. (1997). Complement C3 and factor B cerebrospinal fluid concentrations in bacterial and aseptic meningitis. *Lancet* **349**, 1886-1887.

Stoppini, L., Buchs, P.A., and Muller, D. (1991). A simple method for organotypic cultures of nervous tissue. *Journal of neuroscience methods* **37**, 173-182.

Stringaris, A.K., Geisenhainer, J., Bergmann, F., Balshusemann, C., Lee, U., Zysk, G., Mitchell, T.J., Keller, B.U., Kuhnt, U., Gerber, J*., et al.* (2002). Neurotoxicity of pneumolysin, a major pneumococcal virulence factor, involves calcium influx and depends on activation of p38 mitogen-activated protein kinase. *Neurobiology of disease* **11**, 355-368.

Swann, J.W., Al-Noori, S., Jiang, M., and Lee, C.L. (2000). Spine loss and other dendritic abnormalities in epilepsy. *Hippocampus* **10**, 617-625.

Takeuchi, H., Mizuno, T., Zhang, G., Wang, J., Kawanokuchi, J., Kuno, R., and Suzumura, A. (2005). Neuritic beading induced by activated microglia is an early feature of neuronal dysfunction toward neuronal death by inhibition of mitochondrial respiration and axonal transport. *The Journal of biological chemistry* **280**, 10444-10454.

Tauber, M.G., Khayam-Bashi, H., and Sande, M.A. (1985). Effects of ampicillin and corticosteroids on brain water content, cerebrospinal fluid pressure, and cerebrospinal fluid lactate levels in experimental pneumococcal meningitis. *The Journal of infectious diseases* **151**, 528-534.

Tauber, M.G., and Sande, M.A. (1989). Dexamethasone in bacterial meningitis: increasing evidence for a beneficial effect. *The Pediatric infectious disease journal* **8**, 842-844.

Tauber, M.G., Shibl, A.M., Hackbarth, C.J., Larrick, J.W., and Sande, M.A. (1987). Antibiotic therapy, endotoxin concentration in cerebrospinal fluid, and brain edema in experimental Escherichia coli meningitis in rabbits. *The Journal of infectious diseases* **156**, 456-462.

Tilley, S.J., Orlova, E.V., Gilbert, R.J., Andrew, P.W., and Saibil, H.R. (2005). Structural basis of pore formation by the bacterial toxin pneumolysin. *Cell* **121**, 247-256.

Tomimoto, H., and Yanagihara, T. (1992). Immunoelectron microscopic study of tubulin and microtubule-associated proteins after transient cerebral ischemia in gerbils. *Acta neuropathologica* **84**, 394-399.

Tong, H.H., Blue, L.E., James, M.A., and DeMaria, T.F. (2000). Evaluation of the virulence of a Streptococcus pneumoniae neuraminidase-deficient mutant in nasopharyngeal colonization and development of otitis media in the chinchilla model. *Infection and immunity* **68**, 921-924.

Tseng, C.Y., and Firestein, B.L. (2011). The role of PSD-95 and cypin in morphological changes in dendrites following sublethal NMDA exposure. *The Journal of neuroscience : the official journal of the Society for Neuroscience* **31**, 15468-15480.

van de Beek, D., Farrar, J.J., de Gans, J., Mai, N.T., Molyneux, E.M., Peltola, H., Peto, T.E., Roine, I., Scarborough, M., Schultsz, C*., et al.* (2010). Adjunctive dexamethasone in bacterial meningitis: a meta-analysis of individual patient data. *Lancet neurology* **9**, 254-263.

van Furth, A.M., Roord, J.J., and van Furth, R. (1996). Roles of proinflammatory and anti-inflammatory cytokines in pathophysiology of bacterial meningitis and effect of adjunctive therapy. *Infection and immunity* **64**, 4883-4890.

Verkhratsky, A., and Kirchhoff, F. (2007). NMDA Receptors in glia. *The Neuroscientist : a review journal bringing neurobiology, neurology and psychiatry* **13**, 28-37.

Victorov, I.V., Lyjin, A.A., and Aleksandrova, O.P. (2001). A modified roller method for organotypic brain cultures: free-floating slices of postnatal rat hippocampus. *Brain research Brain research protocols* **7**, 30-37.

Wall, E.C., Gordon, S.B., Hussain, S., Goonetilleke, U.R., Grizfield, J., Scarborough, M., and Kadioglu, A. (2012). Persistence of Pneumolysin in the Cerebrospinal Fluid of Patients With Pneumococcal Meningitis Is Associated With Mortality. *Clinical infectious diseases : an official publication of the Infectious Diseases Society of America*.

Walz, T. (2005). How cholesterol-dependent cytolysins bite holes into membranes. *Molecular cell* **18**, 393-394.

Watanabe, Y., Song, T., Sugimoto, K., Horii, M., Araki, N., Tokumitsu, H., Tezuka, T., Yamamoto, T., and Tokuda, M. (2003). Post-synaptic density-95 promotes calcium/calmodulin-dependent protein kinase II-mediated Ser847 phosphorylation of neuronal nitric oxide synthase. *The Biochemical journal* **372**, 465-471.

Watson, T.F. (1997). Fact and artefact in confocal microscopy. *Advances in dental research* **11**, 433-441.

Wellmer, A., Noeske, C., Gerber, J., Munzel, U., and Nau, R. (2000). Spatial memory and learning deficits after experimental pneumococcal meningitis in mice. *Neuroscience letters* **296**, 137-140.

Wippel, C., Fortsch, C., Hupp, S., Maier, E., Benz, R., Ma, J., Mitchell, T.J., and Iliev, A.I. (2011). Extracellular calcium reduction strongly increases the lytic capacity of pneumolysin from streptococcus pneumoniae in brain tissue. *The Journal of infectious diseases* **204**, 930-936.

Wong, E.H., Kemp, J.A., Priestley, T., Knight, A.R., Woodruff, G.N., and Iversen, L.L. (1986). The anticonvulsant MK-801 is a potent N-methyl-D-aspartate antagonist. *Proceedings of the National Academy of Sciences of the United States of America* **83**, 7104-7108.

Woodruff, G.N., Foster, A.C., Gill, R., Kemp, J.A., Wong, E.H., and Iversen, L.L. (1987). The interaction between MK-801 and receptors for N-methyl-D-aspartate: functional consequences. *Neuropharmacology* **26**, 903-909.

Yuste, J., Botto, M., Paton, J.C., Holden, D.W., and Brown, J.S. (2005). Additive inhibition of complement deposition by pneumolysin and PspA facilitates Streptococcus pneumoniae septicemia. *J Immunol* **175**, 1813-1819.

Zysk, G., Schneider-Wald, B.K., Hwang, J.H., Bejo, L., Kim, K.S., Mitchell, T.J., Hakenbeck, R., and Heinz, H.P. (2001). Pneumolysin is the main inducer of cytotoxicity to brain microvascular endothelial cells caused by Streptococcus pneumoniae. *Infection and immunity* **69**, 845-852.

Acknowledgment

I would like to thank…

…Aspi for being my supervisor. It was a pleasure to work with such a smart and entertaining person. Thanks for giving me the opportunity to join several conferences to present our data. I am also very thankful that you supported my plans to become a toxicologist, although our work was not directly related to that field of science.

…Timothy Mitchell for being my second supervisor, for providing us with toxin and, of course, for the very informative and pleasant time in Glasgow.

…Erich Buchner for being my third supervisor.

…Alexandra Bohl for helping me with the animal experiments. You´re the best cutthroat (that´s what LEO says…) ever. And thanks for being the best and most attentive climbing partner (a.k.a. cc) I can imagine!

…my colleagues Huppi and Tinka for having such a great and funny time in the lab. It was a great pleasure working with you. High throughput!!

…Prof. Roland Nau and Prof. Wolfgang Brück from Göttingen for providing us brain slices from meningitis mice.

…my sister Kathrin Genco for being a big role model for me and, of course, for moving me through the math exams at university. Additionally I would like to thank you for helping me catching the “big fish”…

…Markus Bischoff. You´re the best bedtime story teller ever! I wish that one day I will be able to stay awake till the end of the story. Thanks for proofreading and for calming me down every time I got upset during the writing process (and in general, too ☺).

…Peter Wermke for his course “MS word 2010 – Zielrichtung wissenschaftliche Arbeiten”. I think, without this course, I would have freaked out completely because of all this formatting stuff.

…Bruce Dickinson and all the other guys from Iron Maiden. Your music made the writing process a lot easier.

…Prof. Martin Lohse for interesting discussions.

Last but not least I would like to thank my parents; always letting me know I have a place to go to if everything fails.